

Degradable Phosphate Glasses and Composite Materials for Biomedical Applications

Dissertation

zur Erlangung des akademischen Grades doctor rerum naturalium
(Dr. rer. nat.)

vorgelegt dem Rat der Chemisch-Geowissenschaftlichen Fakultät der
Friedrich-Schiller-Universität Jena

von Dipl.-Chem. Delia S. Brauer
geboren am 28.07.1976 in Berlin-Neukölln

Gutachter:

1. Prof. Dr. Christian Rüssel
2. Prof. Dr. Dörte Stachel

Tag der öffentlichen Verteidigung: 22. Juni 2005

Contents

ZUSAMMENFASSUNG	1
1 INTRODUCTION AND OBJECTIVE	8
2 THEORY AND LITERATURE REVIEW.....	12
2.1 Bone and hard tissue	12
2.2 Implant materials	13
2.2.1 Internal fracture fixation	14
2.2.2 Degradable implants	15
2.3 Glasses and glass properties	17
2.3.1 Glass structure	17
2.3.2 Solubility and degradation.....	19
2.3.3 Phosphate glass fibers.....	23
2.4 Degradable polymers.....	25
2.4.1 Composite materials	27
2.5 Cell experiments	30
2.5.1 Cell compatibility of glasses.....	31
3 EXPERIMENTAL PROCEDURE	35
3.1 Glasses	35
3.1.1 Glass synthesis.....	35
3.1.2 Chemical analysis	36
3.1.3 Glass structure	36
3.1.4 Density, crystallization and viscosity	37
3.1.5 Porous glass cubes	37
3.1.6 Glass fibers	38

3.2	Composites	38
3.2.1	Applied organic polymer	39
3.2.2	Fabrication of composites	40
3.2.3	Mechanical strength and porosity	41
3.3	Solubility experiments.....	42
3.3.1	pH measurements.....	42
3.3.2	Solubility in deionized water	42
3.3.3	Degradation in simulated body fluid.....	42
3.4	Cell experiments	43
3.4.1	Cell culture	43
3.4.2	SEM analysis and HE staining.....	43
3.4.3	Proliferation experiments.....	44
3.4.4	Viability assay	45
3.5	Statistical evaluation	46
3.5.1	Analysis of variance (ANOVA).....	46
3.5.2	Multiple linear regression (MLR).....	46
3.5.3	Neural networks (NN)	47
3.5.4	Modeling of solubility	47
4	RESULTS	49
4.1	Polyphosphate glasses	49
4.1.1	Glass structure	49
4.1.2	Density, crystallization and viscosity	52
4.1.3	Solubility	54
4.2	Pyrophosphate glasses.....	60
4.2.1	Density, crystallization and viscosity	61
4.2.2	Solubility	65
4.2.3	Cell experiments	69
4.3	Porous glasses and composites.....	73
4.3.1	Porosity	73
4.3.2	Compressive strength.....	74
4.3.3	Adhesive shear strength.....	75
4.3.4	Solubility	76
4.3.5	Cell experiments	78

4.4	Glass fibers and composites	81
5	DISCUSSION.....	85
5.1	Polyphosphate glasses	85
5.2	Pyrophosphate glasses.....	87
5.3	Modeling of solubility.....	92
5.4	Composites	94
6	CONCLUSION.....	98
	BIBLIOGRAPHY.....	103
	APPENDIX.....	118
A	Synthetic glass composition.....	118
B	Analytic glass composition.....	120
C	Solubility results	121
D	Glass data.....	124
	FIGURES	127
	TABLES.....	129

Symbols and abbreviations

ANOVA	analysis of variance
DMSO	dimethyl sulfoxide
DPSCs	dental pulp stem cells
DTA	differential thermal analysis
ESEM	environmental scanning electron microscopy
FBS	fetal bovine serum
FDA/EtBr	fluorescein diacetate/ethidium bromide
HA	hydroxyapatite
HBSS	Hank's buffered saline solution
HE	hematoxylin and eosin
HEMA	methacrylic acid 2-hydroxyethylester
HMDS	hexamethyldisilazane
ICP-OES	inductively coupled plasma - optical emission spectroscopy
IPHT	Institut für Physikalische Hochtechnologie, Jena
IR	infra-red
<i>L</i>	average chain length
MAS-NMR	magic angle spinning - nuclear magnetic resonance
MC3T3-E1	a murine osteoblast-like cell line
MC3T3-E1.4	subclone 4 of the MC3T3-E1 cell line
MEM	minimum essential medium
MLR	multiple linear regression
MTT	3-(4,5-dimethylthiazol-2-yl)-2,5-diphenyltetrazolium bromide
<i>n</i>	number of replicates per experiment
<i>n</i>	number of bridging oxygen atoms in PO ₄ (Q ^{<i>n</i>}) groups
NN	neural network
<i>p</i>	statistical significance
PBS	phosphate buffered saline
PBT	poly(butylene terephthalate)
PDS	polydioxanone

PEG 400	polyethylene glycol 400
PGA	poly(glycolic acid)
PHB	polyhydroxybutyrate
PLA	poly(lactic acid)
PLLA	poly(L-lactic acid), poly(L-lactide)
PMMA	polymethyl methacrylate
Q^n	PO_4 group with n = number of bridging oxygen atoms
$[R_2O]$	alkali oxide concentration
$[R'O]$	alkaline earth oxide concentration
SBF	simulated body fluid
SEM	scanning electron microscopy
SR	self-reinforced
TCP	tricalcium phosphate
TCPS	tissue culture polystyrene
T_g	glass transition temperature
WST	4-[3-(4-iodophenyl)-2-(4-nitrophenyl)-2H-5-tetrazolio]-1,3-benzene disulfonate
x	molar metal oxide fraction in glass compositions
XRD	X-ray diffraction

Zusammenfassung

Die Entwicklung von funktionellen Implantatmaterialien als Knochenersatz oder zur Stabilisierung nach Frakturen ist von großer Bedeutung. Ziel bei ihrem Einsatz ist es, nach Unfall, Krankheit oder altersbedingter schmerzhafter Funktionsbeeinträchtigung eine bessere Lebensqualität zu erreichen oder Heilungsprozesse zu unterstützen.

Metallische Implantate, die nur eine temporäre Funktion zu erfüllen haben, werden üblicherweise in einer zweiten Operation wieder entfernt. Dies bedeutet für den Patienten weitere Belastungen und Risiken und verursacht zusätzliche Kosten. Resorbierbare Implantate haben den Vorteil, dass sie im Körper nach Erfüllung ihrer Funktion abgebaut werden oder sich auflösen. Somit entfällt die Operation zu ihrer Entfernung. Außerdem können abbaubare Implantate durch den sukzessiven Verlust ihrer mechanischen Eigenschaften Heilungsprozesse dynamisieren. Abbaubare organische Polymere wie z.B. Polylactide oder Polyglycolide finden seit einigen Jahren Anwendung als bioresorbierbare Schrauben und Nägel. Allerdings haben diese Materialien Nachteile im Bereich der Steifigkeit und der Kraftrelaxation, die ihre Anwendung auf niedrig belastete Implantate beschränkt.

Phosphatgläser bieten eine Alternative für die Entwicklung neuer resorbierbarer Implantatmaterialien. Phosphatgläser des Systems P_2O_5 -CaO-MgO- Na_2O ähneln in ihrer Zusammensetzung dem anorganischen Anteil des Knochens, und ihre Löslichkeit lässt sich durch Variation der Zusammensetzung über weite Bereiche einstellen. Die Löslichkeit hängt dabei u.a. vom Phosphatgehalt der Gläser ab. Polyphosphatgläser, die hauptsächlich aus Phosphatketten aufgebaut sind und deren P_2O_5 -Konzentration zwischen etwa 40 und 50 mol% liegt haben eine deutlich größere Löslichkeit als Gläser mit geringeren Phosphatgehalten. Pyrophosphatgläser haben P_2O_5 -Konzentrationen von weniger als 40 mol% und sind hauptsächlich aus kleinen Phosphateinheiten wie Mono- oder Diphosphatgruppen aufgebaut (Invertstruktur). Aufgrund ihrer geringeren Löslichkeit reagieren sie in wässrigen Lösungen weniger sauer als Polyphosphate. Die Löslichkeit der Gläser lässt sich außerdem durch Zusatz geeigneter Komponenten

beeinflussen. Geringe Konzentrationen an TiO_2 und Al_2O_3 können beispielsweise die Löslichkeit deutlich verringern.

Als Nachteile von Gläsern und Glaskeramiken sind ihre Sprödigkeit, ihre relativ schlechte mechanische Bearbeitbarkeit sowie ihre Steifigkeit zu nennen. Durch Schaffung von Werkstoffverbunden mit resorbierbaren organischen Polymeren können abbaubare Implantatmaterialien mit deutlich verbesserten mechanischen Eigenschaften erhalten werden.

Im Rahmen dieser Arbeit wurden Gläser zweier Gruppen wasserlöslicher Phosphatgläser synthetisiert. In einer ersten Reihe wurde Polyphosphatgläser des Systems P_2O_5 -CaO-MgO- Na_2O - TiO_2 mit Phosphatgehalten zwischen 45 und 50 mol% hergestellt. Die Gläser zeigen eine niedrige Kristallisationsanfälligkeit, weshalb alle Gläser ohne Abpressen der Schmelze glasig erhalten werden konnten. ^{31}P -MAS-NMR-Untersuchungen zeigten, dass das Glas mit 50 mol% P_2O_5 hauptsächlich aus Phosphatketten besteht. Mit Abnahme der P_2O_5 -Konzentration nahm der Anteil an Kettenendgruppen zu, was auf eine Depolymerisation der Phosphatketten hindeutet. Die Gläser waren zunehmend aus kleineren Phosphatbausteinen aufgebaut. Von den Gläsern mit höheren Phosphatgehalten (≥ 46 mol% P_2O_5) wurden Viskositätskurven erhalten. Ihre Viskosität bei 550°C lag zwischen 10^3 und 10^5 dPa s. Bei den Viskositätsuntersuchungen zeigte sich außerdem, dass mit Verringerung der Phosphatanteils im Glas auch die Kristallisationsanfälligkeit zunahm. Von den Gläsern mit 45 mol% P_2O_5 wurden keine Viskositätskurven erhalten, da die Gläser während der Messung kristallisierten.

Das Löslichkeitsverhalten der Gläser wurde zuerst durch pH-Untersuchungen in physiologischer Kochsalzlösung untersucht. Ziel war es, ein Glas zu erhalten, das den pH-Wert des umgebenden Mediums nicht zu weit absenkt. Es wurden 2 g Glasgrieß der Kornfraktion 315 bis $500\ \mu\text{m}$ über 24 h bei 37°C in Kochsalzlösung der Konzentration 9 g/L ausgelaugt. Anschließend wurde der pH-Wert der Lösung bestimmt, die Lösung durch frische NaCl-Lösung ersetzt und der Vorgang wiederholt. Die Untersuchung wurde über mindestens zehn Tage durchgeführt. Für alle Polyphosphatgläser lag der gemessene pH-Wert unter 6,4. Anschließend wurde die Löslichkeit in Anlehnung an DIN ISO 719 (Wasserbeständigkeit von Glasgrieß bei 98°C) untersucht. Glasgrieß der

Kornfraktion 63 bis 315 μm wurde für 60 min in kochendem destilliertem Wasser ausgelaugt. Die resultierende Lösung wurde anschließend mittel ICP-OES (induktiv gekoppeltes Plasma - optische Emissionsspektrometrie) auf ihren Gehalt an Phosphor, Alkali, Erdalkali und Titan analysiert. Es zeigte sich, dass die Löslichkeit der Gläser durch Verringerung des Phosphatgehalts im Glas von 50 mol% auf 45 mol% um zwei Größenordnungen gesenkt werden konnte. Dennoch war die Löslichkeit aller Gläser dieser Gruppe sehr hoch, was auch Ursache für die niedrigen pH-Werte in physiologischer Kochsalzlösung war. Aus diesem Grunde wurde eine zweite Reihe von Gläsern mit niedrigeren Phosphatgehalten hergestellt.

In früheren Untersuchungen am Otto-Schott-Institut hatte sich ein Phosphat-Invertglas des Systems $\text{P}_2\text{O}_5\text{-CaO-MgO-Na}_2\text{O}$ mit einem Phosphatanteil von 37 mol% als geeignet für den Einsatz als resorbierbares Implantatmaterial herausgestellt. Bei Tierversuchen, die vor einigen Jahren in Zusammenarbeit mit der medizinischen Fakultät der Technischen Universität Dresden durchgeführt wurden, war gezeigt worden, dass das Glas Mg5 eine gute Biokompatibilität besitzt und im Körper in einem Zeitraum von über einem Jahr abgebaut wird, ohne Symptome für Entzündungsreaktionen zu zeigen. Ein Nachteil dieses Glases sowie von Invertgläsern allgemein ist die hohe Kristallisationsanfälligkeit im Vergleich zu Polyphosphatgläsern. Ziel war es daher, das Glas Mg5 durch geeignete Zusätze gegen Kristallisation zu stabilisieren.

Basierend auf einem Glas der Zusammensetzung 37 P_2O_5 - 29 CaO - 10 MgO - 24 Na_2O (Mg5) wurden verschiedene Gläser synthetisiert. Bis auf das Glas T5 wurde bei allen Gläsern der Phosphatgehalt konstant bei 37 mol% gehalten. Die anderen Komponenten wurden anteilmäßig gegen die Zusätze ersetzt. Untersucht wurden Gläser mit Zusätzen an Al_2O_3 , F^- , Fe_2O_3 , K_2O , SiO_2 , TiO_2 , ZnO und ZrO_2 . Die Konzentration der Zusatzkomponenten lag zwischen 1 und 10 mol%. Für das Glas T5 wurden die Konzentrationen sämtlicher anderer Komponenten anteilmäßig für den Zusatz von 5.45 mol% TiO_2 reduziert; der Phosphatgehalt lag bei 34.87 mol%. Von sämtlichen Zusätzen verminderte nur die Zugabe von TiO_2 deutlich die Kristallisationsanfälligkeit bereits bei Zugabe geringer Konzentrationen.

Die Kristallisationsanfälligkeit von Glas T5 war so stark herabgesetzt, dass Glasfasern aus einer Preform hergestellt werden konnten. Dazu wurde die Glasschmelze in eine

stabförmige Graphitform gegeben und im Kühllofen von etwa 500 °C auf Raumtemperatur abgekühlt. Der entstandene Glasstab hatte eine Länge von etwa 13 cm und einen Durchmesser von 10 mm. Die Glasfasern wurden bei Temperaturen zwischen 600 und 620 °C gezogen. Es wurden Glasfasern in einer Gesamtlänge von etwa 100 m erhalten, der Faserdurchmesser betrug um 125 µm. Glasfasern sowie die Reststücke der Preform zeigten bei Untersuchungen mittels Polarisationsmikroskop keine Anzeichen von Kristallisation.

Auch die Löslichkeit der Phosphat-Invertgläser wurde mittels pH-Untersuchungen und in Analogie zu DIN ISO 719 untersucht. Die meisten Gläser zeigten in physiologischer Kochsalzlösung einen pH-Wert zwischen 7 und 7,5. Nur für Gläser mit hohen TiO₂-Konzentrationen lag der Messwert niedriger. Dies ist allerdings auf den niedrigen Ausgangs-pH-Wert der physiologischen Kochsalzlösung in Verbindung mit der geringen Löslichkeit der Gläser zurückzuführen. Durch den niedrigen pH-Wert des zur Herstellung der Lösung verwendeten entionisierten Wassers lag der pH-Wert der physiologischen Kochsalzlösung bei etwa 5,8. Nach der Auslaugung bei 98 °C lagen die mittels ICP-OES bestimmten Werte für in Lösung gegangenes P₂O₅ deutlich unter denen der Polyphosphatgläser. Die Löslichkeit der Invertgläser war um drei Größenordnungen kleiner als die der Gläser mit 50 mol% P₂O₅ bzw. um eine Größenordnung geringer als die der Gläser mit 45 mol% P₂O₅.

Poröse resorbierbare Implantate sind interessant für die Regeneration von Knochendefekten, besonders als Ersatz für Spongiosa (Schwammknochen). Außerdem können poröse Implantate als Führungsschiene für die einwachsenden Knochenzellen (Osteoblasten) dienen. Aus diesem Grund wurden in einem Salz-Sinterverfahren poröse Glaskörper hergestellt. Dazu wurde das Glas auf Korngrößen um 10 µm aufgemahlen, anschließend mit Kochsalz der Kornfraktion 250 bis 315 µm im Volumenverhältnis 1:1 gemischt und in würfelförmigen Keramikformen bei Temperaturen um 500 °C für 30 min gesintert. Anschließend wurde das Kochsalz in Wasser herausgelöst. Die resultierenden porösen Glaskörper hatten eine Porosität von etwa 65 %, wobei etwa 15 % auf die Bildung von Mikroporen (< 60 µm) während des Sintervorgangs zurückzuführen waren. Die Makroporen zeigten Durchmesser zwischen 150 und 400 µm.

Für zwei poröse Invertgläser (Grundglas Mg5 und TiO₂-haltiges Glas T5) wurden Abbauprobversuche in simulierter Körperflüssigkeit (SBF) über bis zu 72 Wochen durchgeführt. Dabei wurde alle zwei Wochen die Lösung ausgetauscht. Alle vier Wochen wurden je Glaszusammensetzung zwei Proben entnommen, gereinigt, getrocknet und der Masseverlust bestimmt. Beide Gläser zeigten einen linearen Abbau über die gesamte Versuchsdauer. Allerdings war die Löslichkeit des TiO₂-haltigen Glases deutlich niedriger als die von Glas Mg5. Die Löslichkeit von Glas T5 bei 98 °C in destilliertem Wasser lag nur etwa 35 % unter der von Glas Mg5. Das Abbauverhalten der Gläser in SBF hingegen unterschied sich deutlicher. Über einen Zeitraum von 56 Wochen war das Glas Mg5 zu über 25 ma% gelöst. Glas T5 hingegen zeigte auch nach 72 Wochen keinen deutlichen Abbau, der Masseverlust lag bei etwa 2 ma%. Ob dieser deutliche Unterschied im Abbauverhalten in SBF auf die Bildung von Schutzschichten auf dem Glas zurückzuführen war, konnte bisher nicht geklärt werden. Die Glaszusammensetzung bzw. die Menge des zugesetzten TiO₂ muss somit im Hinblick auf eine geeignete Löslichkeit bei niedriger Kristallisationsanfälligkeit optimiert werden.

Ein weiteres Ziel dieser Arbeit war es, Komposite aus Phosphatgläsern geeigneter Löslichkeit und Polymeren auf Basis von Methacrylat-modifizierten Oligolactiden herzustellen. Die Kompositmaterialien wurden in Zusammenarbeit mit Innovent Technologieentwicklung Jena e.V. hergestellt, wo das Polymer entwickelt und synthetisiert wurde. Komposite mit offener Makroporosität sowie Komposite mit gerichteter Struktur durch Einbettung von Glasfasern in die Polymermatrix wurden auf ihre mechanischen Eigenschaften, ihr Abbauverhalten in wässrigen Medien sowie ihre Cytokompatibilität untersucht.

Das Polymersystem eignete sich sehr gut sowohl zur Herstellung poröser Polymerkörper als auch zum dünnflächigen Beschichten poröser Glassinterkörper. Die Druckfestigkeit der porösen Sinterkörper konnte durch eine Beschichtung der inneren Porenoberfläche unter Beibehaltung der offenen Porosität um eine Größenordnung erhöht werden. Durch Herstellung von Polymerkörpern mit eingebettetem Glaspulver konnten poröse Körper mit noch deutlich höherer Druckfestigkeit erhalten werden. Im Gegensatz zu den porösen Glassinterkörpern lassen sich die Komposite gut mechanisch bearbeiten wie z.B. schneiden oder schleifen. Aus den Glasfasern und dem Polymer wurden Faserkomposite hergestellt, die im Gegensatz zu den porösen Materialien

elastisches Verhalten zeigten. Bei Biegebruchuntersuchungen ergab sich eine Bruchfestigkeit von 115 MPa. Die Faserkomposite zeigten keinen glatten Bruch sondern Delaminierungen und Rissverzweigungen.

Das Abbauverhalten der porösen Kompositmaterialien wurde in SBF untersucht, wie für die porösen Glassinterkörper bereits beschrieben. Es zeigte sich, dass der Masseverlust der Polymerkörper zu Beginn, d.h. über die ersten vier Wochen, sehr groß war (bis zu 13 ma%). Anschließend zeigten die Materialien einen linearen Abbau über die restliche Versuchszeit. Offensichtlich wird das Polymer deutlich schneller abgebaut als die Glaskomponente.

Bei ersten Untersuchungen zur Zellverträglichkeit zeigten weder die verwendeten Gläser noch das Polymer Anzeichen von Cytotoxizität. Zur Untersuchung der Cytokompatibilität einiger ausgewählter Phosphat-Invertgläser wurden Proliferationstests mit osteoblastenähnlichen MC3T3-E1.4-Zellen und odontoblastenähnlichen Zellen (DPSCs, *dental pulp stem cells*) durchgeführt. Bei Untersuchungen an polierten Gläsern mit MC3T3-E1.4-Zellen über 24 h und 72 h zeigte sich kein Einfluss der Glaszusammensetzung. Die Zellen proliferierten auf allen Materialien. Allerdings waren die Zellkonzentrationen niedriger als auf der Kontrollprobe ohne Glas. DPSCs proliferierten nur auf Glas T5, das die niedrigste Löslichkeit hatte, eindeutig. Die Proliferation von MC3T3-E1.4-Zellen auf porösen Sinterglaskörpern war deutlich geringer als auf polierten Gläsern. Nach 24 h war nur auf Glas T5 die Zellkonzentration eindeutig größer als die ausgesäte Zellkonzentration. Jedoch proliferierten die Zellen über 72 h eindeutig, so dass auf allen untersuchten Proben die Zellkonzentration nach drei Tagen deutlich über der ausgesäten Konzentration lag. Offensichtlich verhinderte die poröse Struktur zu Beginn das Adhärenzieren einiger Zellen, jedoch nicht die Zellproliferation auf den Materialien.

Zur Bestimmung der Zellkompatibilität der Kompositmaterialien wurde die Zellvitalität mittels Tot/Lebendfärbung untersucht. Als Proben dienten poröse Polymerkörper mit eingebettetem Glaspulver (Mg5 und T5) sowie poröse Polymerkörper mit CaCO₃ als Kontrolle. Die Probekörper wurden mit MC3T3-E1-Preosteoblasten besiedelt. Im Ergebnis der Cytotoxizitätstests wurde gefunden, dass nach einem Tag und nach vier Tagen auf den Probekörpern aus Polymer/Calciumcarbonat- und Polymer/Phosphatglas-

(Mg5 und T5) Kompositen weniger als 5 % tote Zellen vorhanden waren. Die Zellen wuchsen als adhärenente Zellen auf der gesamten Oberfläche gleichmäßig an und besiedelten auch Poren und Hohlräume der Proben. Nach vier Tagen lag eine deutlich höhere Zelldichte vor als nach einem Tag, d. h. die Zellen proliferierten. Somit konnte in diesem Test eine sehr gute Zellverträglichkeit der Trägermaterialien nachgewiesen werden.

Abschließend kann gesagt werden, dass wasserlösliche Phosphatgläser vielversprechend für die Herstellung abbaubarer Implantatmaterialien sind. Die untersuchten Polyphosphatgläser reagierten jedoch in wässriger Lösung zu sauer für einen Einsatz im menschlichen Körper und ihre Löslichkeit war zu hoch. Da jedoch die Gläser aufgrund ihrer geringen Kristallisationsanfälligkeit interessant für die Herstellung von Glasfasern sind, sollte untersucht werden, ob die Löslichkeit nicht durch geeignete Zusätze, wie z.B. Erhöhung der TiO_2 -Konzentration, herabgesetzt werden kann. Die untersuchten Invertgläser zeigten in ersten Zellversuchen eine gute Biokompatibilität. Ihre Löslichkeit lag deutlich unter jener der Polyphosphatgläser. Allerdings wiesen die Invertgläser eine deutlich höhere Kristallisationstendenz auf. Durch geeignete Zusätze wie z.B. TiO_2 kann die Kristallisationsanfälligkeit zwar vermindert werden. Gleichzeitig wird jedoch die Löslichkeit drastisch herabgesetzt. Die Menge an Zusätzen muss daher optimiert werden.

Durch die Kombination von Phosphatgläsern und Polymeren in Werkstoffverbunden konnten Implantatmaterialien mit deutlich verbesserten mechanischen Eigenschaften erhalten werden. Die Druckfestigkeit der porösen Komposite lag deutlich über jener der porösen Glassinterkörper. Durch Einbetten von Glasfasern in die Polymermatrix wurden Komposite mit gerichteten Strukturen erhaltenen. Diese Werkstoffverbunde sind beispielsweise interessant für die Entwicklung von Nägeln und Schrauben als temporäre Osteosynthesematerialien.

Da außerdem die Zelluntersuchungen an Gläsern und Kompositen eine gute Biokompatibilität der Materialien zeigten, kann abschließend gesagt werden, dass sowohl die untersuchten Phosphat-Invertgläser als auch das Polymer auf Basis Methacrylat-modifizierter Oligolactide vielversprechend für die Entwicklung abbaubarer Implantatmaterialien sind.

1 Introduction and objective

Materials which are in direct contact with human tissue are known as biomaterials. The use of certain materials as surgical implants is not new. Substitutions of bone parts for repairing serious damages in the human body have been reported for centuries [1,2]. However, general success was only achieved in the course of the 20th century. Leading thought in the development of implant materials is to improve life conditions for those who are subject to malfunctions caused by accidents, age or birth defects by reconstructing damaged or missing parts of the human body.

Biomaterials can be divided into different groups according to their biocompatibility [1]. Biocompatible materials release substances only in non-toxic concentrations. They do not cause negative reactions of the body and are not rejected by the body tissue. Bioactive materials provoke positive reactions of the tissue, e.g. the formation of bone on the implant tissue interface. Resorbable implants are hydrolytically or enzymatically degradable, i.e. they eventually disappear after implantation. Characterization of the biocompatibility of implant materials is essential. As animal tests cannot be carried out in an early stage of materials development, *in vitro* cell tests provide an alternative.

The ideal implant material for bone replacement or fracture fixation would be biocompatible, chemically related to the surrounding tissue, and would be degraded at the same rate at which new tissue was formed. The rate of resorption should not exceed the rate of bone formation, and the rate at which the implant weakens should closely match the increase in tissue strength to ensure a gradual stress transfer. By using implant materials which promote bone regeneration the removal of osteosynthesis materials like plates and screws could be avoided. This would be a substantial benefit both economically and to the patient being treated.

Metals and alloys are commonly used for internal fracture fixation to promote bone union at the fracture site. But while these metal devices provide stability during the healing process they are much stiffer than the bone and therefore often require removal after bone healing.

Ceramics, glasses and glass-ceramics as implant materials have opened new possibilities in medicine as their chemical composition can be adjusted to obtain the desired properties [2-9]. Applications of glass-ceramics also include biocompatible and machinable glass-ceramics as long-term stable implants [3] or glass-ceramics with oriented structures [8]. Since the late 1960s the biocompatibility of a range of silica-based glasses (Bioglass[®]) has been demonstrated [10-15]. This material is stable to hydrolysis because of its high silica content but it promotes osteoblast cell attachment and proliferation.

Phosphate-based glasses can provide an alternative to silica-based glasses [16-18]. They are water-soluble and the degradation rate can be adjusted by altering their composition. They therefore offer great possibilities for application as temporary bioresorbable implant materials. Their good processibility, e.g. low melting and glass transition temperatures, and their adjustable solubility makes them potentially useful for promoting the regeneration of soft as well as hard connective tissue. Recent work focused on polyphosphate glasses with phosphate concentrations between 40 mol% and 50 mol% [19-23]. Vogel *et al.* developed phosphate invert glasses for medical applications which have been tested successfully *in vitro* and *in vivo* [24-26]. A drawback of these invert glasses is their relatively high crystallization tendency compared with polyphosphate glasses.

Organic polymers are extensively used as temporary implants in surgery, e.g. as bioabsorbable polymeric pins. Polylactides and polyglycolides are commonly used resorbable polymers but recent work also focused on other degradable organic polymers [27-29]. While glasses can provide good chemical properties, their mechanical properties can be disadvantageous. Even if they possess the correct mechanical properties for bone augmentation, their use is hindered by the brittle nature and difficulties in manufacturing patient-specific parts. The lack of sufficient strength can be compensated by the production of composites with organic polymers. Composites of glasses and organic polymers also provide improved machinability [12,30-35]. Composite materials with oriented structures can be obtained by embedding glass fibers or whiskers into a matrix of organic polymers, if required followed by an alignment procedure.

Objective

The aim of this study was the development and characterization of novel phosphate glasses and composites for use as bioresorbable bone replacement or fracture fixation materials and degradable scaffolds in tissue engineering. Bone regeneration by use of degradable implants or fixation devices is a promising approach in orthopedic surgery. Absorbable implants obviate the need for surgical removal. They allow for the gradual transfer of load to the healing bone, thereby eliminating the problem of stress shielding. The goal is the development of resorbable implant materials which provide sufficient strength and degrade in a timely accordance with bone healing or formation.

Phosphate-based glasses are an interesting range of materials, as they may dissolve completely in water depending on the chemical composition. Furthermore, the solubility can be tailored to suit the end application. Glasses of the system P_2O_5 -CaO-MgO- Na_2O with suitable additives were to be synthesized with focus on optimized solubility. This glass system allows variation of properties such as solubility or crystallization tendency by only minor chemical adjustments. The components released from the glasses during dissolution should consist of substances which naturally exist in the human body. Hence, good biocompatibility and low toxicity were expected. The degradation rate also affects cell adhesion and subsequently cell proliferation. Optimization of the degradation rate facilitates cell proliferation and improves biocompatibility and bioactivity of the material. Therefore, solubility of the glasses in aqueous media was to be investigated and adjusted.

In comparison with silica based glasses some phosphate glasses show a relatively high crystallization tendency. However, for use as resorbable implant materials, glasses which show a uniform dissolution are favored. To improve producibility of the glasses and, for example, enable the production of glass fibers, the crystallization tendency needs to be controlled as well. Hence, glasses should show neither phase separation nor crystallization.

Composite materials made of phosphate glasses and degradable organic polymers based on methacrylate-modified polylactides were to be produced in cooperation with Innovent Technologieentwicklung e.V., Jena. Composites with an open interconnective porosity are of interest for resorbable implants in general and for replacement of

cancellous bone in particular. By contrast, composites with aligned structures are interesting for the development of degradable fracture fixation devices because of their good mechanical properties. Composite materials should show sufficient strength for application as implant material. Hence, mechanical properties of the composite materials (compression or bending strength, respectively) needed to be determined and adjusted. For degradable biomaterials, control of solubility and degradation rate is a key issue. Therefore, long-term degradation behavior of the composite materials was to be evaluated.

For biomaterials in general, biocompatibility tests represent a major part of the characterization procedure. Implant materials should promote osteoblast proliferation and differentiation. Therefore, investigations on the applicability of the glasses and composites as implant materials or tissue engineering scaffolds were to be carried out using *in vitro* techniques.

2 Theory and literature review

2.1 Bone and hard tissue

The mechanical function is one of the main functions of the human skeleton. Skeletal elements protect vital internal organs from external forces and provide internal support. The composition of bone depends on species, age, sex, the specific bone, the type of bone (cortical or trabecular), and whether or not the bone is affected by disease. About 70 wt% of the bone are formed by inorganic, i.e. mineralized, components, the remaining 30 wt% consist of organic matter (cells and organic matrix) [1]. The main protein of the matrix is collagen type I. It represents about 70 to 90 % of the non-mineralized components of bone [36]. The mineral component of mature bone is made of calcium phosphates, the most important of which is hydroxyapatite, $\text{Ca}_{10}(\text{PO}_4)_6(\text{OH})_2$, with a calcium deficiency ranging between 5 and 10 %. The bone apatite is characterized by carbonate substitutions and a certain degree of loss of crystallographic order; it also contains small amounts of fluorine, chlorine, sodium and magnesium. The combination of different constituents (i.e. the crystals of the mineral phase (apatite), the fibrils of type I collagen and water), their different mechanical properties and the different relative proportions of each component make bone a true composite material [2,36].

Bone architecture can be divided into two categories, compact bone (or cortical bone) and trabecular cancellous bone. The main difference between the two types is their porosity. The ratio between the volume of bone tissue and the volume occupied by pores is large in compact bone while the inverse relationship applies to cancellous bone. The compact bone is a dense tissue of a continuous solid mass in which the only empty spaces are meant for blood vessels and bone cells or osteocytes. The trabecular bone consists of a network of septa or trabeculae occupied by bone marrow.

Bone is able to undergo spontaneous regeneration and to remodel its micro and macro structure. This is accomplished through osteogenic (bone forming) and osteoclastic

(bone removing) processes. Bone can adapt to a new mechanical environment by changing the equilibrium between osteogenesis and osteoclasts [37]. Osteoblasts are specialized cells which are characteristic of bone, belonging to the more general category of fibroblasts, which are cells typical of connective tissue of any organ. Osteoblasts play a prominent role in both the formation and calcification process of bone matrix. The morphology of an osteoblast is subject to variation depending on its functional state. Osteoblasts are localized particularly in the periosteum membrane which envelops the external part of medium and long bones and in the endosteal membrane, which develops over the inner bone wall of the medullary canal. Osteoblasts, enclosed within their osteoid shell inside bone matrix, are converted to osteocytes when reaching the end of their activity. Osteocytes represent the population of stable living cells of bone and have the task of keeping bone in the form of living tissue [2].

The elastic (Young's) modulus of cortical bone ranges from 17 to 24 GPa, depending upon the age and location of the specimen [38]. Due to its structure, bone exhibits effects of anisotropy in the tensile and compressive strengths. Tensile and compressive strengths of human bone tissue in axial directions are about 130 MPa and 200 MPa, respectively. The strengths in tension and compression in an angle of 90° with respect to the long axis of the bone are 50 MPa and 130 MPa, respectively [36,39,40].

2.2 Implant materials

A wide diversity and sophistication of materials is currently being used in medicine and biotechnology. Only a few decades ago, common commercial polymers and metals were used in implants and medical devices. Over the years, the need for new and improved materials, implants and devices was recognized.

Metallic implants have a significant clinical and economic impact on the biomaterials field due to their favorable mechanical properties. Applications include joint prostheses, instrumentation devices and bone replacement materials. Besides orthopedics, metals are used in oral and maxillofacial surgery (e.g. dental implants, craniofacial plates and screws) and cardiovascular surgery (e.g. parts of artificial hearts, pacemakers) [2,41]. The use of pure metals is limited because of their softness and tendency to corrode

quickly. To overcome these limitations, most metals are commonly used as alloys, e.g. titanium alloys used in screws, joint components and nails and stainless steel found in fracture plates and vascular stents [42].

Ceramics, glasses and glass-ceramics have been essential in medical industry for diagnostic instruments, flasks and fiber optics. Ceramics are also widely used in dentistry as restorative materials. For use as implants, relatively few ceramics, glasses and glass-ceramics have achieved clinical success [3,6,43]. While metallic implant materials provide good mechanical properties, it can be important to avoid or reduce contact of their surface with the surrounding tissue. Therefore there is a major interest in coating the surface of metallic implants. Materials used in prosthesis coating include plasma-sprayed alumina (Al_2O_3) and hydroxyapatite coatings. As these, however, do not possess elastic properties resembling those of metals, recent research also focused on glasses that can be enameled onto alloys yielding a reliable coating while retaining bioactivity [2,13].

Porous bioactive glasses appear to provide the possibility of hosting tissue offshoots in the cavities into which they penetrate, thereby establishing bonds that in the corresponding non-porous glasses would be developed only superficially. Histological investigations have shown that bone in-growth leads to intra-membranous ossification on porous glasses. Porous bioactive glasses have been used as coating materials but did not meet the same percentage of success as compact coatings [2]. Porous inorganic or hybrid inorganic-organic matrices and scaffolds can be produced with controlled rates of resorption. Hydroxyapatite (HA) powders and blocks have applications in bone surgery, e.g. to fill in defects. Since porous ceramics are brittle, attempts have been made to increase their toughness by combining them with polymers. Coating porous HA externally or internally with poly(lactic acid) or polymethyl methacrylate increased the strength of the porous scaffolds considerably [44,45].

2.2.1 Internal fracture fixation

The main goals of fracture treatment are rapid healing and restoring function without general or local complications. In the selection of treatment method, excessive motion between bone fragments is to be avoided. Common treatments include non-surgical or surgical methods. Examples of non-surgical treatments are immobilization with casting

(plaster or resin) and bracing with a plastic apparatus. The surgical treatments are divided into external fracture fixation, which does not require opening the fracture site, or internal fracture fixation, which requires opening the fracture. With external fracture fixation, the bone fragments are held in alignment by pins placed through the skin onto the skeleton. With internal fracture fixation, the bone fragments are held by wires, screws, plates or other devices (Figure 2.1) [37,46,47].

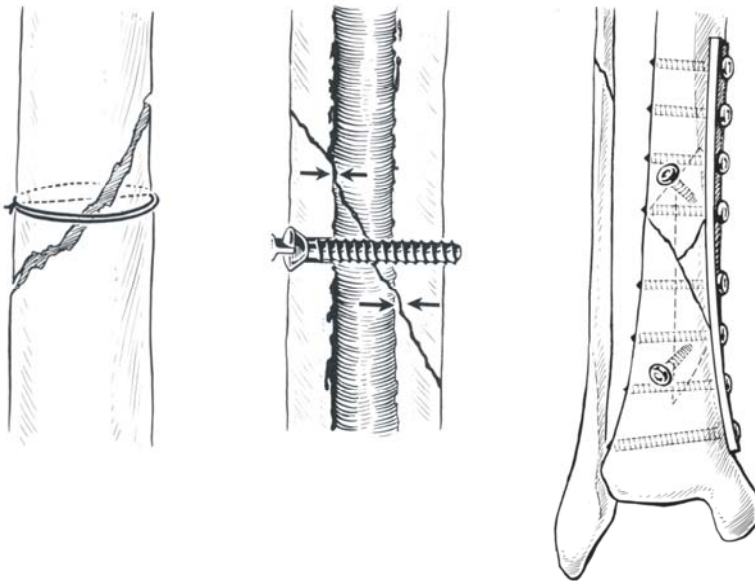


Figure 2.1: Internal fracture fixation using wires (left), screws (center and right) and plates (right) (after Matzen [46])

Internal fixation devices should meet the general requirements of biomaterials, i.e. biocompatibility, sufficient strength and corrosion resistance, and should provide a suitable mechanical environment for fracture healing. From this perspective, stainless steel, cobalt-chrome alloys and titanium alloys are the most suitable materials. However, most internal fixation devices persist in the body after the fracture has healed, often causing discomfort and requiring removal. Biodegradable polymers (cf. Chapter 2.4) have been used to treat minimally loaded fractures, thereby eliminating the need for a second surgery for implant removal [48].

2.2.2 Degradable implants

Different terms (e.g. degradable, absorbable, resorbable) are used to indicate that a given material or device will eventually disappear after being introduced into a living organism. Since a degradable implant does not have to be removed surgically once it is

no longer needed, degradable materials are of value in short-term applications that require only the temporary presence of an implant. They reduce the potential for long-term implant complications associated with foreign materials. Biodegradable materials, however, need to meet more stringent requirements than non-degradable materials. Key issues include the biocompatibility, the possibility of leaching toxic contaminants (e.g. residual monomers and stabilizers) and the potential toxicity of degradation products and metabolic residues [49,50].

If a natural tissue is weakened by disease, injury, or surgery (e.g. a healing wound or broken bone) it requires artificial support. Sutures and bone fixation devices (e.g. bone nails, screws or plates) would be the corresponding applicances. In these instances, the degradable implant would provide temporary mechanical support until the natural tissue healed and regained its strength. The degradation rate of the implant needs to be adjusted to the healing of the surrounding tissue. For example, if a material is designed for fracture fixation the rate of resorption should not exceed the rate of bone formation, and the rate at which the implant weakens should closely match the increase in tissue strength to ensure a gradual stress transfer. Biomaterials that enhance the regeneration of natural tissues would be desirable. Regeneration of tissue would include restoration of structure and function as well as restoration of metabolic and biochemical behavior and biomechanical performance. This represents one of the major challenges in the design of a temporary scaffold [44,48,51-53].

In spite of extensive research efforts only degradable polymers are currently used to any significant extent in the formulation of degradable implant materials (cf. Chapter 2.4). Examples of biodegradable products which have been used successfully in orthopedic surgery include resorbable sutures, pins, screws and some bone plates used for spine fusion. The variety of available and suitable biodegradable materials is still too limited to cover the wide range of materials properties needed for producing implants and other biomedical devices. Thus, considerable research effort is being put into the development and modification of materials and formulations. One key feature is the creation of well-defined hierarchical levels of organization. Many biocomposite systems have at least one distinct structural feature at the molecular, nanoscopic, microscopic and macroscopic scales. These levels are organized into a hierarchical composite system designed to meet a complex spectrum of functional requirements. Bone and wood are

good examples of natural composite materials of a hierarchical structure. As synthetic composites increase in complexity, they are known to function at higher levels of performance. However, the connection between hierarchical design and final properties still needs to be understood in real products [49,53]. The lack of available biomaterials suitable for all the required needs has forced the development of composite biomaterials. One advantage of composites is that they can be designed, within defined limits, to tailor their mechanical or physical properties depending on the selection of their components (cf. Chapter 2.4.1).

2.3 Glasses and glass properties

2.3.1 Glass structure

Oxides used in glasses can be divided into three groups: network forming oxides, network modifying oxides and intermediate oxides. SiO_2 , B_2O_3 and P_2O_5 are the primary glass formers, they can form single component glasses. By volume, silica based glasses are the most common. Silicon dioxide has a high melting point, so components are added to reduce the processing temperatures. Phosphorus pentoxide is very reactive and hygroscopic, so by adding other components its durability can be increased. Thus, the reasons for adding other components depend on the network former used [4,18]. Structures of the network forming silicate and phosphate tetrahedra are shown in Figure 2.2.

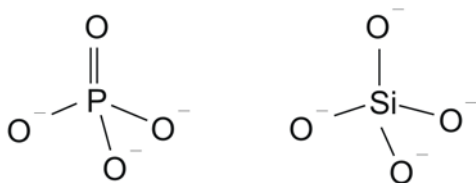


Figure 2.2: Basic phosphate and silicate tetrahedra in glass structures

The structure of phosphate glasses is usually described in Q^n groups. Q^n groups are XO_4 tetrahedra (such as PO_4 or SiO_4); n indicates the number of bridging oxygen atoms and depends on the degree of condensation. In condensed phosphates three main building groups exist, which are the Q^1 or end unit, the Q^2 or middle unit and the Q^3 or branching unit. Isolated orthophosphate groups are accordingly denoted as Q^0 groups. The PO_4 tetrahedra can be attached to a maximum of three neighboring tetrahedra forming a

three-dimensional network as in vitreous P_2O_5 [22,54-63]. The addition of metal oxide leads to a depolymerization of the network with metal ions breaking the P-O-P links and creating non-bridging oxygen atoms in the glass. However, the modifying cations can provide ionic cross-linking between non-bridging oxygen atoms of two phosphate chains. This cross linking can increase the bond strength and chemical durability of these glasses. Thus, the properties of phosphate glasses are directly related to their chemical composition. Sodium and calcium are typical network modifiers and are most commonly used in binary phosphate glasses [64,65].

Corresponding to their structure, phosphate glasses can be divided into three groups: acidic phosphate glasses (ultraphosphate glasses) consist of three-dimensional networks of PO_4 tetrahedra which are connected via bridging oxygen atoms at the three corners of most tetrahedra. Therefore, merely glasses with more than 50 mol% P_2O_5 , i.e., with a molar metal oxide fraction $x < 0.5$ (cf. Equation 3.2), form two-dimensional phosphate networks. Polyphosphate glasses containing 50 mol% P_2O_5 or less ($x \geq 0.5$) are formed by PO_4 tetrahedra chains or rings possessing different chain lengths. By contrast, phosphate invert glasses (pyrophosphate glasses, $x \geq 0.667$) are formed by ortho- (PO_4^{3-}) and pyrophosphate ($P_2O_7^{4-}$) groups exclusively, where isolated orthophosphate groups are present in glasses with metal oxide fractions $x \geq 0.75$. In these cases the glassy state is neither caused by a relatively stiff network nor by entangled chains but by the interaction of cations and phosphate groups (Figure 2.3) [56,57].

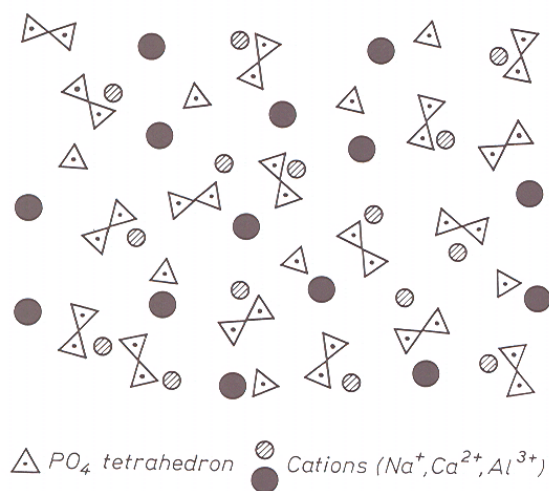


Figure 2.3: Schematic of the invert glass structure (after Vogel [4])

2.3.2 Solubility and degradation

In contrast to many silicate or borosilicate glasses, the importance of phosphate glasses is relatively small. Especially due to their high solubility, phosphate glasses are not as commonly used. However, from a biomedical point of view, the fact that phosphate glasses dissolve completely in aqueous media is a great advantage and offers various possibilities for their application as degradable implant materials. A significant amount of work has focused on the dissolution behavior of polyphosphate glasses in the ternary system P_2O_5 -CaO- Na_2O . In these studies solubility was tested in different ways. In some cases cell response was investigated as well and is discussed in Chapter 2.5.1.

Bunker *et al.* [66] prepared glasses with chemical compositions of $50 P_2O_5 - x CaO - (50-x) M_2O$ where $M = Na, Li$ and x is 10 and 20 mol% respectively. To characterize the dissolution behavior of the glasses, they did pH measurements on glass powder as well as leaching experiments on glass disks. They determined on the one hand weight loss and on the other hand measured dissolved ions using ICP-OES. The durability of the glasses was found to be very sensitive to the glass composition. The more alkali the glass contained, the lower the durability. Solution analysis indicated that at all times all of the phosphate glasses dissolved uniformly. There was no selective alkali leaching as observed in silicate glasses. Leaching rates in deionized water lay between 10^{-7} and 10^{-5} g/(cm² min). Tests also revealed a strong pH dependence for dissolution rates. The glasses investigated were most durable from pH 5 to pH 9. In acidic solutions the rate of dissolution increased dramatically. Dissolution rates also increased with temperature regardless of the pH of the solution. In contrast to many silicate glasses the dissolution rates of the phosphate glasses investigated showed no dependence on the ratio of the surface area of the glass to the volume of the leachant. One reason for that is according to the authors that the uniform dissolution of the glasses does not result in the extreme pH changes induced by the selective leaching of silicate based glasses. Although the pH changed slightly during phosphate glass dissolution, it remained within the range where the dissolution rate is roughly constant. For the dissolution mechanism the authors suggest a simple hydration of entire phosphate chains rather than chain hydrolysis. This model can explain why the phosphate glasses dissolved faster in acidic solutions. In acids, phosphate chains are protonated, which disrupts ionic cross-links between chains. Water can then penetrate the glass faster, leading to rapid chain hydration and uniform

dissolution. In basic leaching solutions, crystalline precipitates appeared on the glass surface after several days of leaching. X-ray powder diffraction patterns revealed that they were crystals of hydroxyapatite, $\text{Ca}_5(\text{PO}_4)_3\text{OH}$, which is known to be the least soluble calcium orthophosphate compound in basic solution.

Franks *et al.* [67] investigated ternary phosphate glasses with phosphate contents fixed at 45 mol%. Glass disks with compositions in the range $45 \text{ P}_2\text{O}_5 - x \text{ CaO} - (55-x) \text{ Na}_2\text{O}$ with x between 12 and 36 mol% were leached in distilled water and Hank's buffered saline solution (HBSS) over up to 8 weeks. Weight loss per unit area and pH were measured to characterize the solubility. Solubility showed a strong dependence on glass composition and the medium in which the test was carried out. Increasing CaO content resulted in decreased solubility. Solubility in distilled water lay between 10^{-5} and $10^{-4} \text{ g}/(\text{cm}^2 \text{ h})$ but was much lower in HBSS. pH values during dissolution in distilled water varied between 5 and 9.

Ahmed *et al.* [20,68] investigated the solubility of bulk glasses and glass fibers of phosphate glasses with a chemical composition in a similar range. They prepared various compositions based on the $\text{P}_2\text{O}_5\text{-CaO-Na}_2\text{O}$ glass system with phosphate contents of 55, 50 and 45 mol%, CaO contents of 40, 35 and 30 mol% and Na_2O concentrations of 25, 20 and 15 mol%. They measured the weight loss per unit area of glass disks in distilled water at 37°C and did pH and ion measurements over up to 8 days. Again, a decrease in solubility with increasing CaO content was seen. However, this dependence on the composition was much stronger for glasses with 45 and 50 mol% P_2O_5 respectively than for glasses with a phosphate content of 55 mol%. Glasses with a P_2O_5 content fixed at 45 mol% showed an initial increase in pH. The values almost approached neutral from a starting value of around 6 then declined over time to a value of about 6.4. For glasses with phosphate contents of 50 and 55 mol% respectively, the starting pH is around 5.5 and 5 and a gradual decrease of pH over time is observed to between 4.5 and 2.5 depending on the CaO concentration of the glasses. Phosphate glass fibers showed a higher solubility than the bulk glass due to the increase in surface area.

Franks *et al.* [21] also tested solubility behavior and cell proliferation for glasses in the system $45 \text{ P}_2\text{O}_5 - (32-x) \text{ CaO} - x \text{ MgO} - 23 \text{ Na}_2\text{O}$. MgO was used as a CaO substitute in

glasses investigated in [67]. Tests were carried out over up to 34 days. pH measurements were carried out in distilled water and showed a significant increase in pH from a starting value of around 5 up to neutral and then followed by a slow decline to around 6. This is similar to the pH change found in the ternary system [67], however, the glass with the highest MgO content showed a smaller decrease in pH even at longer periods of time. Degradation experiments were carried out in distilled water at 37 °C determining the weight loss per unit area of glass disks. By systematically replacing CaO with MgO, the solubility curves lost their exponential nature and the solubility was reduced.

Knowles *et al.* [69] determined the solubility of glasses in the system P₂O₅-CaO-Na₂O-K₂O; P₂O₅ concentration was 45 mol%, potassium oxide concentrations were between 0 and 25 mol%. The authors tested the solubility of glass disks in distilled water at 37 °C and determined the weight loss per unit area as described in [67]. pH values were measured as well over a period of 30 days and showed an initial increase to values of 7 to 8 and then a steady decrease with time to values of around 5.

Results of the solubility tests showed an increase in solubility with increasing K₂O content. This also explained the results of the pH measurements, as with increasing solubility, irrespective of how the solubility was varied, there will be an increase in the ion levels in solution which results in a change of pH. According to the authors, addition of potassium oxide to the glasses increases the solubility because of the ionic radius of potassium. Having a larger ionic radius in comparison to sodium, it has a larger disrupting effect on the structure as a network modifier and thus will weaken the network. Although the glass system investigated was a mixed alkali system, the authors did not find any correlation of the solubility behavior with the mixed alkali effect (mobile ion effect).

Clément *et al.* [54] investigated the structural changes of two ternary phosphate glasses (P₂O₅-CaO-Na₂O with P₂O₅ contents of 44.5 and 50 mol% respectively) during their dissolution in simulated body fluid (SBF), which chemical composition is similar to that of human blood plasma. Studies revealed the formation of a hydrated layer during glass dissolution. Raman spectroscopy and X-ray analysis showed that this layer was composed of calcium orthophosphate groups. This indicated the formation of an apatitic

phase at the surface of the glass. SBF seemed to play an important role in the formation of this layer as it could not be detected during dissolution in distilled water. These observations can be related to the dissolution mechanisms described by Bunker *et al.* [66].

Navarro *et al.* [22,23] investigated a similar glass system in which sodium oxide was partially replaced by titania ($44.5 \text{ P}_2\text{O}_5 - 44.5 \text{ CaO} - (11-x) \text{ Na}_2\text{O} - x \text{ TiO}_2$ with $x = 0, 3, 5, 8$). Solubility tests of glass cubes in deionized water and SBF showed that the solubility of the glasses in SBF was lower than in deionized water. This was on the one hand due to the fact that SBF is a concentrated solution with respect to the different ions present in the glass. On the other hand the glasses decreased the pH in deionized water from 7 to 5.8 whereas the pH in SBF, which is a buffered solution, stayed constant. In both media the solubility of the glasses decreased as the titania content increased; the weight loss of the glasses was already greatly reduced with the incorporation of only 3 mol% TiO_2 . Environmental electron scanning microscopy (ESEM) experiments revealed that for the same period of time, the glass without TiO_2 presented a surface much more degraded than the titania containing glasses.

The incorporation of Fe_2O_3 in phosphate glasses was investigated as well. Ahmed *et al.* [70] investigated the glass system $\text{P}_2\text{O}_5\text{-CaO-Na}_2\text{O-Fe}_2\text{O}_3$ which is similar to those described in [20,68]. As biocompatibility studies had revealed that the glasses and fibers in the ternary system were too soluble for cell attachment and proliferation, sodium oxide was partially replaced by Fe_2O_3 . Degradation behavior was tested using glass disks and fibers. Incorporation of Fe_2O_3 gave lower dissolution rates resulting in an improvement of biocompatibility (cf. Chapter 2.5.1). The decrease in solubility was attributed to the replacement of P-O-P bonds in the glass by Fe-O-P bonds, and to the strong cross-linking of the phosphate chains by the iron ions. However, it was not clear if the iron was incorporated in form of Fe(II) or Fe(III). Lin *et al.* [71] investigated four ternary glass compositions in the system $\text{P}_2\text{O}_5\text{-CaO-Fe}_2\text{O}_3$ with phosphate contents between 56.9 and 73.5 mol% and iron oxide concentrations between 3.6 and 16.9 mol%. Glass rods were kept in buffered solutions of pH 7.4, 6.4 and 5.4 at 37 °C and weight loss per unit area was determined. The dissolution rate of calcium phosphate glass was decreased by the addition of iron oxide. The dissolution rates of the iron-

containing phosphate glasses were influenced by the pH of the buffer solution. These results agree with the ones obtained by Ahmed *et al.* [70].

Vogel *et al.* [72] tested the solubility of a wide range of glasses in the system P_2O_5 -CaO-MgO-Na₂O-TiO₂-Al₂O₃. In analogy to DIN ISO 719 [73] glass of the grain fraction from 63 to 315 μm was soaked for 60 min in 50 mL deionized water (initial pH 5.8) and diluted hydrochloric acid (HCl, initial pH 4) at 98 °C. The resulting solutions were analyzed using ICP-OES. Results show that in contrast to conventional silicate glasses, phosphate glasses show an increase in dissolution rates while decreasing the pH even to a relatively small extent (from pH 5.8 to pH 4). The dissolution behavior could be controlled to a large extent by the glass composition. The chain structure of metaphosphates was less stable against chemical attacks than in invert glass structure. The incorporation of alumina or titania lead to the stabilization of the invert glass structure by linking mono- and diphosphate groups by AlO_4 , TiO_4 or TiO_6 structural units. This affects the dissolution rates of invert glasses in acidic media to a larger extent than those of metaphosphate glasses. The chemical attack was decelerated after a comparatively short time and a relatively stable state was reached. According to the authors, the formation of protective layers may play an important role. According to Walter *et al.* [57] decreasing the P_2O_5 content makes the phosphate glasses more resistant to moisture attack but restricts the glass formation area.

2.3.3 Phosphate glass fibers

The excellent properties of glass fibers have already opened a broad field of applications. As an example, the high tensile strength of glass fibers has provided fiber-reinforced plastics as a group of new materials with very low weight for highest mechanical and chemical stresses. There is high interest in bioactive fibers for tissue engineering scaffolds. However, crystallization of glass fibers can have deleterious effects on fiber production and mechanical properties [74]. Furthermore, crystallization of phosphate glass fibers influences solubility and hence degradation rate and cell response. Therefore attempts have been made to avoid crystallization by alternative processing methods or by altering the melt composition.

Not only the properties but also the structure of the glass fibers differ from that of the bulk glass (cf. above). Strong anisotropies resulting in smaller Young's and shear

moduli have been reported for alkali metaphosphate glass fibers [75-77]. Alkali metaphosphate glasses are more easily orientable in contrast to silicate glass fibers due to the chain structure of the phosphate glasses. The fibers are composed of long chains of PO₄ tetrahedra with two bridging oxygen atoms (Q² units), while the double-bonded and the oxygen atoms connected with alkali ions are acting as non-bridging oxygen atoms. The axes of these chains have a strong preference for lying along the fiber axis direction.

In contrast, alkaline earth metaphosphate glass fibers are not composed by long double chains, connected by the bivalent alkaline earth ions, but form a very strong cross-linked chain structure, which has more similarity with a network of borates and silicates than with the linear chain structure of alkali metaphosphate glass fibers [75]. The bivalent alkaline earth ions form junctions with relatively high bonding forces between the phosphate chains. In this way a partly three-dimensional network is formed, however, not in such a strict manner as in silicate glasses or glass fibers.

Ahmed *et al.* [68] developed ternary calcium sodium phosphate fibers with 45, 50 and 55 mol% P₂O₅, respectively, for use as cell delivery vehicles for cell transplantation purposes. Glass fibers were obtained from the 50 and 55 mol% P₂O₅ compositions. However, no fibers were obtained from the 45 mol% P₂O₅ compositions. This was attributed to the network connectivity, cross-link density and average chain length of the glasses. However, the resulting glass fibers were too soluble for cell attachment and proliferation. Therefore, a quaternary component (Fe₂O₃) was added in low concentrations (1-5 mol%) to reduce the dissolution rates by increasing the cross-link density [70]. Glass fibers were obtained of iron phosphate glasses with a phosphate content of 50 mol% using a crucible method. Lin *et al.* [71] developed iron oxide containing bioabsorbable phosphate glass fibers in the ternary system P₂O₅-CaO-Fe₂O₃ with phosphate contents between 56.9 and 63.7 mol% and iron oxide concentrations between 3.6 and 16.9 mol%. Fibers were drawn continuously from a three-hole platinum bushing.

Abou Neel *et al.* [78] developed copper oxide containing phosphate glass fibers for use in wound healing applications. Glass fibers in the quaternary system P₂O₅-CaO-Na₂O-CuO with a phosphate content of 50 mol% and CuO concentration up to 10 mol% were

obtained using a crucible fiber drawing method. Shah *et al.* [79] developed glass fibers of the composition 62.9 P₂O₅-21.9 Al₂O₃-15.2 ZnO for production of three-dimensional phosphate glass fiber constructs for craniofacial muscle engineering. Fibers were obtained using a fiber-pulling rig. Resulting fibers had diameters of 6.5 μm and were arranged in a fibrous meshwork prior to cell adhesion tests.

Choueka *et al.* [38] investigated the effect of annealing temperature on the degradation of reinforcing fibers for absorbable implants. Fibers in the system P₂O₅-CaO-Na₂O-Fe₂O₃-ZnO were drawn at 1000 °C using a crucible method. Annealing fibers at higher temperatures slowed degradation. Fibers annealed at the highest temperatures underwent a mode of degradation that allowed them to maintain their structural integrity in aqueous media for longer time periods. This made high temperature annealed phosphate glass fibers most suitable for reinforcement of biodegradable implants.

2.4 Degradable polymers

Polymeric materials have been used for years in orthopaedic surgery; typical applications include tissue replacement, augmentation and support of tissues and the delivery of drugs. Because of their physical properties similar to those of soft tissue, their applications include wound dressings, tendon replacements and vascular prostheses. Polymers used for these devices are classical polymers like polyethylene or polyurethanes. Sutures were the earliest, successful application of synthetic degradable polymers in human medicine. The most important surgical bioabsorbable polymers are aliphatic polyesters (polymers and copolymers) of α-hydroxy acid derivatives. The first synthetic degradable sutures were made of poly(glycolic acid) (PGA) in the 1970s. Unreinforced PGA was found to be too brittle and absorbed too rapidly to be adequate for osteosynthesis [38]. Poly(lactic acid) (PLA) is highly resistant to hydrolysis and therefore degrades much more slowly than PGA. Later copolymers of PGA and PLA, poly(lactic-co-glycolic acids), were developed. Sutures made of polydioxanone (PDS) became available in the 1980s [51,52,80].

Bioabsorbable materials should fulfill certain criteria and requirements. The bioabsorbable materials must be non-mutagenic, non-antigenic, non-carcinogenic, non-toxic, non-teratogenic, antiseptic and tissue compatible. They should not cause

morbidity and must provide adequate mechanical stiffness and strength. Degradation should preferably occur by hydrolysis in aqueous media, although it is faster in the presence of certain enzymes. The degradation products should be water-soluble, comprise small molecules, be naturally occurring metabolites and be excreted via the kidneys and the lungs [45,81].

Bioabsorbable implants in current use are sutures, fiber constructions, porous composites and drug delivery systems [82]. Many macromolecular compounds are bioabsorbable, but only a few possess the properties necessary for internal bone fixation such as high mechanical strength and stiffness. Low implant stiffness allows too much bone motion for satisfactory healing. Compared to stainless steel, unreinforced biodegradable polymers are as much as 36 % as strong in tension and 54 % as strong in bending, but only 3 % as stiff in either test mode [38]. The strength characteristics of implants, e.g. rods and screws, have been improved by a fiber-reinforced composite texture in which the polymer matrix is reinforced with the same material (self-reinforced, SR). SR-PLLA exhibits an elastic modulus of 10 GPa and a bending strength of 300 MPa in comparison to 3 GPa and 119 MPa for non-reinforced PLLA [83]. The application of biodegradable SR composites such as rods and screws is expanding rapidly and has increased steadily over the past years. The latest SR composites are strong enough for fractures of load-bearing cancellous bones to be fixed without a plaster cast and with an early mobilization of the patient [45]. Results indicate that besides their beneficial use in bone fracture fixation the degradable polymers show osteoconductive potential and can initiate new bone formation [84].

Today research focuses on the development of degradable polymeric materials for use as internal fixation material and resorbable temporary scaffold for tissue engineering. Ishaug *et al.* [85] investigated bone formation *in vitro* in three-dimensional poly(D,L-lactic-co-glycolic acid) foams with pore sizes ranging from 150 to 710 μm . Their results suggested the use of the scaffolds for the transplantation of autogenous osteoblasts to regenerate bone tissue. Deschamps *et al.* [86] performed *in vivo* degradation studies on poly(ether ester)s based on polyethylene glycol (PEG) and poly(butylene terephthalate) (PBT). The copolymers degraded slowly under *in vivo* conditions. Results indicated that part of the PBT fraction might remain in the body at late stages of degradation. However, crystalline PBT fragments seemed to be tolerated by the body. Guan *et al.*

[87] characterized biodegradable poly(ether ester urethane)urea elastomers based on poly(ether ester) triblock copolymers with putrescine as chain extender. Resulting polymers exhibited tensile strengths ranging from 8 to 20 MPa and breaking strains from 325 % to 560 % and did not show evidence of cytotoxicity. The polymers showed potential for applications that require high strength and flexibility. Vogt *et al.* [88,89] developed highly porous scaffold materials based on functionalized oligolactides for bone tissue engineering. Degradable or osteoconductive fillers were tested as additives to modulate the materials properties. The scaffolds exhibited a continuous degradation *in vitro* with varying degradation rates depending on the composition. *In vitro* cell experiments revealed their excellent biocompatibility.

2.4.1 Composite materials

One of the major challenges during development of both conventional and degradable implant materials for fracture fixation is the mechanical compatibility between implants and bone. While metals and alloys have been used successfully for internal fixation, the rigid fixation from bone plating can cause stress protection atrophy resulting in loss of bone mass and osteoporosis. While the elastic modulus of cortical bone ranges from 17 to 24 GPa, common alloys have moduli ranging from 100 to 200 GPa. This large difference in stiffness can result in high stress concentrations as well as relative motion between the implant and bone upon loading [90]. In contrast, the strength and stiffness of polymeric materials are too low for application as load bearing implants. Polymeric self-reinforced screws showed higher tensile and bending strength in comparison with homogeneous polymeric screws. However, elastic moduli were still too low resulting in bending of the screws which limited the use [53]. Therefore the fabrication of composite materials can provide an alternative.

Composite biomaterials are composed of at least two materials that are different in composition, structure and properties, defining a continuous phase (matrix) and at least one reinforcing phase. The reinforcement should be homogeneously dispersed in the matrix at the microscopic scale and at the macroscopic scale the material should behave as a homogeneous material [49,83,90,91].

Polymer matrix composites are being increasingly studied [35,79,92-95]. Applications are ranging from coatings to load-bearing implants. The research concerning

biodegradable composites has been mostly centered on the use of poly(α -hydroxy esters) (cf. above). For the development of biodegradable implant materials, both the matrix and the reinforcement should be resorbable. However, research includes both degradable and stable materials as fillers. Currently the most studied reinforcement materials for bone-driven implants are bioactive fillers. Examples of those fillers are hydroxyapatite (HA), tricalcium phosphate (TCP) and bioactive glasses. Embedding particles of these materials into the polymer matrix is known to promote bone bonding properties and increase both the elastic modulus and the strength of the resulting composite. Additionally, the ceramic phase can act as hydrolysis barrier, delaying the degradation of the polymer. While sintered HA exhibits low absorption kinetics, non-sintered HA and TCP are bioactive and completely absorbable [49].

HA is the most-used ceramic in such composites as it is similar to the inorganic phase existing in mineralized bone and has high biocompatibility and bioactivity. Ural *et al.* [96] developed composite materials based on elastomeric D,L-lactide and ϵ -caprolactone copolymers and HA powder. Incorporation of HA significantly increased the elastic modulus and decreased degradation rates. Marra *et al.* [97] developed composites of polymer blend (poly[caprolactone] and poly[D,L-lactic-*co*-glycolic acid]) and HA granules. The resulting composite specimens showed good biocompatibility *in vitro* and the elastic modulus was increased considerably by adding HA. Knowles *et al.* [95] developed composites based on polyhydroxybutyrate (PHB) and HA which were bioactive and showed good bonding to the surrounding tissue *in vivo*. Helwig *et al.* [98] produced composite materials by ring-opening polymerization of lactones in the presence of HA.

Other composites include bioactive glasses (Bioglass[®]) as reinforcing phase. These glasses are silica based and therefore stable to hydrolysis. But their bioactivity and high osteoinductive potential induces an excellent biochemical compatibility, which is a very important quality for artificial bone [90]. Resulting composites are partially bioabsorbable devices. Lu *et al.* [31] developed three dimensional porous composites of polylactide-*co*-glycolide and 45S5 bioactive glass granules. The addition of bioactive glass resulted in a structure with higher compressive strength. In addition, the composite supported adhesion, growth and mineralization of human osteoblast-like cells *in vitro*. Stamboulis *et al.* [92] tested the mechanical properties of biodegradable polymer

sutures coated with bioactive glass. After 28 days immersion in SBF the residual tensile strength of the coated sutures was significantly higher than that of the uncoated ones. This result indicated a protective function of the Bioglass[®] coating. Maquet *et al.* [99] investigated porous composites of poly-D,L-lactide and polylactide-*co*-glycolide containing different amounts of bioactive glass. The presence of bioactive filler was found to delay the degradation rate of the polymer foams.

For totally biodegradable composite materials both the continuous phase and the reinforcement should be completely degradable. Therefore, the use of phosphate glasses as filler is of special interest. Knowles *et al.* [100] produced completely degradable composite scaffolds of PHB and glass particles of the system P_2O_5 -CaO- Na_2O (phosphate content between 39 and 54.3 mol%). *In vitro* degradation studies showed that mass loss and mechanical property change could be correlated with the solution rate of the reinforcing glass. *In vivo* studies showed a slight inflammatory reaction, but otherwise good compatibility. With time, the inflammatory reaction disappeared and therefore had probably been caused by the high solubility of the glass. Prabhakar *et al.* [101] tested the effect of glass composition on the degradation properties of phosphate glass/polycaprolactone composites. Composites containing 20 vol% of glass powder of the system $45 P_2O_5-x CaO-(55-x) Na_2O$ with x between 24 and 36 mol%. Degradation rates of the composite could be adjusted by changing the glass composition.

Statistically homogenous but anisotropic media represent an important class of composite materials, e.g. polymer composite reinforced with glass fibers. Anisotropic composites offer superior strength and stiffness in comparison with isotropic ones. material properties in one direction are gained at the expense of properties in other directions [39]. Vallittu *et al.* [102] investigated the tensile strength of unidirectional glass fiber/polymethyl methacrylate (PMMA) composite for use in dentures. An increased amount of fibers in the PMMA matrix resulted in a considerable increase in tensile strength. Slivka *et al.* [94] characterized the fiber-matrix interface in completely degradable composite materials consisting of calcium phosphate glass and poly(L-lactic acid) (PLLA). The continuous fiber-reinforced composite showed an elastic modulus suitable for fixing cortical bone fractures (42 GPa). However, its rapid deterioration of mechanical properties and fiber-matrix interfacial shear strength limited its use.

One of the key parameters in controlling the successful design of polymer matrix composites is the control of the interface properties between the matrix (i.e. biodegradable polymer) and the filler. The interface can be improved by either chemical bonding or by physical interlocking between the matrix and the reinforcement. The goal is to obtain a good transfer of load from the continuous phase to the reinforcement [49].

2.5 Cell experiments

Tissue culture is a generic term that refers to both organ culture and cell culture and the terms are often used interchangeably. Cell cultures are derived from either primary tissue explants or cell suspensions. Primary cell cultures typically will have a finite life span in culture whereas continuous cell lines are, by definition, abnormal and are often transformed cell lines.

Cells used for cytocompatibility tests in this study include MC3T3-E1 and MC3T3-E1.4 cells. The clonally derived murine MC3T3-E1 cell line originates from cells extracted from the skull of newborn mouse calvaria. Although MC3T3-E1 cells comprise a cell line rather than primary osteoblasts, it has been shown that they express parameters of the osteoblast phenotype, including type I collagen synthesis, alkaline phosphatase, and nodular extracellular matrix mineralization resembling woven bone [103,104]. However, their capability to proliferate and differentiate is significantly reduced after a finite period of time. Cells above passage 60 were found to be less proliferative as well as less osteogenic than cells at passage 20 or lower. Furthermore, serial passage diminished osteoblastic function [105]. For this reason the MC3T3-E1 cell line became phenotypically heterogenous due to prolonged passaging and its mesenchymal origin [13]. Wang *et al.* [106] derived a series of subclonal cell lines from MC3T3-E1 cells which differed in their ability to mineralize a collagenous extracellular matrix and express osteoblast-related genes. The MC3T3-E1.4 cell line was derived from subclone 4 which showed a high differentiation/mineralization potential.

Other cell tests were carried out using post-natal human dental pulp stem cells (DPSCs). These cells possess stem cell-like qualities, including self-renewal capability and multi-lineage differentiation. They have the ability to form a dentin/pulp-like complex and are possibly a precursor population of odontoblasts [107,108]. DPSCs were included into

this research to test the applicability of degradable phosphate glasses as tissue culture scaffolds for culturing of dentin-forming cells.

Once a cell is explanted from its normal *in vivo* environment, the question of viability becomes fundamental. Furthermore, many experiments carried out *in vitro* are for the sole purpose of determining the potential cytotoxicity of the compounds being studied. Many cytotoxicity assays concentrate on aspects that influence cell growth or survival. Cell growth is usually taken to show the regenerative potential of cells [109]. There are several ways to determine the number of cells in a proliferation assay. Cell number can be determined directly, by counting using a microscope and a hemocytometer, or indirectly, e.g. by measuring metabolic activity of cellular enzymes.

MTT (3-[4,5-dimethylthiazol-2-yl]-2,5-diphenyltetrazolium bromide) is a substrate which is converted by means of a complex enzymatic system corresponding to the mitochondrial respiratory chain to yield a dark blue formazan product [110]. This system is known as the mitochondrial succinate-tetrazolium-reductase system and is active only in viable cells. The intensity of the color produced is directly related to the number of living cells *in vitro*. The amount of formazan produced can easily be determined using a spectrophotometer. WST (4-[3-(4-iodophenyl)-2-(4-nitrophenyl)-2H-5-tetrazolio]-1,3-benzene disulfonate) is another tetrazolium salt which is used in assays to determine the number of metabolically active cells.

2.5.1 Cell compatibility of glasses

Over the last years the interest in phosphate glasses for use as degradable implant materials was on the rise. However, most of the research focused on glasses containing 45-50 mol% P_2O_5 or above. Bitar *et al.* [19] investigated the cellular response on glasses in the system $50 P_2O_5 - x CaO - (50-x) Na_2O$ with x between 30 and 48 mol%. Solubility of these glasses is described by Ahmed *et al.* [20] (cf. Chapter 2.3.2). Bitar *et al.* assessed the biocompatibility of the glasses using human osteoblasts and fibroblasts which were seeded directly on glass disks. Besides adhesion, survival and proliferation maintenance of osteoblast and fibroblast phenotype was assessed. Results indicated that a higher calcium content supported the attachment, growth and maintenance of differentiation of both human osteoblasts and fibroblasts. This was probably due to the

fact that an increasing CaO content decreases the solubility of the glasses (cf. Chapter 2.3.2).

Salih *et al.* [111] tested the cell compatibility of glasses in the system $45 \text{ P}_2\text{O}_5 - x \text{ CaO} - (55-x) \text{ Na}_2\text{O}$ (x between 8 and 40 mol%) using two human osteosarcoma cell lines. Solubility behavior of these glasses is described in [67] (cf. Chapter 2.3.2). Cells were cultured using glass extracts rather than glass samples and proliferation and antigen expression were assessed. Results showed that extracts of highly soluble phosphate glasses caused inhibition of growth and antigen expression while glasses with lower solubility apparently up-regulated proliferation of cells and expression of various antigens.

However, the use of glass extracts in cell experiments can give results which are less distinct than those obtained by culturing cells in direct contact with the glass samples as shown by Navarro *et al.* [23]. They tested the cytocompatibility of two glasses in the system $44.5 \text{ P}_2\text{O}_5 - 44.5 \text{ CaO} - (11-x) \text{ Na}_2\text{O} - x \text{ TiO}_2$ where x was 0 and 5 mol%, respectively. Experiments were carried out on the one hand culturing the human skin fibroblasts using extracts of the glasses and on the other hand directly on glass plates. Toxicity and proliferation were measured using the WST assay. Their results clearly demonstrated that the information given by the extracts method and the direct contact method cannot be considered as equivalent. They also showed that the *in vitro* behavior (toxicity, adhesion and proliferation) of soluble phosphate glasses is modulated by the solubility of the glass. While the glass devoid of titania, which showed a solubility 10 times higher than the titania containing glass, showed a more toxic response in cell cultures, cell adhesion was enhanced. Navarro *et al.* also demonstrated that it is difficult to extrapolate the *in vitro* results to the *in vivo* behavior of the material. The titania-free glass was evaluated in rabbits dorsal subcutaneous tissue. It showed a good biocompatibility and did not present any adverse reaction, despite its solubility. This can probably be explained by the fact that *in vivo*, the local chemical changes are buffered by the physiological environment and local conditions can be smoothed by the continuous circulation of body fluids.

Franks *et al.* [21] investigated the response of a human osteosarcoma cell line (MG63) to glasses of the quaternary system $45 \text{ P}_2\text{O}_5 - (32-x) \text{ CaO} - 23 \text{ Na}_2\text{O} - x \text{ MgO}$, where x

was between 0 and 22 mol%. Again, glass extracts in different dilutions were used to derive the cell compatibility of the glasses; cell proliferation was measured using the MTT test. Results of the assay suggested that the growth of MG63 cells in the presence of glass extracts of four different dilutions remained largely unaffected. After five days in culture, cell proliferation increased in some cases, particularly for those glasses containing 7 mol% MgO or more. However, the reasons for the apparent beneficial effect of these glasses remained unclear.

Ahmed *et al.* [70] developed phosphate based fibers for use as cell delivery vehicles for cell transplantation purposes. Fibers in the system P_2O_5 -CaO- Na_2O - Fe_2O_3 containing 50 mol% P_2O_5 and 1 to 5 mol% Fe_2O_3 were tested with focus on their biocompatibility using a conditionally immortal MPC cell line (muscle precursor cells). Cells were cultured directly on the glass surface and their ability to replicate and differentiate *in vitro* was studied. It was found that adding 4 to 5 mol% Fe_2O_3 to the original P_2O_5 -CaO- Na_2O ternary composition was sufficient to achieve cell attachment and proliferation. This was attributed to the enhanced chemical durability of the iron-phosphate glasses (cf. Chapter 2.3.2). Glasses of the ternary system P_2O_5 -CaO- Na_2O had been too soluble for cell attachment and proliferation on the glass surface [20,68,111].

Lee *et al.* [103] used a murine pre-osteoblast MC3T3-E1 cell line to determine the cytocompatibility of glasses in the system P_2O_5 -CaO- CaF_2 -MgO-ZnO with about 44 mol% P_2O_5 . Cells were cultured in direct contact with the glasses and proliferation, differentiation and calcification were assessed. As cell proliferation on the phosphate glass was not significantly different from proliferation of the cells on tissue culture polystyrene (TCPS) controls, it was concluded that the glass was non-cytotoxic. Alkaline phosphatase activity was significantly enhanced and promotion of bone-like nodule formation by the calcium phosphate glass was observed after 7 days and thereafter. Apparently the phosphate glass enhanced both differentiation and calcification of MC3T3-E1 cells.

In summary, soluble phosphate glasses are promising for use as degradable hard tissue substitution materials. The results presented in the literature can be significant for some applications in the field of materials for bone regeneration or also in the field of the development of substrates for tissue engineering with controlled degradation rates. The

control of degradation rates seems to be a key issue. Adjustment of solubility seems to be important not only for the manufacturing of implant materials with resorption rates matching the growth rates of bone (cf. Chapter 2.2.2) but also for satisfying results in cell experiments and tissue engineering.

3 Experimental procedure

3.1 Glasses

3.1.1 Glass synthesis

The glasses were prepared by melting mixtures of carbonates and metaphosphates of calcium, sodium and magnesium and different oxides (e.g. titania, silica and alumina) in silica crucibles at temperatures between 1200 and 1350 °C using an electrically heated furnace. After quenching between copper blocks the glasses were remelted in platinum crucibles for 30 min. Melting times were kept short to minimize losses through evaporation. After casting the glasses were quenched to prevent surface crystallization and annealed. Synthetic glass composition is given in Appendix A.

Table 3.1: Synthetic glass composition (mol%) of polyphosphate glasses

glass	P ₂ O ₅	CaO	MgO	Na ₂ O	TiO ₂
G1	50.00	20.00	2.00	25.00	3.00
G2	48.00	24.00	4.00	21.50	2.50
G5	46.00	20.00	4.00	28.50	1.50
G6	45.00	20.00	4.00	29.50	1.50
G7	46.00	16.00	8.00	28.00	2.00
G8	45.00	16.00	8.00	29.00	2.00

Glasses of the system P₂O₅-CaO-MgO-Na₂O-TiO₂ with a phosphate concentration of 45 to 52.5 mol% (polyphosphate to ultraphosphate region) were produced (cf. Table 3.1 and Appendix A). As the glass Mg5 was shown to be biocompatible in previous experiments [26,32,112,113], another set of glasses in the pyrophosphate region (34 to 37 mol% P₂O₅) was produced (cf. Table 3.2). Different additives (Al₂O₃, F⁻, Fe₂O₃, K₂O, SiO₂, TiO₂, ZnO and ZrO₂) were added at concentrations between 1 and 10 mol% to control solubility and crystallization. For glass T5, all components (P₂O₅, CaO, MgO and Na₂O) were proportionally substituted for TiO₂. For all other glasses, the phosphate content was kept constant at 37 mol%. For the N series, CaO, MgO and Na₂O were proportionally substituted for the additives. For the B glasses, CaO and MgO were

substituted for TiO₂ while the Na₂O content was kept constant as well. In the C glass series, Na₂O was substituted for K₂O.

Table 3.2: Synthetic glass composition (mol%) of pyrophosphate glasses

glass	P ₂ O ₅	CaO	MgO	Na ₂ O	additive	
Mg5	37.00	29.00	10.00	24.00	-	
T5	34.87	27.45	9.65	22.57	5.45	TiO ₂
NT1	37.00	28.54	9.84	23.62	1.00	TiO ₂
BT1	37.00	28.26	9.74	24.00	1.00	TiO ₂
CK1	37.00	29.00	10.00	23.00	1.00	K ₂ O
NA1	37.00	28.54	9.84	23.62	1.00	Al ₂ O ₃
NH1	37.00	28.54	9.84	23.62	1.00	F ⁻
NS1	37.00	28.54	9.84	23.62	1.00	SiO ₂

3.1.2 Chemical analysis

For chemical analysis of the glass composition, 200 mg of glass powder were dissolved completely in 50 ml of 37 % hydrochloric acid p.a. (HCl) in a 100 mL graduated flask at 98 °C. After cooling, the flasks were filled with deionized water. 25 mL were removed, transferred to a clean 100 mL flask and filled to 100 mL with deionized water. The resulting concentration was 50 mg glass/100 mL of deionized water with about 5 % HCl. The solutions were analyzed using inductively coupled plasma – optical emission spectroscopy (ICP-OES). Analyses were done in triplicates.

3.1.3 Glass structure

Glass structure was investigated using ³¹P MAS-NMR spectroscopy. Spectra were collected at 161.9 MHz on a NMR spectrometer (AMX 400, Bruker GmbH, Reinstetten). The ³¹P chemical shifts were obtained from slow spinning MAS spectra with spinning speeds of 5 kHz. All chemical shifts are expressed in ppm relative to an 85 % H₃PO₄ solution.

The measured ³¹P MAS-NMR spectra were decomposed into Gaussian components and the relative total area of each approximated isotropic peak was used as a measure of the respective site concentration. Theoretical average chain length (*L*) was determined according to Bunker *et al.* [66] and Ahmed *et al.* [68] according to the following equation

$$L = \frac{2}{\frac{x}{1-x} - 1} \quad (3.1)$$

where x is the molar metal oxide fraction

$$x = \frac{[R_2O] + [R'O]}{[R_2O] + [R'O] + [P_2O_5]} \quad (3.2)$$

$[R_2O]$ and $[R'O]$ are the alkali and alkaline earth oxides concentrations and $[P_2O_5]$ is the phosphate concentration of the glass.

3.1.4 Density, crystallization and viscosity

Glass transition temperatures and crystallization temperatures were determined using differential thermal analysis (DTA, heating rate 10 K/min) (DTA 50, Shimadzu, Kyoto, Japan) or dilatometry. Crystallization behavior of the phosphate glasses was investigated by tempering glass rods of approximately $5 \times 5 \times 8 \text{ mm}^3$ at temperatures between 480 and 600 °C for 30 min in an electrically heated furnace (Programat P80, Ivoclar AG, FL). Afterwards the samples were ground to expose the desired crystal-glass interface and polished. The progress of crystal growth was then easily followed by optically measuring the thickness of the crystallized layer under an optical microscope (Stereomikroskop Technival, Zeiss AG, Jena) [114,115]. The crystalline phases were identified using X-ray diffraction (XRD; Diffraktometer D5000, Siemens AG). Spectra were obtained from powdered samples and from crystalline surfaces. Densities of the glasses were determined using a helium pycnometer (Accupyc 1334, Micromeritics GmbH, Mönchengladbach). Viscosity measurements were carried out using a rotating viscometer ($\lg \eta = 1$ to 5) and a beam bending viscometer ($\lg \eta = 9$ to 15). For rotating viscometry, 13.8 cm^3 of glass frit were used for the experiments. Measurements were carried out at rotations of 10 min^{-1} and 250 min^{-1} . For bending viscometry, two glass rods of $4 \times 5 \times 45 \text{ mm}^3$ and $5 \times 5 \times 45 \text{ mm}^3$, respectively, were used.

3.1.5 Porous glass cubes

Porous glass cubes were produced from the pyrophosphate glasses (Mg5 based: Mg5, T5, N, B and C series). For fabrication of porous specimens the glass was crushed after cooling, the glass frit was mixed with isopropanol and milled for 3 h using an agate planetary mill (Pulverisette, Fritsch GmbH, Idar-Oberstein). The resulting suspension

was kept over night at 120 °C to remove the isopropanol. The resulting glass powder had a grain size smaller than 20 μm [116]. The porous structure was obtained by sintering mixtures of glass powder and sodium chloride (grain size 250-315 μm) in a glass/salt ratio of 1:1 at temperatures above T_g (470 to 520 °C) for 30 min in ceramic molds (15 x 15 x 13 mm). After sintering, the salt phase was dissolved in water.

3.1.6 Glass fibers

Of the pyrophosphate glasses only glass T5 (5.5 mol% TiO_2) was used for the fabrication of fibers. Fibers were produced using a preform technique at the Institut für Physikalische Hochtechnologie, Jena (IPHT). The preform was obtained by casting the glass melt into a preheated rod shaped graphite mold and subsequent annealing at 500 °C. The resulting glass rod was about 13 cm in length and had a diameter of 10 mm. The fibers were drawn at temperatures between 600 and 620 °C at a rate of 6 m/min, sized and wound up on a rotating drum. Viscosity during fiber drawing was 10^4 to 10^5 dPa s. As sizing, the oligomer/HEMA mixture described in Chapter 3.2.1 was used. A schematic of the fiber rig at the IPHT is shown in Figure 3.1.

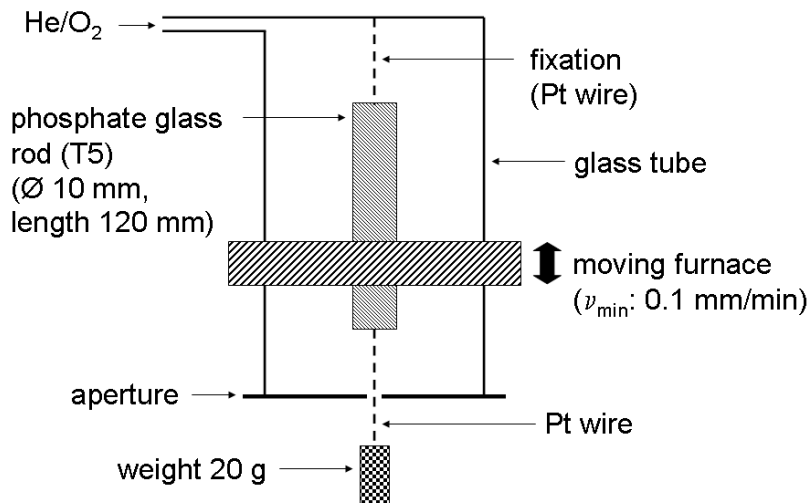


Figure 3.1: Schematic of the fiber rig (IPHT)

3.2 Composites

Composites were prepared of phosphate glasses and degradable organic polymers [27,32] to obtain bioresorbable composite materials. The composites were produced in

cooperation with Innovent Technologieentwicklung e.V., Jena, where the polymer was developed and synthesized.

3.2.1 Applied organic polymer

The degradable polymer used in this study is based on oligo-L-lactide macromers which were prepared in a two-step procedure [89,117]. For the ring-opening oligomerization of L-lactide in the first step, a mixture of dianhydro-D-glucitol (initiator, 35.1 g, 0.24 mol), L-lactide (69.2 g, 0.48 mol) and stannous ethylhexanoate (stannous isooctanoate $\text{Sn}(\text{Oct})_2$, catalyst, 0.43 g, 1.05 mmol) was stirred under nitrogen and exclusion of moisture at 150 °C for 2 h. The melt was allowed to cool and was dissolved in dichloromethane (160 mL). The solution was filtered and the oligolactide was precipitated by pouring into heptane (1400 mL). Finally, the solvent was removed and the isolated oligolactide (102.4 g, yield 98%) was dried under vacuum at 25 °C to constant weight.

The macromer was synthesized in a second step. The oligolactide (102.4 g) was dissolved in dichloromethane (160 mL). After adding triethylamine (147.5 mL, 1.06 mol), methacryloyl chloride (68.7 mL, 0.707 mol) was slowly added under stirring at 0 – 5 °C under moisture exclusion. The mixture was extracted several times with 1 M HCl (300 mL), saturated aqueous solution of NaHCO_3 (600 mL) and distilled water (300 mL). The organic phase was dried over Na_2SO_4 , filtrated and treated with silica gel to remove colored impurities. *p*-Methoxyphenol (0.12 g) was added to the filtrated macromer solution and the solvent was removed under reduced pressure. Drying of the resulting residue in vacuum produced the product as a yellow viscous oil (84.5 g, yield 63 %). The reaction schematic is shown in Figure 3.2.

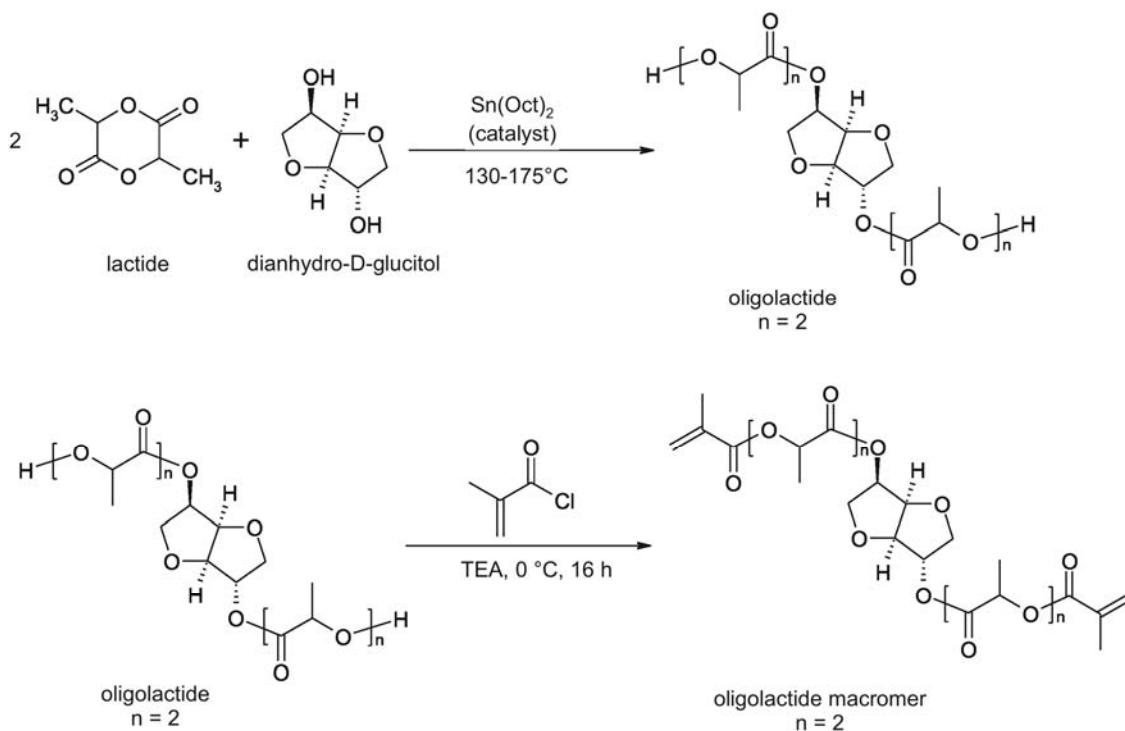


Figure 3.2: Reaction schematic of the macromer synthesis

Using the macromer and methacrylic acid 2-hydroxyethyl ester (HEMA) as comonomer (10 wt%), polymeric coating systems were produced. For polymerization dibenzoyl peroxide was used as starter and the mixture was cured at 110°C for one hour.

3.2.2 Fabrication of composites

Three types of composite materials were produced. As a first set of composites porous sintered glasses (cf. Chapter 3.1.5) with polymer coating were produced. Purpose of this procedure was the improvement of the mechanical properties and machinability while maintaining the interconnective porous structure of the specimens. Therefore the inner surface of porous glass specimens was coated with polymer. A silicon mold possessing the same dimensions as the porous glass samples was used for the coating process. The bottom of the mold was perforated and connected to a vacuum line. The glass cubes were placed in the mold and completely infiltrated with the macromer/dibenzoyl peroxide mixture using a low vacuum. Supernatant liquid was sucked off through the perforation. The coated glass specimens were cured as described above.

In addition, porous glass powder-reinforced polymer were produced. The aim was to obtain porous specimens with improved mechanical properties and to avoid partly

crystallized glass parts in the composites. Production of the polymer is described above. 15.0 g macromer mixture (57.9 wt% macromer, 6.4 wt% HEMA, 32.2 wt% acetone and 3.5 wt% dibenzoyl peroxide), 24.0 g glass powder (cf. Chapter 3.1.5), 2.0 g polyethylene glycol 400 (PEG 400) and 15.4 g sodium chloride were thoroughly mixed. The mixture was given into cylindrical silicone molds and cured. The salt was removed in boiling distilled water until the water had a constant electrical conductivity. The specimens were dried at 70 °C.

For the fabrication of glass fiber composites, the fibers were coated with macromer without starter directly after drawing before winding up on a rotating drum. Later the fibers were cut into shorter pieces of about 50 cm in length, bunched, soaked in macromer/dibenzoyl peroxide mixture and cured as described above.

3.2.3 Mechanical strength and porosity

Compressive strength of the porous samples and 4-point and 3-point bending strength of the fiber composites were determined using a hydraulic testing machine (Universalprüfmaschine UPM 1445, Zwick GmbH, Ulm). Porosity of sintered porous glass cubes and of porous polymer cylinders (reinforced with glass powder or calcium carbonate) was determined using a Helium pycnometer (AccuPyc 1330, Micromeritics GmbH).

The breaking behavior of the composite materials was investigated under a scanning electron microscope (DSM 940 A, Zeiss AG, Oberkochen). Fiber composites were clamped into a small 3-point bending device in which a screw could be used for bending the sample. The composite was bended, carbon sputter-coated and the fracture was investigated under the SEM.

To test the adhesion between the glasses and the polymer adhesive shear strength was determined. Glass plates of the dimensions 7 x 7 x 3 mm³ were glued onto glass plates with the dimensions 10 x 20 x 3 mm³. Gluing was accomplished by giving macromer between the glass plates and curing as described above. A schematic of the measurement procedure is shown in Figure 3.3. Tests were carried out both with annealed polished glass samples and sintered non-porous glass plates.

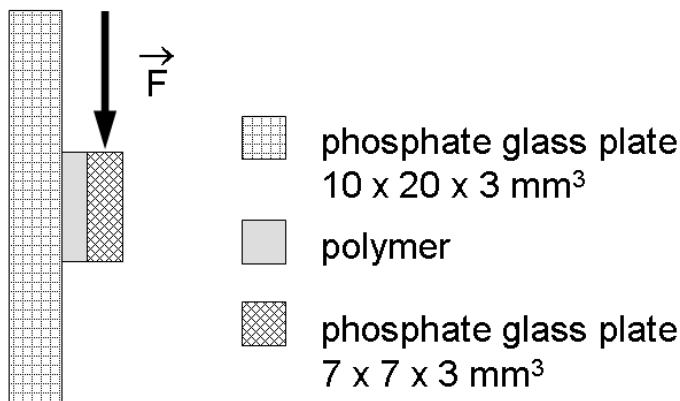


Figure 3.3: Schematic of the adhesive shear strength measurement procedure

3.3 Solubility experiments

3.3.1 pH measurements

pH measurements were carried out in physiological NaCl solution with a concentration of 9.0 g/L. 2.0 g glass of the grain fraction 315 to 500 μm were soaked in 200 mL physiological NaCl solution at 37 °C over a period of at least 10 days. The pH of the solution was determined every 24 hours and afterwards the solution was exchanged for a fresh one. After 10 days, the weight loss of the glass was determined.

3.3.2 Solubility in deionized water

Solubility experiments were carried out in analogy to DIN ISO 719 [72,73]. For time-constant experiments 2 g glass of the grain fraction 63 to 315 μm were soaked for 60 min in 50 mL deionized water at 98 °C. For time-dependent experiments, 1 g glass of the same grain fraction was soaked in deionized water at 98 °C for 60, 120, 300 and 480 min, respectively. The experiments were done in duplicates. The resulting solutions were analyzed using ICP-OES.

3.3.3 Degradation in simulated body fluid

Degradation experiments in SBF (simulated body fluid) at 37 °C were carried out over up to 72 weeks. SBF is an acellular solution that has the same pH and contains the same inorganic ions as human blood plasma in similar concentrations but is devoid of proteins or other organic constituents [118]. Degradation in SBF was tested for sintered

porous glass cubes ($1.5 \times 1.5 \times 1 \text{ cm}^3$) with and without polymer coating and for porous phosphate glass-reinforced polymer cylinders of glasses Mg5 and T5. The specimens were kept in 15 mL SBF per sample. The SBF medium was exchanged every two weeks and every four weeks two samples were removed, cleaned, dried, weighed and the weight loss was determined. Tests were carried out in duplicates.

3.4 Cell experiments

3.4.1 Cell culture

Biocompatibility of the glasses was tested using MC3T3-E1 and MC3T3-E1.4 murine pre-osteoblast cell lines and human dental pulp stem cells (DPSCs) from third molars (wisdom teeth) of juveniles. Cells were grown in an incubator at $37 \text{ }^\circ\text{C}$ and 5 % CO_2 atmosphere. MC3T3-E1 and MC3T3-E1.4 cells were cultured in α -modified minimum essential medium supplemented with 10 % fetal bovine serum (FBS) and 1 % antibiotic/antimycotic (penicillin, streptomycin and fungizone). DPSCs were grown in Eagles minimum essential medium with Earle's balanced salt solution supplemented with 10 % FBS, 1 % penicillin-streptomycin and 0.1 % ascorbic acid. Cells were passaged every 4 to 5 days and used between passages 10 and 20.

Cell tests were carried out on non-porous polished and porous samples with tissue culture polystyrene (TCPS) as control. Glasses were cut into rectangular samples using a low speed diamond saw. The non-porous samples were polished to eliminate influence of sample topography on the results. Cells were seeded at an initial density of $50,000 \text{ cells/cm}^2$ in $500 \text{ }\mu\text{L}$ aliquots on the center of each sample and control material. Then another $500 \text{ }\mu\text{L}$ of cell culture medium were gently added. In all experiments 1 mL medium per well was consistently used to reduce variability of glass dissolution.

As the polymer samples were heat sensitive, sample sterilization was done by γ -irradiation over night ($2.6 \cdot 10^5 \text{ rd}$ total after 15 h). As a control, one set of polished glass samples was sterilized using dry heat (1 h at $250 \text{ }^\circ\text{C}$).

3.4.2 SEM analysis and HE staining

For scanning electron microscopy (SEM) analysis samples with cells were treated as follows: Cells were washed three times with phosphate buffered saline (PBS) without

calcium or magnesium ions prior to fixation with 10 % phosphate buffered formalin solution. Afterwards cells were dehydrated with a series of graded ethanol solutions (30 % to 100 % ethanol), treated with hexamethyldisilazane (HMDS) and sputter-coated with gold-palladium (200 nm).

For HE (hematoxylin and eosin) staining cells were seeded at a concentration of 50,000 cells/cm² as described above. After three days, cells were fixed and dehydrated in 100 % ethanol for one hour. They were stained in hematoxylin for 2 min and washed in tap water to remove supernatant staining solution. Afterwards the samples were treated with acid-alcohol (1 % HCl in 70 % ethanol) for about 30 seconds to remove staining from the glass. After washing with tap water the specimens were immersed in Scott's water (bluing solution) for 30 seconds to turn the nuclei blue by adjusting the pH. Samples were treated with eosin staining for 1 min to turn the cytoplasm pink, then rinsed several times in 95 % and 100 % ethanol. The glasses were embedded in epoxy resin and cut into slices using a low-speed diamond saw.

3.4.3 Proliferation experiments

Cell proliferation of MC3T3-E1.4 cells and DPSCs was assayed according to the following schedule: on day 1, cells were seeded as described above; on day 2, cells were synchronized by serum starvation for 48 hours replacing the medium with a fresh one containing 1 % FBS. On day 4, cells were allowed to re-enter the cell cycle by replacing the medium with a fresh one containing 10 % FBS. After 24 h and 72 h respectively, the cell concentration was determined using a commercial MTT assay (CellTiter 96[®], Promega Corp., Madison, WI, USA). MTT (3-[4,5-dimethylthiazol-2-yl]-2,5-diphenyltetrazolium bromide) is converted by a mitochondrial enzyme, which is active in living cells, to yield a dark blue formazan product. The intensity of the color produced is directly related to the number of viable cells and thus to their proliferation *in vitro*.

To assess the cell number the rectangular glass samples were removed from the original culture plate and placed into the wells of a new one. This way only the cells actually growing on the samples were assessed. Cell culture medium was added keeping the ratio of solution volume to sample surface area constant at 5 mL/mm². This was done to compensate for the difference in surface area available to the cells as the samples did

not cover the bottom of the wells completely. After adding the MTT solution (0.15 μL dye solution/ μL medium) the wells were incubated for 4 h at 37 °C. To dissolve the formed formazan product a solubilization/stop solution was added (5 μL solution/ mm^2 sample surface area). The overnight protocol was chosen to ensure complete solubilization. Absorption was measured at 570 nm in a spectrophotometer (Genesys 5, Spectronics Instruments, Rochester, NY, USA). A calibration curve was determined to convert absorbance into cell concentration.

Cell experiments were performed in triplicate with $n = 3$ for each sample in each experiment. Multiple groups of data were compared by ANOVA; $p < 0.05$ was considered significant.

3.4.4 Viability assay

Cytocompatibility of porous composites was tested using the FDA/EtBr (fluorescein diacetate/ethidium bromide) viability assay. Cell viability of MC3T3-E1 cells after 1 and 4 days was assayed on porous polymer samples with Mg5 and T5 glass powder reinforcement. Porous polymer samples with calcium carbonate (CaCO_3) reinforcement were used as control. Scaffold slices of about 10 mm in diameter and 3 mm in height were transferred each into a separate well of a 24 well culture plate. After disinfection with 1 mL of 70 % ethanol for 1 h, scaffolds were stored in complete cell culture medium for at least 2 h. The medium was changed and 50,000 cells suspended in 1 mL of culture medium were seeded into each well onto the scaffolds. The culture medium was renewed every day. After 1 and 4 days, respectively, the culture medium was replaced by phosphate buffered saline (PBS), the scaffolds were placed onto microscopic slides, overlaid with 0.05 mL of two-fold concentrated staining solution (0.030 mg/mL fluorescein diacetate, 0.008 mg/mL ethidium bromide in PBS), covered with a cover slide and evaluated microscopically. Green and red fluorescence were monitored after 1 min using an Axiotech microscope (Zeiss AG, Jena) with filter sets 09 and 14. Photomicrographs were recorded using a CCD fluor microscope imager MP 5000 (Intas GmbH, Göttingen). Imaging was supported by Image Express software (Media Cybernetics, Inc., Silver Spring, MD, USA). The percentage of dead cells was calculated from the ratio of orange-fluorescent nuclei of dead cells and green-fluorescent living cells.

3.5 Statistical evaluation

3.5.1 Analysis of variance (ANOVA)

The purpose of analysis of variance (ANOVA) is to test differences in means (for groups or variables) for statistical significance [119,120]. This is accomplished by analyzing the variance, i.e., by partitioning the total variance into the component which is due to true random error and the components which are due to differences between means. These latter variance components are then tested for statistical significance. If significant, the null hypothesis of no differences between means is rejected and the alternative hypothesis that the means (in the population) are different from each other is accepted.

The statistical significance (p -value) of a result is the probability that an observed relationship (e.g., between variables) or a difference (e.g., between means) in a sample occurred by pure chance, and that in the population from which the sample was drawn, no such relationship or differences exist. Using less technical terms, one could say that the statistical significance of a result tells us something about the probability to which the result is true (in the sense of being representative of the population). More technically, the value of the p -value represents a decreasing index of the reliability of a result. The higher the p -value, the less we can believe that the observed relation between variables in the sample is a reliable indicator of the relation between the respective variables in the population. In many areas of research, the p -value of 0.05 is customarily treated as a border-line acceptable error level.

3.5.2 Multiple linear regression (MLR)

The general purpose of multiple regression is to learn more about the relationship between several independent or predictor variables and a dependent or criterion variable. Multiple linear regression attempts to model the relationship between two or more explanatory variables and a response variable by fitting a linear equation to observed data [119-121]. Every value of the independent variable x is associated with a value of the dependent variable y . In the least-squares model, the best-fitting line for the observed data is calculated by minimizing the sum of the squares of the vertical deviations from each data point to the line (if a point lies on the fitted line exactly, then

its vertical deviation is 0). Because the deviations are first squared, then summed, there are no cancellations between positive and negative values.

3.5.3 Neural networks (NN)

Neural networks are sophisticated modeling techniques capable of modeling extremely complex functions. In particular, neural networks are non-linear. For many years linear modeling has been the commonly used technique in most modeling domains since linear models have well-known optimization strategies. Where the linear approximation was not valid (which was frequently the case) the models suffered accordingly.

Artificial neural networks work in a way which mimics the fault-tolerance and capacity to learn of biological neural systems by modeling the low-level structure of the brain [119,120]. Hidden nodes play the role of the synapses and by strengthening and weakening the coefficients in an iterative way, the learning process is simulated. However, the NN model can also be described as a non-linear regression model which uses standard non-linear least squares regression methods. Hence, a neural network is just a set of non-linear equations that predict output variables from input variables in a flexible way using layers of linear regressions and transfer functions.

The signal transfer in biological neurons is simulated in the artificial neuron by multiplication of the input signal with the synaptic weight to derive the output signal. In general, neural networks consist on the one hand of an input layer that receives the input signals (cf. Figure 3.4). Between the input layer and the output layer, hidden layers may be arranged, which consist of hidden nodes. The neuron receives from other neurons the input signals, aggregates them by using the weights of the synapses and passes the result after suitable transformation as the output signal. Modeling is achieved by repeated discrete iterations until a stable state of the network is achieved.

3.5.4 Modeling of solubility

The aim was to find a correlation between the solubility behavior of the glasses and their chemical composition. To reduce the number of variables, only glasses of the system P_2O_5 -CaO-MgO- Na_2O - TiO_2 were included in the modeling investigations. In this work, 21 glasses in this system were produced and characterized with respect to their solubility in deionized water. To increase the amount of data available for

modeling, results of previous solubility investigations by Deutschbein [122] were included. Experiments in this work were carried out according to DIN ISO 719 [73] as described in [72]. Therefore results for phosphate glass solubility obtained by Deutschbein and in this work should be comparable. 10 glasses of the system P_2O_5 -CaO-MgO- Na_2O - TiO_2 were prepared and analyzed by Deutschbein (cf. Appendix C).

Modeling of solubility behavior of the glasses was accomplished by use of multiple linear regression (MLR) as an example for a linear method and artificial neural networks (NN) as a non-linear method. Statistical evaluation and modeling were accomplished using Statistica 7 (StatSoft Europe GmbH, Hamburg) and JMP 5.1 (StatCon, Witzenhausen). For neural network experiments, a model including one hidden layer of three hidden nodes as shown in Figure 3.4 was used. Maximum number of iterations was 50.

Input layer

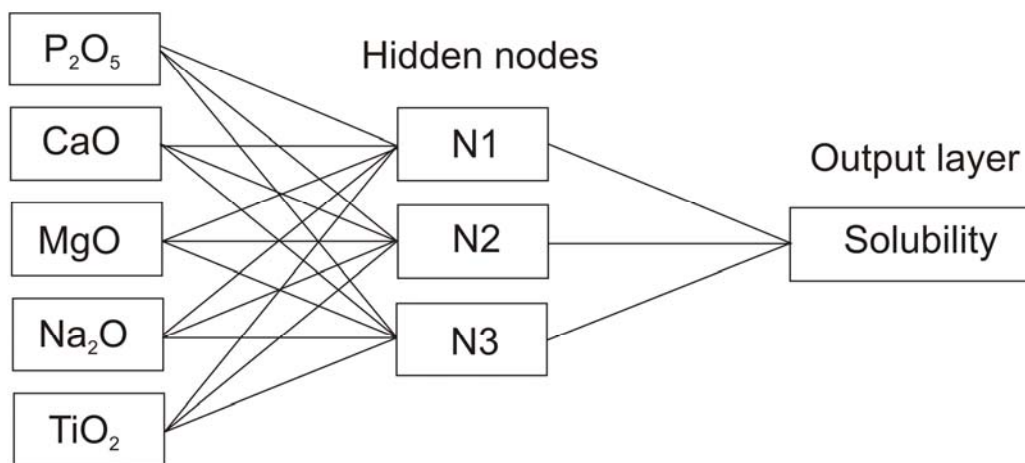


Figure 3.4: Schematic of the neural network used for modeling investigations

4 Results

4.1 Polyphosphate glasses

All polyphosphate glass compositions were obtained in a glassy state. Glasses were transparent and showed a yellowish/brownish coloration which became more intense with increasing titanium oxide content.

Glass compositions were analyzed using ICP-OES analyses. As shown in Appendices A and B, synthetic and analytic glass compositions were comparable. No systematic changes in composition, e.g. due to evaporation of phosphate, were observed. Synthetic glass compositions of all glasses prepared are given in Appendix A.

4.1.1 Glass structure

Glass structure of glasses G1, G2, G5 and G6 was investigated using ^{31}P MAS-NMR spectroscopy. Glass compositions and the metal oxide fraction x (cf. Equation 3.2) are given in Table 4.1.

Table 4.1: Glass compositions in mol% and metal oxide fraction (x) of glasses G1, G2, G5 and G6

glass	P_2O_5	CaO	MgO	Na_2O	TiO_2	x
G1	50.0	20.0	2.0	25.0	3.0	0.50
G2	48.0	24.0	4.0	21.5	2.5	0.52
G5	46.0	20.0	4.0	28.5	1.5	0.54
G6	45.0	20.0	4.0	29.5	1.5	0.55

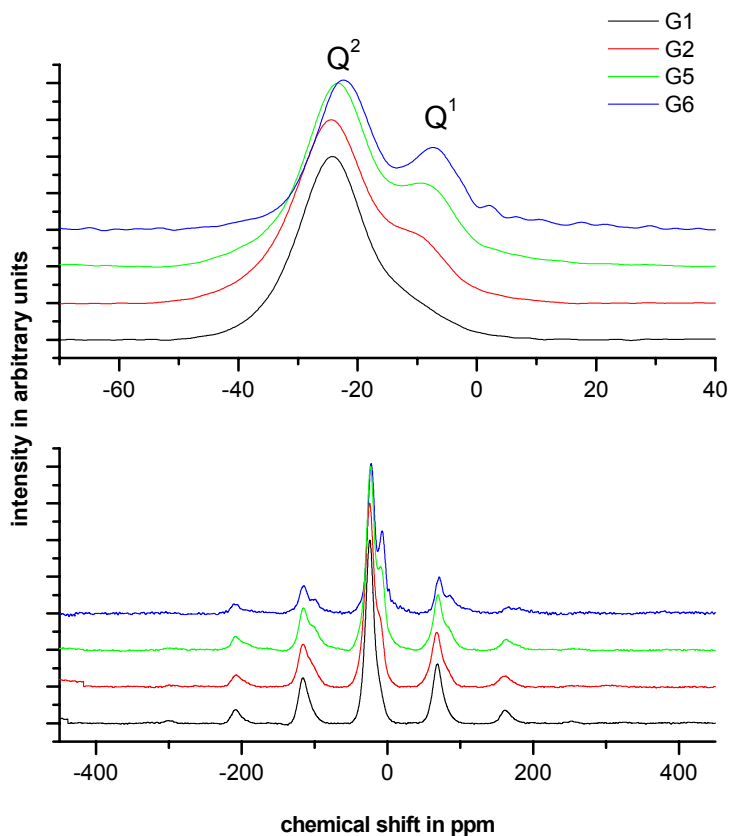


Figure 4.1: ^{31}P MAS-NMR spectra (bottom) and central resonances (top) of glasses G1, G2, G5 and G6

Figure 4.1 shows the ^{31}P MAS-NMR spectra and the central resonances of all four glasses. All glasses yield a central peak with a chemical shift in the range from -24.5 ppm (G1) to -22.3 ppm (G6). The spectra are similar in shape, however, glasses with $x > 0.5$ clearly produce a second peak at shifts in the range from -8.6 ppm (G2) to -7.3 ppm (G6) (cf. Table 4.2). The central peak of glass G1 is clearly asymmetric. Thus central peaks of all glasses were fitted by two Gaussian functions (Figure 4.2).

Table 4.2: ^{31}P MAS-NMR chemical shifts in ppm for Q¹ and Q² groups

glass	Q ¹	Q ²
G1	-8.9	-24.5
G2	-8.6	-24.5
G5	-7.3	-23.5
G6	-7.3	-22.3

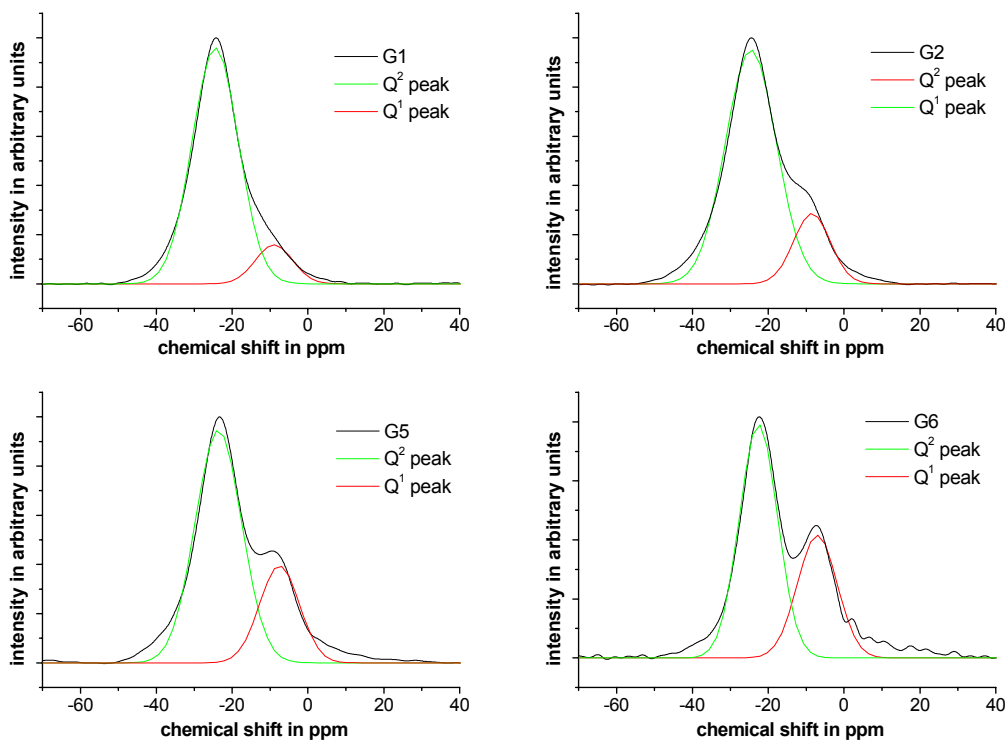


Figure 4.2: ^{31}P chemical shifts: Gauss fit of Q^1 (red curves) and Q^2 (green curves) peaks of glasses G1, G2, G5 and G6

The peaks with chemical shifts in the range of -25 ppm to -20 ppm can be attributed to Q^2 groups, i.e., chain middle groups. Q^1 end groups show shifts in the range of -10 ppm to -7 ppm [56,57,64]. While glasses with smaller P_2O_5 contents still consist of phosphate chains, as can be seen by the presence of Q^2 middle units, the increasing amount of Q^1 end units shows that they consist of shorter phosphate chains. Thus the depolymerization of the phosphate chains with decreasing P_2O_5 content from 50 mol% (G1) to 45 mol% (G6) is reflected in the increasing amount of Q^1 groups and the decrease in the number of Q^2 groups. Therefore it can be easily followed by ^{31}P MAS-NMR.

Table 4.3: Relative concentrations of the Qⁿ units determined by ³¹P MAS-NMR and experimental and theoretical average chain lengths L

glass	Q ² fraction	Q ¹ fraction	L (experimental)	L (theoretical)
G1	0.88	0.12	17	∞
G2	0.82	0.18	11	24
G5	0.74	0.26	8	12
G6	0.65	0.35	6	9

The relative concentrations of Q¹ and Q² groups were calculated from Gaussian peak areas in Figure 4.2. Theoretical average chain lengths were obtained from synthetic glass composition according to Equation 3.1. Experimental average chain lengths were obtained from the relative concentrations of Qⁿ groups. Results are given in Table 4.3.

4.1.2 Density, crystallization and viscosity

Glasses in the system P₂O₅-CaO-MgO-Na₂O-(K₂O)-TiO₂ with phosphate contents between 45 and 50 mol% had densities between 2.58 and 2.64 g/cm³. Glass transition temperatures were between 336 and 394 °C. No systematic changes in T_g and in density with structural changes in the glass (cf. Chapter 4.1.1) were observed for glasses G1, G2, G5 and G6. This might be due to water contents in the glass. Glass D4, which has a P₂O₅ content of 52.5 mol% (ultraphosphate glass), had a density of 2.56 g/cm³ and a transition temperature of 360 °C. All glass data are summarized in Appendix D.

Viscosity measurements using a rotating viscometer were carried out with glasses D4, D3T3, D3T2, G1, G2, G5 and G6. Viscosity curves are shown in Figure 4.3. Viscosity of the glasses at 550 °C and 600 °C is given in Table 4.4. Glass D4 was the only investigated ultraphosphate glass (composition in mol%: 52.5 P₂O₅ - 23.7 CaO - 4.3 MgO - 19.5 Na₂O). It showed a viscosity between 10² and 10⁵ dPa s for the temperature range from 680 to 480 °C. Glass D4 was the only titania-free glass which was used for viscosity measurements. It showed a low crystallization tendency which can be attributed to the high phosphate content [57].

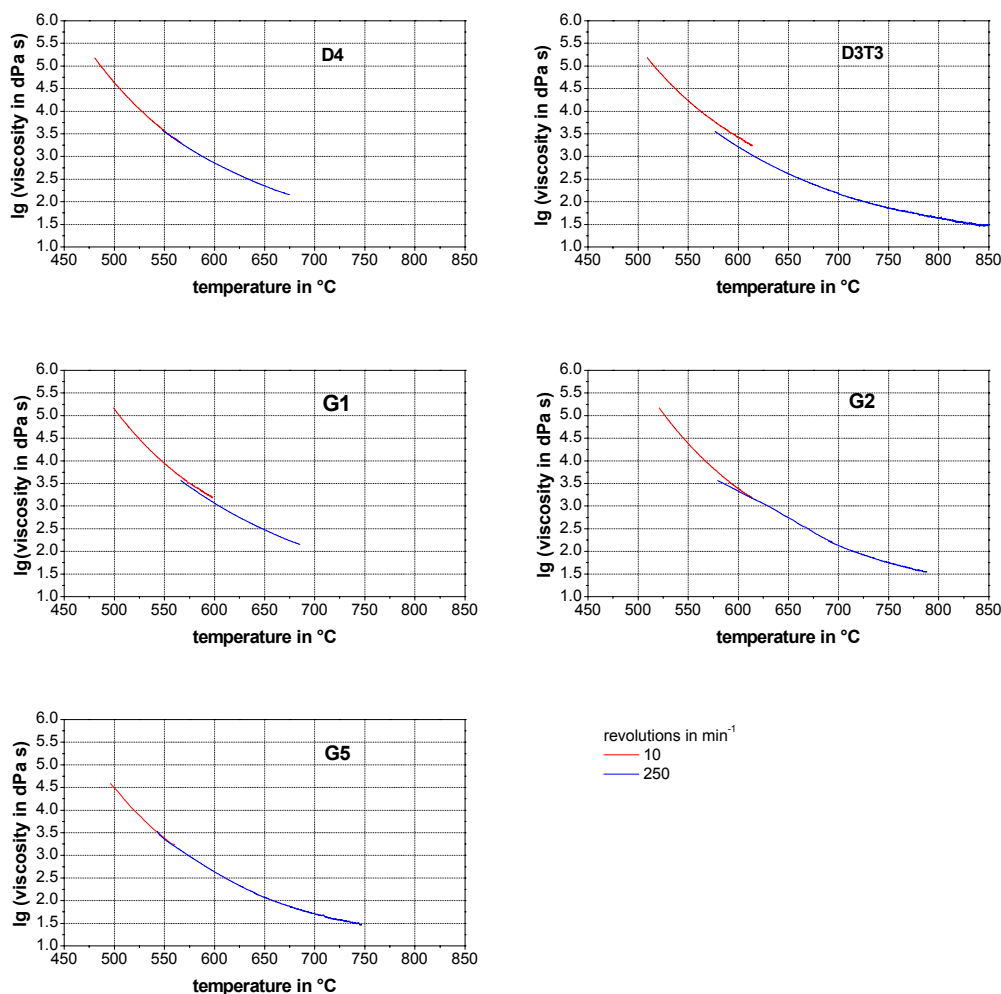


Figure 4.3: Viscosity (rotating viscometer) of glasses D4, D3T3, G1, G2 and G5

Glass G1 (composition cf. Table 4.1) showed a viscosity similar to that of glass D4. As Figure 4.3 demonstrates, however, the viscosity was different for different revolutions (10 and 250 min⁻¹). This non-Newtonian behavior can be attributed to the chain structure of the glass and is typical for phosphate glasses mainly consisting of phosphate chains as shown in extrusion experiments [123-126]. It is caused by entangled phosphate chains which hinder rotation during the measurement procedure. At higher rotations, the phosphate chains become aligned, hence, they offer less resistance to the movement of the rotating viscometer.

Glass D3T3 (composition in mol%: 48.3 P₂O₅ - 24 CaO - 4.4 MgO - 19.6 Na₂O - 3.7 TiO₂) gave a viscosity in a similar range (Figure 4.3) and also showed non-

Newtonian flow. Glass D3T2 crystallized during the experiment, so no viscosity curve was obtained. This stronger crystallization tendency was probably due to the lower titania content in comparison with glass D3T3 (2.5 mol% TiO₂ vs. 3.7 mol%). Of glass G2, which had a composition similar to that of glass D3T2 (48 mol% P₂O₅ and 2.5 mol% TiO₂ but less MgO and a higher Na₂O content), a viscosity curve was obtained (Figure 4.3); however, at temperatures around 600 °C and below the measurement was affected by crystallization.

Table 4.4: Viscosity (η) at 550 °C and 600 °C

glass	P ₂ O ₅ conc. mol%	lg(η) at 550°C η in dPa s	lg(η) at 600°C η in dPa s
D4	52.5	3.57	2.86
G1	50.0	3.94	(3.21/3.42)*
D3T3	48.3	4.24	(3.06)*
G2	48.0	4.40	(3.39)**
G5	46.0	3.38	2.64

* affected by non-Newtonian flow

** affected by crystallization

Although glass G5 had a phosphate content of only 46 mol%, a low titania concentration (1.5 mol% TiO₂) and contained a significant amount of Q¹ groups (cf. Chapter 4.1.1), a viscosity curve was obtained (Figure 4.3). Glass G6, which had a similar composition but contained only 45 mol% P₂O₅ and an alkali concentration increased by 1 mol%, showed a crystallization tendency too high for viscosity measurements. This can be attributed to the higher concentration of Q¹ groups, i.e., the significant amount of depolymerization in the glass in comparison with the other glasses (cf. Chapter 4.1.1).

The viscosity results obtained were interesting for fiber production using crucible techniques. However, crystallization of some of the glasses was too high and needs to be controlled.

4.1.3 Solubility

pH measurements

pH of the glasses in physiological salt solution was tested over 10 days. The pH of the solution was measured every 24 hours, afterwards the salt solution was exchanged.

Figure 4.4 shows mean values for some representative glasses as well as the confidence interval. Results for all glasses are given in Appendix D. The aim was to develop a glass which did not lower the pH of the surrounding medium too much but gave a pH near to physiological pH which is around 7.36. As the physiological salt solution used was not buffered and the pH of the salt solution is low due to the low pH of the deionized water, the results of the pH measurements can only give a faint hint on which glasses to use in further experiments. Especially for glasses with low solubility (cf. Chapter 4.2.2) the pH obtained in the experiment is lower than it would have been if the initial pH of the physiological NaCl solution had been around 7.36. However, for glasses with higher solubility, the results of the pH measurements agree with the results of further tests, e.g. of biocompatibility as shown in [127].

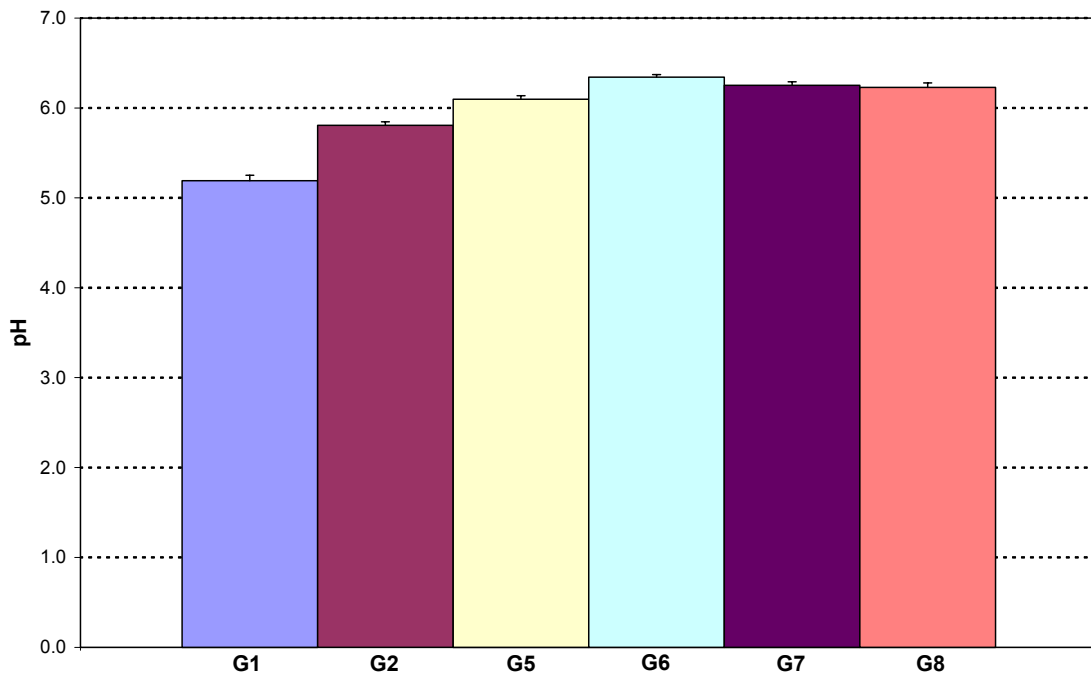


Figure 4.4: pH of polyphosphate glasses in physiological NaCl solution (mean \pm standard deviation)

For all glasses the pH was below 6.4. Except for glass D4, all glasses showed a relatively constant pH over the measurement period. The pH of glass D4 increased linearly within the entire period of time studied (cf. Figure 4.5). Therefore the pH of this glass was tested over 16 days instead of 10 days. During this time the pH rose from 2.9 to 4.7; after 16 days the glass was completely dissolved. The change in pH showed that the glass did not dissolve uniformly.

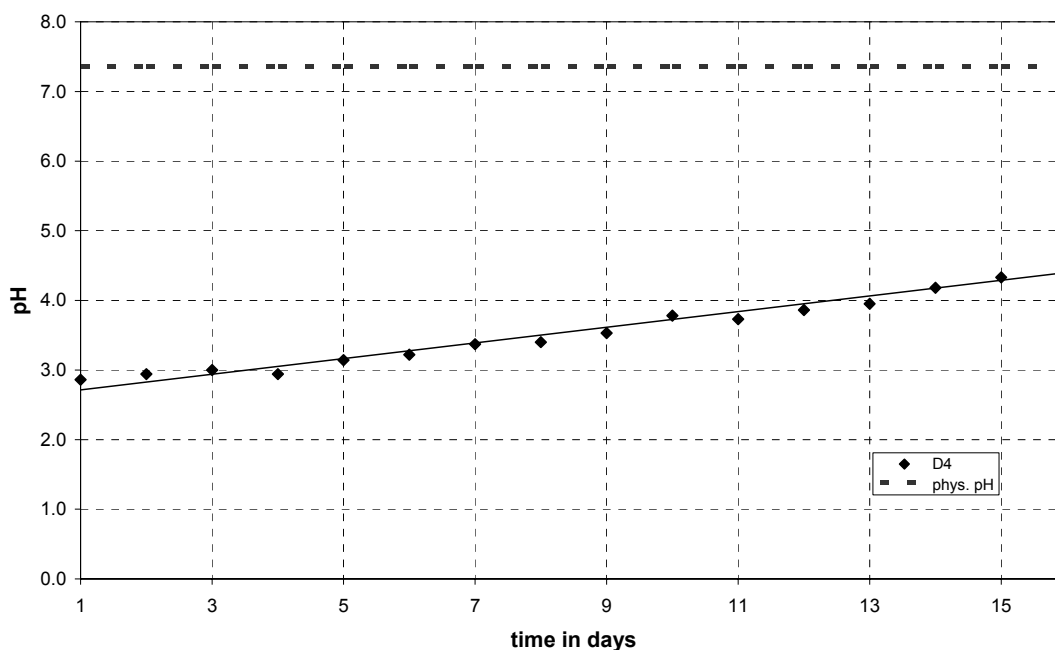


Figure 4.5: pH of glass D4 in physiological NaCl solution over 16 days (line: regression line)

Time-constant solubility in deionized water

The solubility of polyphosphate glasses in the system P_2O_5 -CaO-MgO- Na_2O -(K_2O)- TiO_2 with phosphate contents between 45 and 50 mol% was tested in time-constant and time-dependent degradation tests. All results are given in Appendix C. Results of time-dependent tests are discussed later. Solutions were analyzed using ICP-OES with respect to the concentration of phosphate, alkali, alkaline earth, titania, silica and other components. However, as P_2O_5 is the network forming component, dissolved phosphate is directly linked with dissolution of the glass structure, i.e. the phosphate network. Therefore discussion of the dissolution behavior will focus on the dissolution of phosphate. The phosphate glasses showed a uniform dissolution. Figure 4.6 shows the ratio P_2O_5 /other oxides in solution vs. ratio P_2O_5 /other oxides in the glass composition. No selective alkali leaching, which is known from silica based glasses, was observed. Hence, dissolved phosphate reflects the amount of other oxides dissolved.

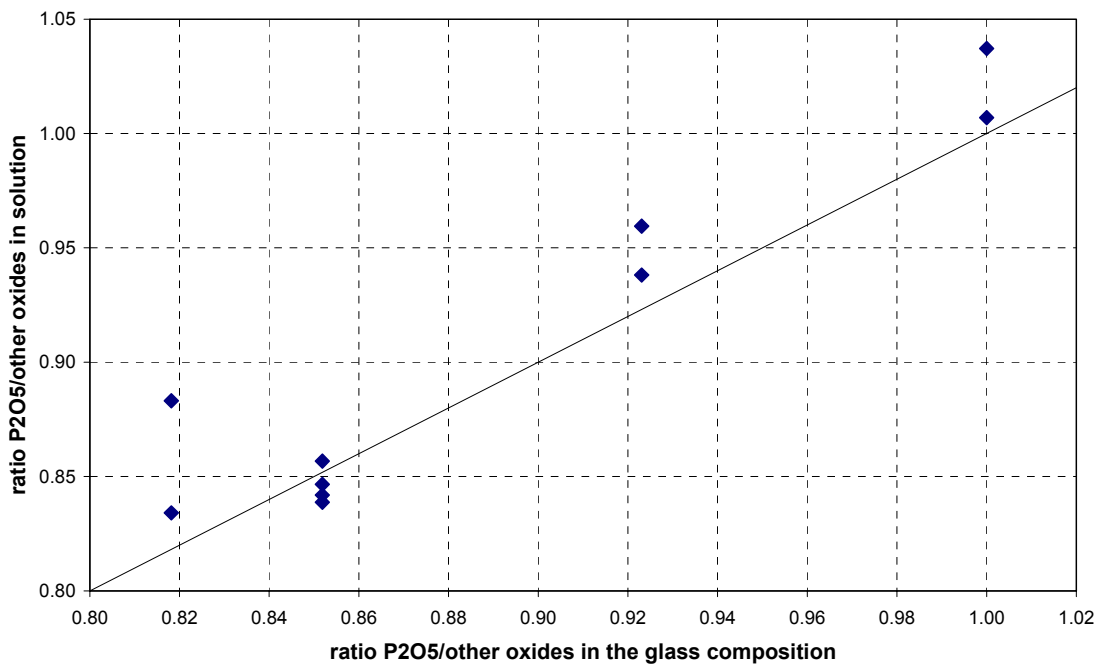


Figure 4.6: Ratio P_2O_5 /other components in solution vs. ratio P_2O_5 /other components in the glass (line: ratio 1:1)

Solubility of the glasses strongly depends on the glass composition. Especially the phosphate content influences the dissolution rate. Figure 4.7 shows the dissolved P_2O_5 for glasses with phosphate contents between 45 and 50 mol%. As the results demonstrate, the amount of dissolved oxides was reduced by two orders of magnitude by reducing the phosphate content from 50 to 45 mol%. Glass G1, which had a P_2O_5 content of 50 mol%, showed the highest solubility and gave an amount of about 10 g/L dissolved P_2O_5 . Glass G6 (45 mol% P_2O_5) showed the lowest solubility of about 250 mg/L P_2O_5 .

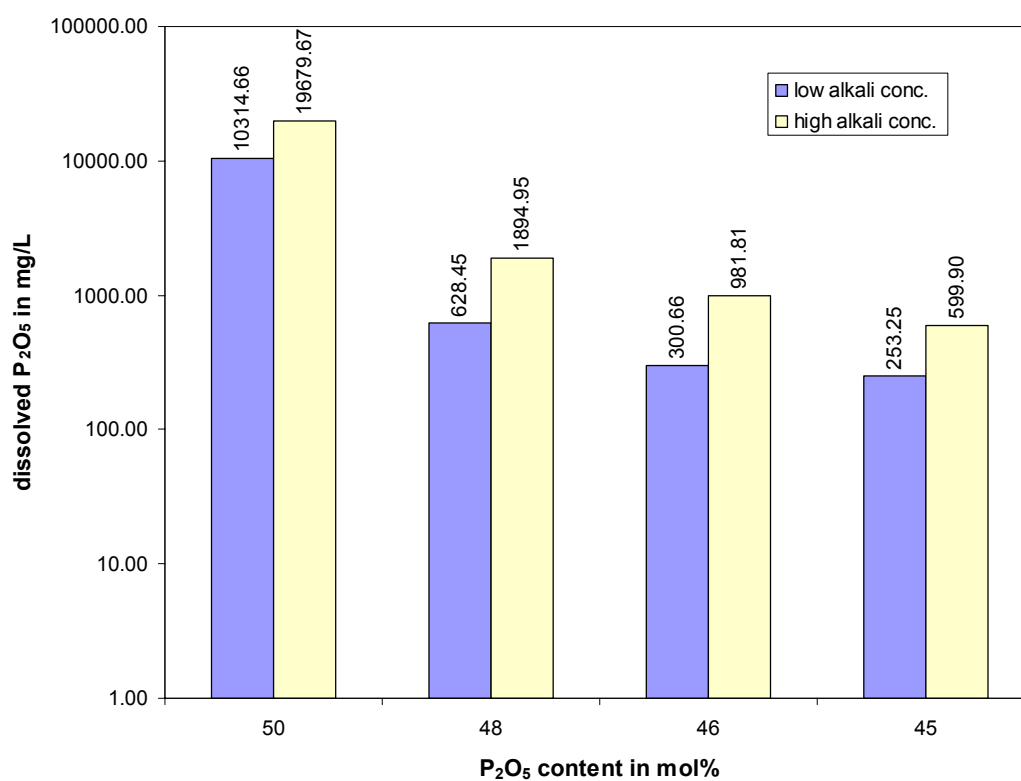


Figure 4.7: Dissolved P₂O₅ vs. P₂O₅ content in the glass for low (left) and high (right) alkali oxide contents

Figure 4.7 shows the amount of dissolved phosphate as a function of alkali oxide concentration in the glass. Additional alkali oxide (sodium oxide and potassium oxide) was added while the amount of calcium oxide and magnesium oxide was reduced. The increase in alkali oxide content, i.e. the reduction of CaO and MgO contents, resulted in a significant increase in solubility. For glasses G1 and G1N30, increasing the sodium oxide content from 25 to 30 mol% (which corresponds to a decrease in CaO concentration from 20 to 15.5 mol% and a decrease in MgO concentration from 2 to 1.5 mol%) doubled the amount of dissolved phosphate (10 g/L to 20 g/L). For the other glasses, results are similar. Glass G2 (21.5 mol% Na₂O, 24 mol% CaO, 4 mol% MgO) gave about 630 mg/L P₂O₅ while G2N25 (25 mol% Na₂O, 21 mol% CaO, 3.5 mol% MgO) gave an amount of dissolved P₂O₅ which was three times larger (1.89 g/L).

Modeling of solubility

Results for modeling and chemometric evaluation of the glass solubility are given in Chapter 4.2.2.

Time-dependent solubility in deionized water

In order to determine the dissolution as a function of time, glasses were soaked in deionized water at 98 °C for 1, 2, 5 and 8 hours respectively. Figure 4.8 shows the leaching behavior of glass G1, which showed the highest solubility in time-constant experiments (cf. above). The dissolution rate was high at the beginning but decelerated with time. Dissolution in the range from 300 to 480 min was nearly constant.

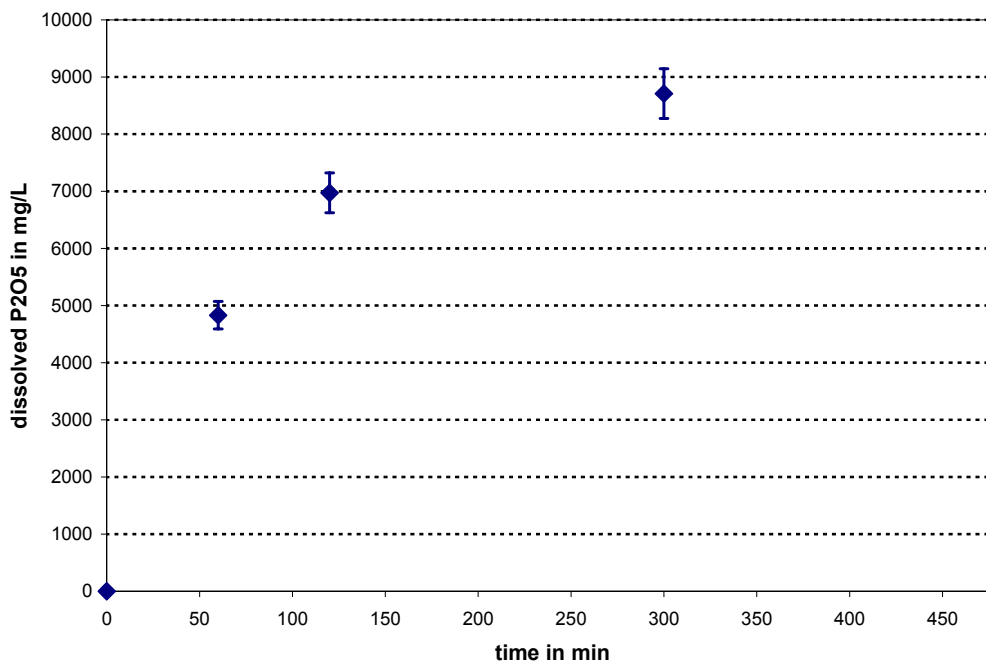


Figure 4.8: Time-dependent solubility of glass G1

Figure 4.9 shows the dissolution curves of the glasses G2, G5, G6, G7 and G8. All glasses showed a linear dissolution behavior. None of the glasses showed a deceleration in dissolution rate as it was seen for glass G1. Dissolution experiments over a longer period would show if this deceleration occurred later. However, maximum dissolution time was 480 min. G2 showed the highest dissolution rate of the five glasses; still, the solubility is significantly lower than the one of G1. This corresponds to the results of the time-constant experiments (cf. above). Glasses G5, G6, G7 and G8 show considerably lower dissolution rates, i.e. they are more stable to hydrolysis than glasses G1 and G2. This is due to the smaller P₂O₅ contents of the glasses. Decreasing the P₂O₅ concentration makes the glasses more stable to moisture attack. This can be attributed to the fact that Q² units, i.e. chain middle groups, are most susceptible to hydrolysis [57].

According to ^{31}P MAS-NMR results (cf. Chapter 4.1.1) glasses G5 and G6 show much larger amounts of Q^1 units in comparison with glasses G1 and G2. This depolymerization of phosphate chains results in a decreased tendency for hydration and subsequently in a decrease in solubility.

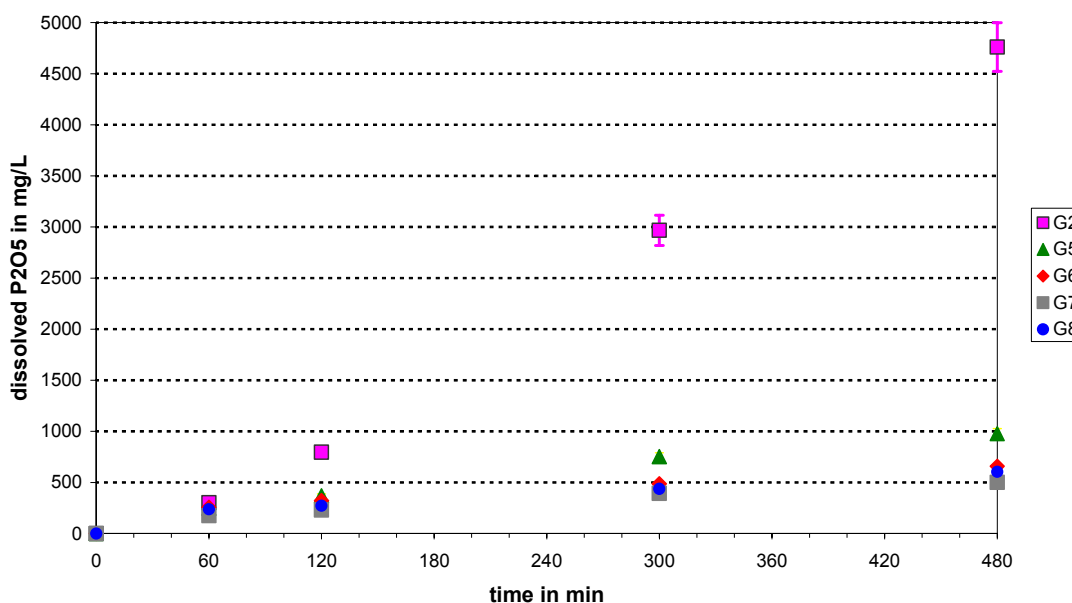


Figure 4.9: Time-dependent solubility of glasses G2, G5, G6, G7 and G8

All polyphosphate glasses investigated showed high dissolution rates. By changing the chemical composition, the solubility of the glasses was reduced by several orders of magnitude. However, solubility of the glasses was still too high for use as degradable implant material. Furthermore, the glasses were too acidic, i.e. the pH of the glasses in physiological salt solution was too low. Therefore glasses in the pyrophosphate region with phosphate contents below 40 mol% were prepared and their dissolution behavior was tested.

4.2 Pyrophosphate glasses

A range of invert glasses based on glass Mg5 (cf. Table 3.2) were produced. In previous experiments glass Mg5 was shown to have an invert glass structure mainly consisting of diphosphate groups (> 90 %), with less than 5 % of phosphate chains and

orthophosphate groups, respectively [128]. Furthermore, the good biocompatibility of glass Mg5 was shown in animal experiments [112,113].

In spite of the relatively high crystallization tendency of some of the glasses all glasses were obtained in a glassy state by quenching the glass melt between copper blocks. Crystallized parts were mechanically removed before accomplishing any further experiments. Resulting glasses were transparent and colorless. Only glasses with high titania concentrations showed a light yellowish or purple/brownish coloring.

Glass compositions were analyzed using ICP-OES analyses. As shown in Appendices A and B, synthetic and analytic glass compositions were comparable. No systematic changes in composition, e.g. due to evaporation of phosphate, were observed.

4.2.1 Density, crystallization and viscosity

Glasses with phosphate contents between 34 and 37 mol% had densities between 2.67 and 2.77 g/cm³. Glass transition temperatures were in the range from 411 to 487 °C. The change in density and T_g for glasses containing TiO₂ and Al₂O₃ clearly show a densification of the network and an increase in glass transition temperature. Incorporation of 1 mol% (NA1) and 5 mol% Al₂O₃ (NA5) resulted in a increase in T_g from 422 °C (base glass Mg5) over 437 °C (NA1) to 472 °C (NA5). Results for incorporation of TiO₂ were similar. In glasses NT1, NT5 and NT10, CaO, MgO and Na₂O were proportionally substituted for titania. This resulted in an increase in T_g from 433 °C (NT1) to 487 °C (NT10). Simultaneously, the density of the glasses changed from 2.74 g/cm³ (NT1) to 2.78 g/cm³ (NT1). The density of base glass Mg5 was 2.73 g/cm³. Results for other glasses with incorporated titania (BT1-10) were similar.

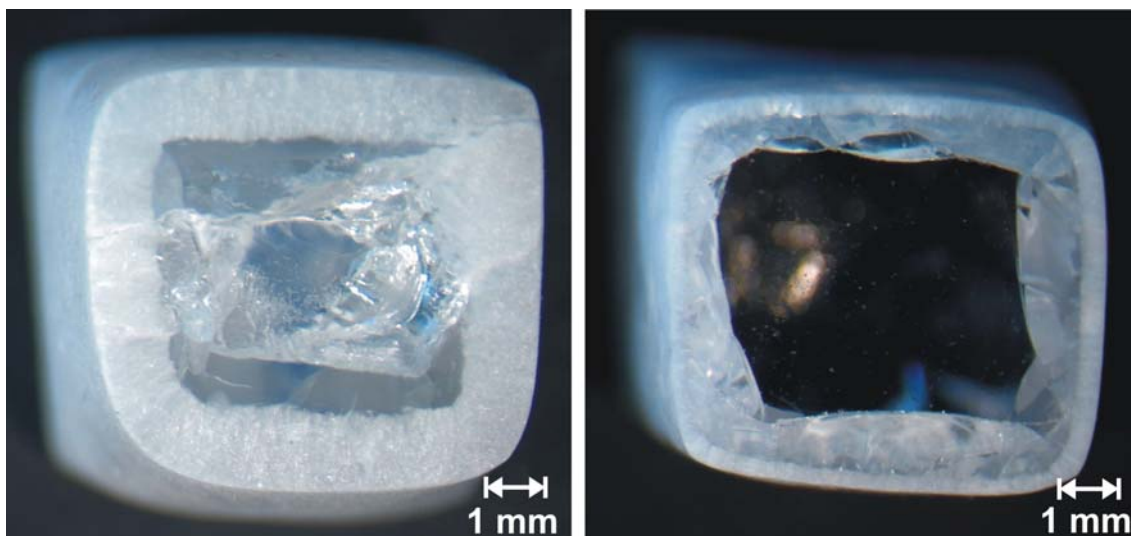


Figure 4.10: Crystalline surface layers after tempering for 30 min at 540 °C: Glasses Mg5 (left) and T5 (right)

Glasses in the pyrophosphate region generally show a larger crystallization tendency than polyphosphate glasses [57]. All investigated pyrophosphate glasses showed surface crystallization. The crystallization behavior of the glasses was investigated by measuring the thickness of the crystallized layer on the surface of cubic samples. Micrographs of the crystalline surface layers of glasses Mg5 and T5 are shown in Figure 4.10. Crystallization of glass NH1 (1 mol% F⁻) could not be investigated using this procedure as the glass showed surface crystallization as well as volume crystallization and therefore the thickness of the crystalline surface layer could not be measured properly. Crystal phases of the crystalline surface layers were mainly diphosphates of calcium, magnesium and sodium. Crystal phases of all investigated glasses are given in Appendix D. X-ray spectra of powdered samples and of crystalline surface layers (Figure 4.11) showed significant differences, which is a sign for a textured structure. The peak at about 29.6 ° is the maximum peak in X-ray spectra of crystalline surfaces. It can be attributed to either magnesium phosphate (MgP₂O₇, (012) peak) or calcium phosphate (CaP₂O₇, (008) peak). This points at a texture in (008) direction, which agrees with the assumption of crystals growing in an angle of 90 ° from the surface into the sample.

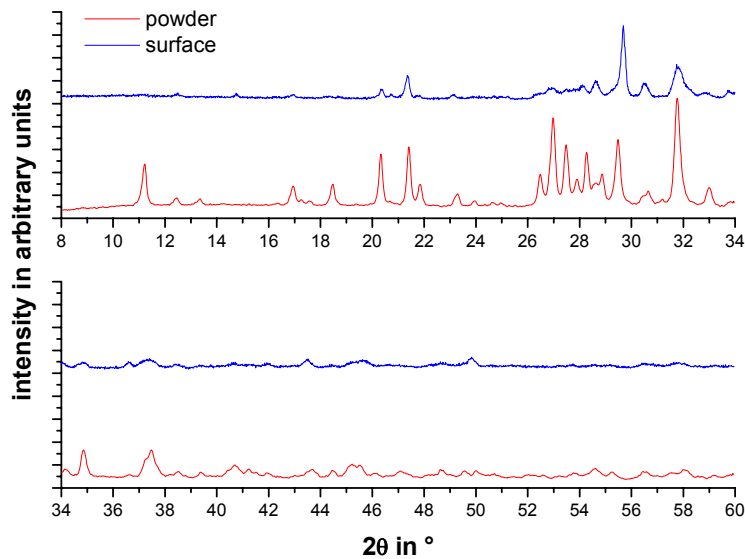


Figure 4.11: X-ray spectra of powder and crystalline surface of glass T5 (tempered for 30 min at 600 °C)

Crystallization curves of glasses Mg5 (basic glass), NS1 (1 mol% SiO₂), NA1 (1 mol% Al₂O₃) and CK1 (1 mol% K₂O) showed no significant differences (Figure 4.12). The addition of 1 mol% SiO₂, Al₂O₃ or K₂O had no apparent influence on the crystallization behavior in the temperature range investigated. Glasses with additions of 1 mol% and 5.45 mol% TiO₂ showed formation of a crystalline surface layer at higher temperatures than the other glasses. Hence, addition of 1 and 5.45 mol% reduced the crystallization tendency of the glasses in the temperature range which is of interest for the fabrication of porous specimens and glass fibers. However, all glasses in the pyrophosphate region investigated showed a crystallization tendency which was considerably higher than crystallization tendencies of polyphosphate glasses (cf. Chapter 4.1.1).

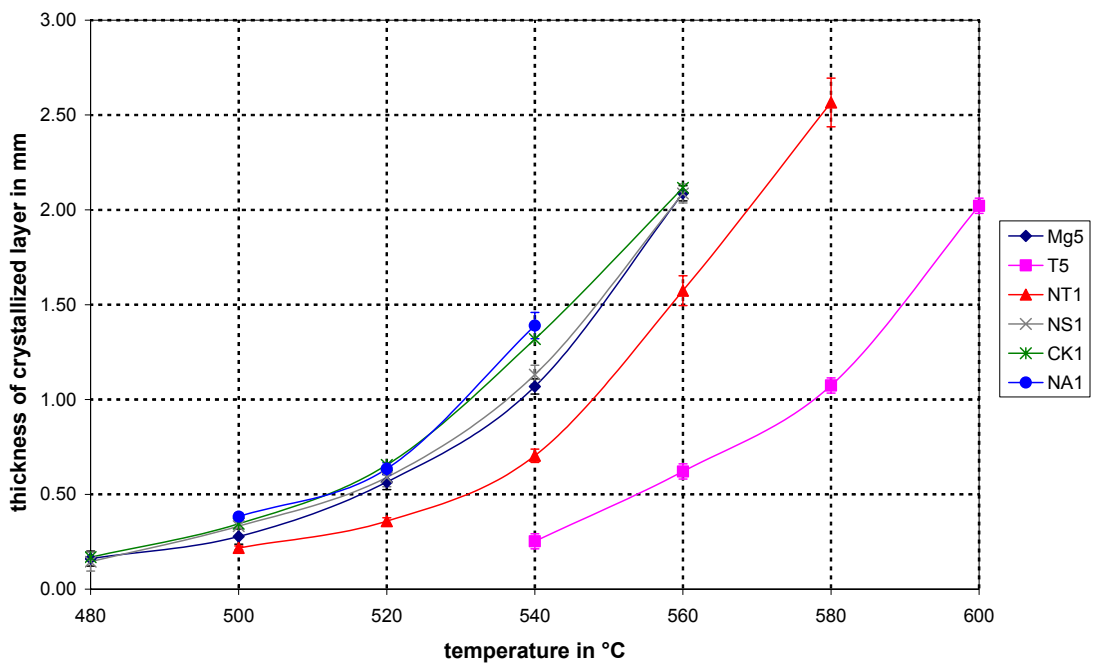


Figure 4.12: Crystallization of pyrophosphate glasses (tempered for 30 min)

Glass T5 was the pyrophosphate glass which showed the smallest tendency to crystallize. The viscosity curve for the temperature range from 480 to 520 °C is shown in Figure 4.13.

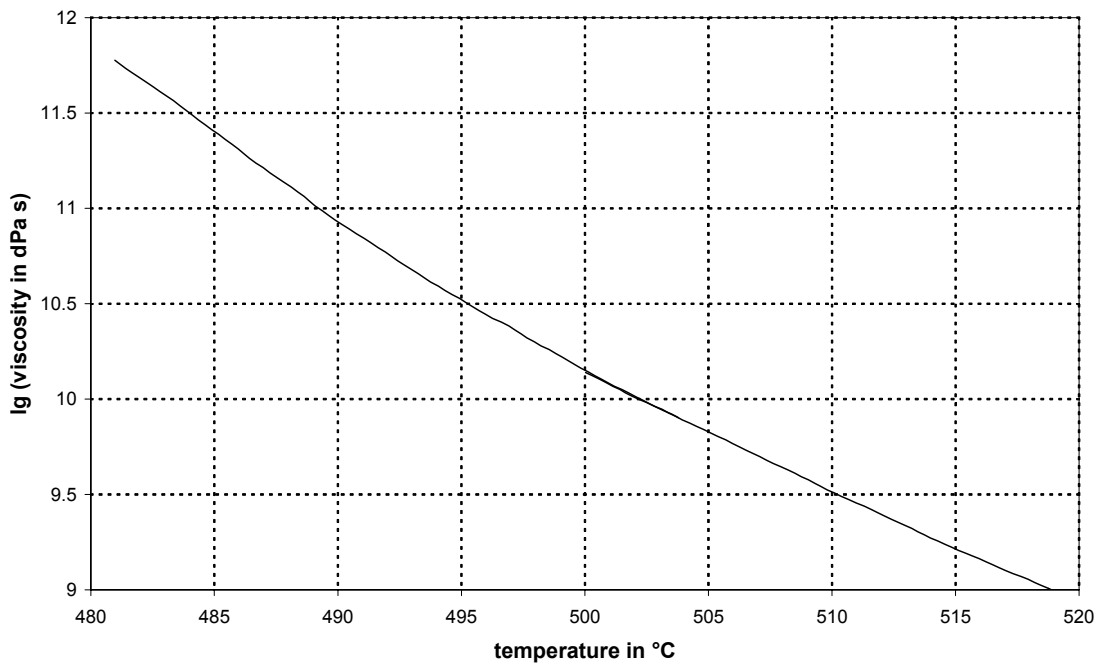


Figure 4.13: Viscosity curve (beam bending viscometer) of glass T5

4.2.2 Solubility

pH measurements

Glasses with phosphate contents between 34 and 37 mol% showed pH values in physiological sodium chloride solution between 6.6 and 7.5. However, the lower pH values were due to the low solubility of the glasses and the slightly acidic pH of the deionized water used. Figure 4.14 gives the mean pH values and weight loss for some of the glasses after immersion in physiological NaCl solution over 10 days; all results are given in Appendix D.

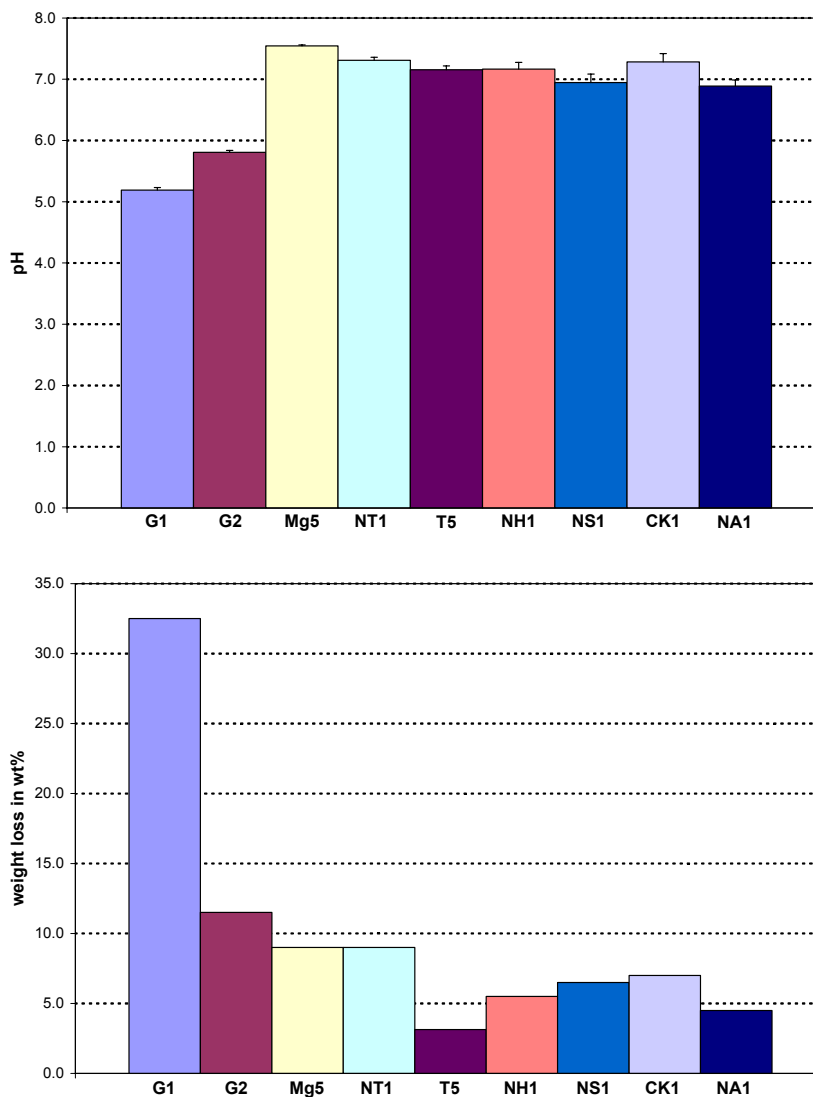


Figure 4.14: pH of glasses in physiological NaCl solution (mean \pm confidence interval) (top); weight loss after 10 days in physiological NaCl solution (bottom)

Solubility in deionized water

Different additives (Al_2O_3 , F-, Fe_2O_3 , K_2O , SiO_2 , TiO_2 , ZnO , ZrO_2) were given to a base glass (Mg5) in concentrations between 1 and 10 mol% and their influence on the solubility was investigated. Solubility in deionized water at 98 °C over 60 min was tested. Results for some of the glasses investigated are shown as total oxides dissolved in Figure 4.15. All results are given in Appendix C. Solubility of pyrophosphate glasses in deionized water was considerably lower than solubility of polyphosphate glasses (cf. Chapter 4.1.3).

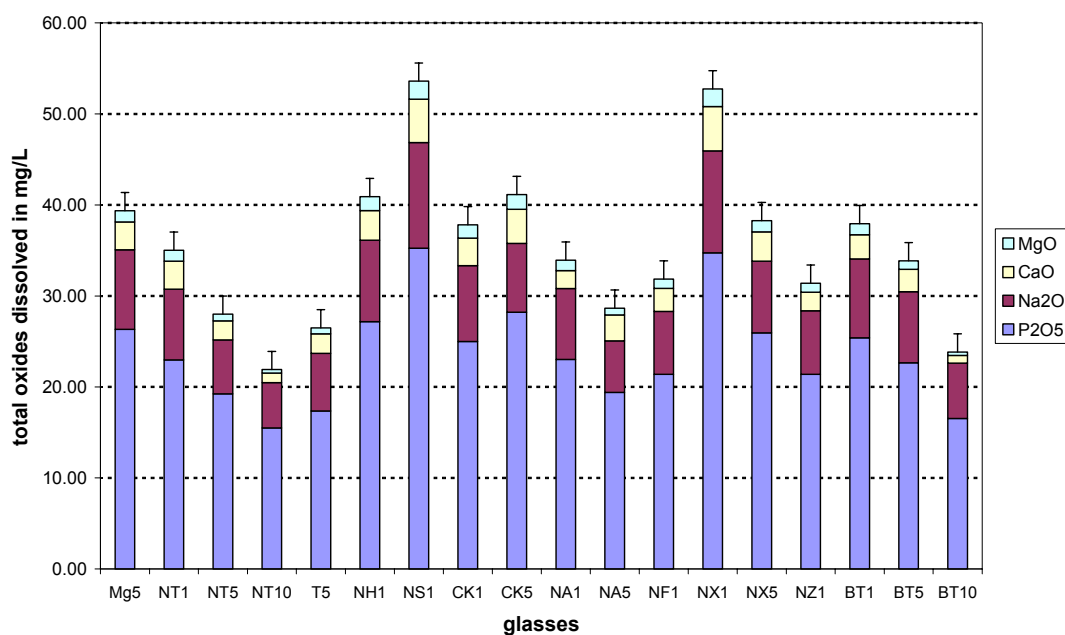


Figure 4.15: Total oxides dissolved (mean \pm 95% confidence interval)

Only addition of SiO_2 clearly increased the solubility of the glass. Glasses with additions of fluoride, ZnO and K_2O showed somehow ambivalent results. The solubility of the fluoride containing glass (NH1) was not significantly higher than the solubility of MgO. Addition of 5 mol% K_2O (CK5) increased the solubility significantly whereas the addition of 1 mol% K_2O (CK1) had no apparent influence. Addition of 1 mol% ZnO (NX1), however, increased the solubility considerably, while the glass with 5 mol% ZnO (NX5) showed a solubility similar to that of MgO.

As expected, addition of TiO_2 and Al_2O_3 reduced the solubility of the glasses [72,129]. Addition of 1 mol% TiO_2 (NT1) gave an amount of P_2O_5 dissolved which was 14 % lower than the original one. The solubility of the glass with 5 mol% TiO_2 (NT5) and

10 mol% TiO₂ (NT10) was reduced by 28 % and 42 %, respectively. The results for glasses BT1, BT5 and BT10 were similar. Again, TiO₂ was added in concentrations of 1, 5 and 10 mol%, respectively. But in contrast to glasses of the N series, P₂O₅ and Na₂O concentrations were kept constant while CaO and MgO were partially substituted for titania. This resulted in a decrease in solubility of 5 % (BT1), 15 % (BT5) and 48 % (BT10) with respect to the amount of dissolved P₂O₅. For glass T5 (5.45 mol% TiO₂) all components, i.e. P₂O₅, CaO, MgO and Na₂O, were proportionally substituted for TiO₂. T5 gave an amount of dissolved P₂O₅ which was 35 % less than for glass Mg5. Addition of 1 mol% Al₂O₃ (NA1) and 5 mol% Al₂O₃ (NA5) resulted in a decrease in solubility of 14 % and 27 %, respectively. Both glass NF1 (1 mol% Fe₂O₃) and NZ1 (1 mol% ZrO₂) showed an amount of dissolved P₂O₅ which was 20 % less than for glass Mg5.

Modeling of solubility

As values of dissolved P₂O₅ in mg/L seemed to increase exponentially with increasing P₂O₅ content (cf. Figure 4.7 in Chapter 4.1.3) MLR was used to describe lg(dissolved P₂O₅) as a linear function of glass components, i.e. concentrations of P₂O₅, CaO, MgO, Na₂O and TiO₂. Figure 4.16 shows the graph of observed P₂O₅ dissolved vs. predicted P₂O₅ dissolved and the 95 % confidence interval. The correlation coefficient was 0.93 and several data points were lying outside the confidence band.

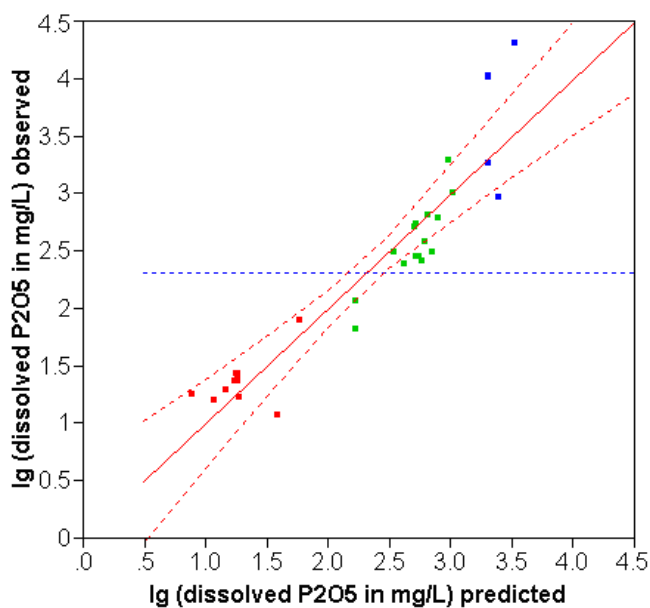


Figure 4.16: MLR: observed by predicted plot and 95 % confidence band (correlation coefficient: 0.93; red: pyrophosphate glasses, green: polyphosphate glasses, blue: meta-/ultra-phosphate glasses)

Therefore artificial neural networks were used since they are non-linear and hence should be more suitable for describing and modeling the correlation between solubility and glass composition. The network employed calculated values for dissolved P_2O_5 from the glass composition. Figure 4.17 shows the observed vs. predicted plots. The correlation coefficient was 0.9996.

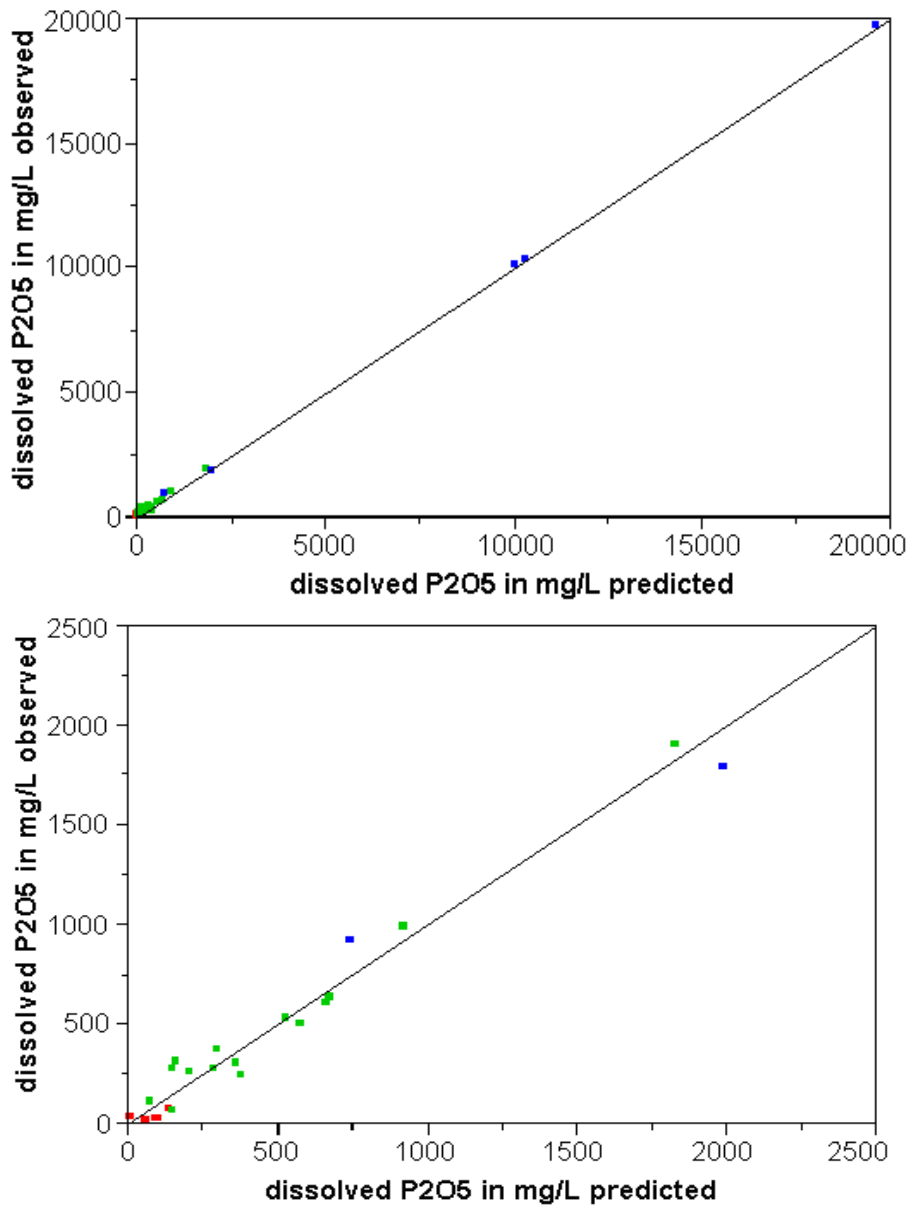


Figure 4.17: NN: observed by predicted plot (correlation coefficient: 0.9996; red: pyrophosphate glasses, green: polyphosphate glasses, blue: meta-/ultraphosphate glasses)

4.2.3 Cell experiments

Proliferation of MC3T3-E1.4 cells

Proliferation of MC3T3-E1.4 osteoblast-like cells was tested on six different glass compositions (Mg5, NT1, T5, NH1, NS1 and CK1) over 24 hours. Results are shown in Figure 4.18. Cells proliferated on all six glasses; the cell concentration at 24 h was significantly higher than the cell concentration seeded (50,000 cells/cm²). There were no significant differences between cell concentrations on the different substrates (ANOVA, $p > 0.05$). However, at 24 h cell concentration on all six glasses was significantly lower than on TCPS control (ANOVA, $p < 0.05$).

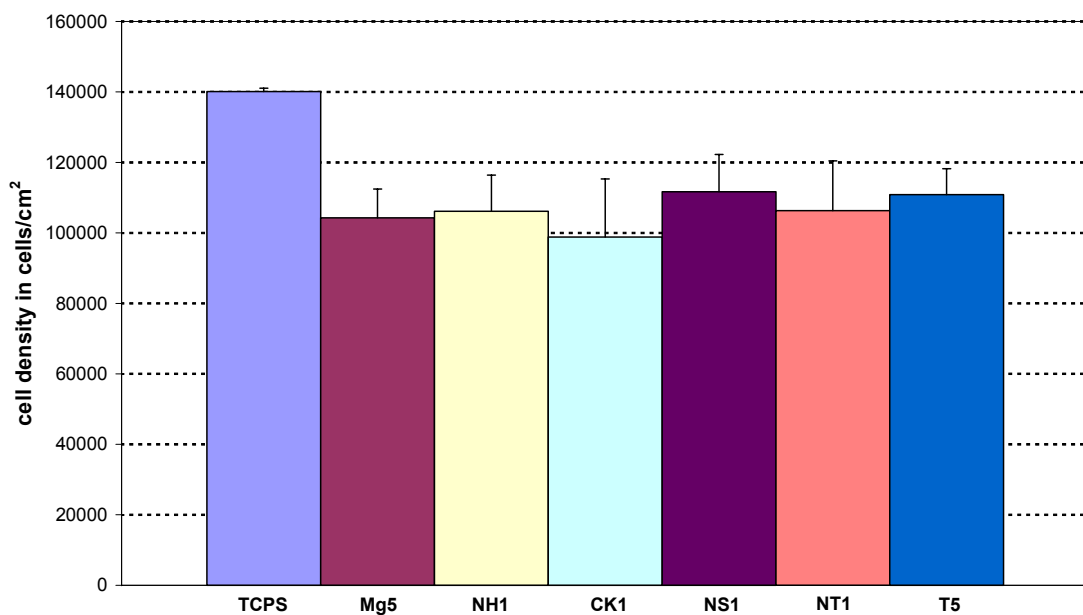


Figure 4.18: MC3T3-E1.4 concentration on polished glasses at 24 h (mean \pm standard deviation)

For three of the glasses (Mg5, NT1 and T5) proliferation over 72 h was investigated as well. Results are shown in Figure 4.19. Cell numbers at 72 h were higher than at 24 h but not proportionally higher. This was probably due to the fact that the cell layer at 24 h was already nearly confluent and therefore the sample surface area limited further cell growth. This was confirmed by SEM investigations. Figure 4.20 shows SEM micrographs of a confluent cell layer on glass Mg5 after cell cultivation over 24 h. The cracks around the cell nuclei on the left hand side micrograph were caused by an

incomplete dehydration process prior to critical point drying. The picture on the left hand side shows the exposed glass surface with scratches, which are artefacts of the polishing procedure, and the cell layer. However, during the dehydration and fixation process, cell layers of some samples were washed off the glass surface. This indicates that cell adhesion on the glasses was affected by glass dissolution.

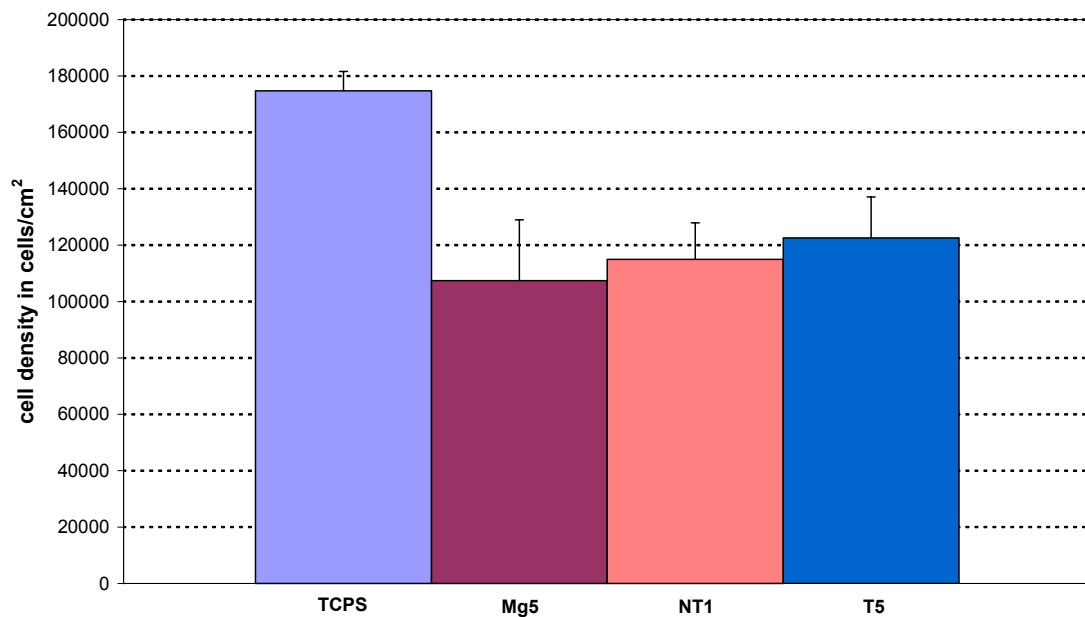


Figure 4.19: MC3T3-E1.4 concentration on polished glasses at 72 h (mean \pm standard deviation)

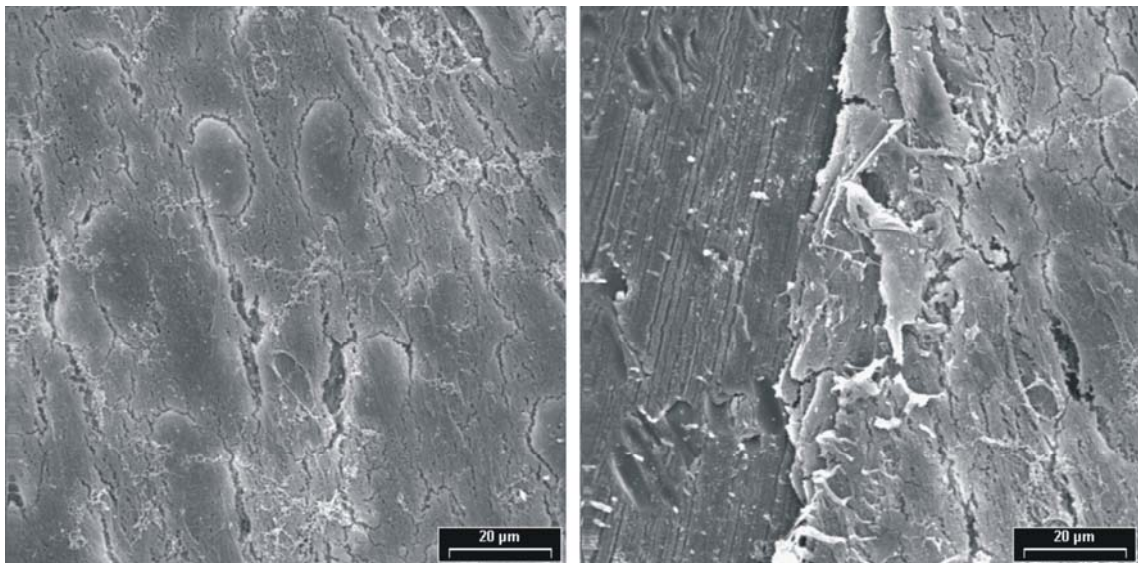


Figure 4.20: MC3T3-E1.4 cell layer on polished glass Mg5 at 24 h (left: confluent cell layer; right: cell layer and exposed glass surface)

Proliferation of dental pulp stem cells

Additional cell tests were carried out using human dental pulp stem cells (DPSCs). Cell proliferation was tested on polished non-porous glasses Mg5, T5 (5.45 % TiO₂) and NT1 (1 % TiO₂) over 24 hours. Results are shown in Figure 4.21. Cells proliferated only on glass T5 while cell concentrations on glasses Mg5 and NT1 were lower than the cell concentration seeded. Cell numbers were significantly different on each sample and significantly lower than on TCPS (ANOVA $p < 0.05$).

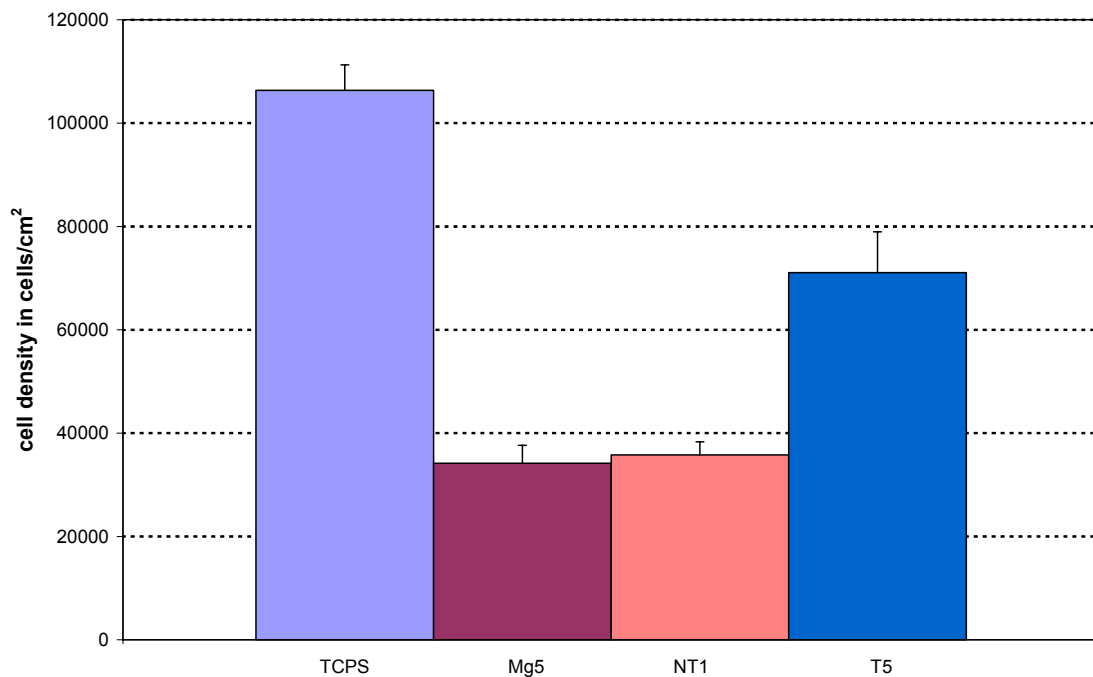


Figure 4.21: DPSC concentration on polished glasses at 24 h (mean \pm standard deviation)

Sterilization

For cell experiments glasses and composites were sterilized using γ -irradiation over night ($2.6 \cdot 10^5$ rd total after 15 h). During the sterilization process the glasses turned slightly red. This color formation can be attributed to radiation defects caused by γ -radiation. γ -rays can cause partial rupture of chemical bonds, partial destruction of the network, reduction of specific ions, introduction of defects, discoloration or fluorescence [130]. Optical spectroscopy measurements of γ -irradiated polished glass plates were carried out (UV-3101PC, Shimadzu, Kyoto, Japan). Absorbance between

350 and 700 nm corrected by absorbance of non-treated specimens is shown in Figure 4.22. The absorbance maximum is at 500 nm.

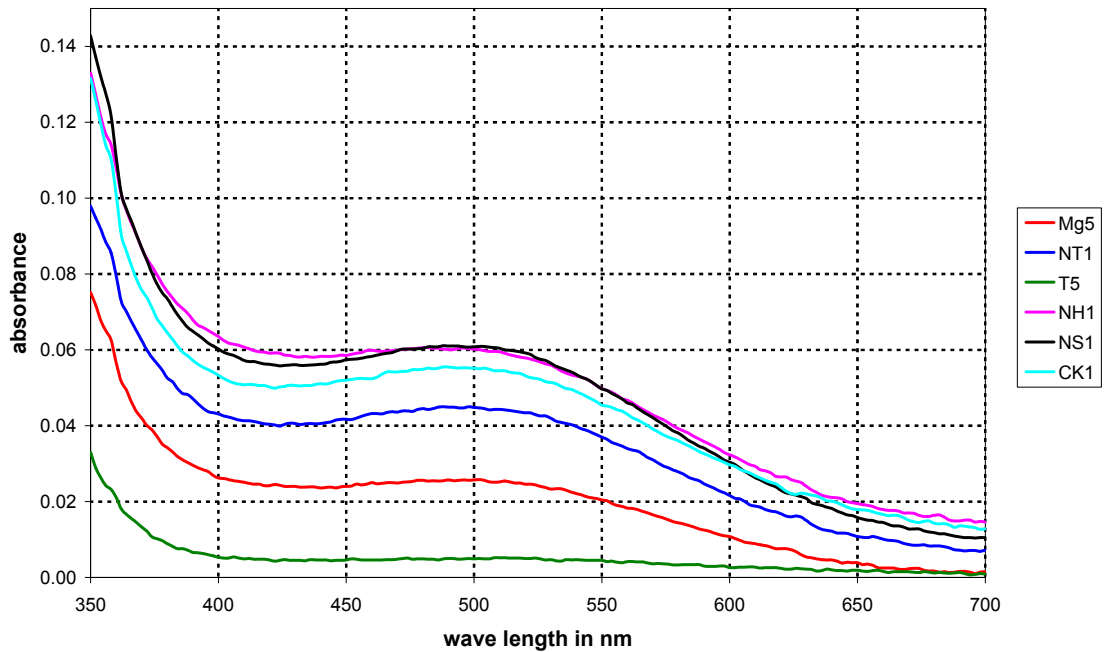


Figure 4.22: Absorbance of γ -irradiated glasses corrected by absorbance of non-irradiated glasses

To ensure sterilization method had no influence on cell proliferation one set of polished glasses was sterilized using dry heat as a control. After standardizing the results using the TCPS cell concentrations, no influence of the sterilization protocol was seen (ANOVA $p > 0.05$). Results are shown in Figure 4.18 (γ -irradiated specimens, cf. above) and Figure 4.23 (heat sterilized specimens).

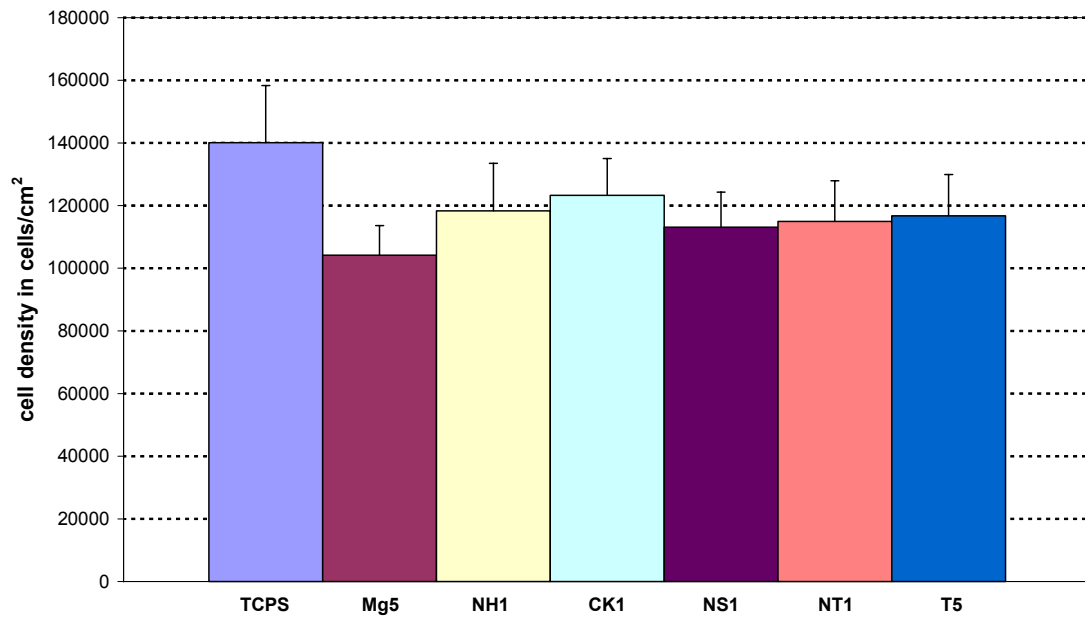


Figure 4.23: MC3T3-E1.4 concentration on heat-sterilized polished glasses at 24 h (mean \pm standard deviation)

4.3 Porous glasses and composites

4.3.1 Porosity

For sintered porous glass cubes, previous experiments showed that the porosity was around 65 % with about 15 % caused by micropores ($< 60 \mu\text{m}$) [116]. The pore diameters of the macropores were between 150 and 400 μm while the micropores caused by the sintering process showed pore diameters between 0.2 μm and 60 μm . Figure 4.24 shows SEM micrographs of macropores and micropores.

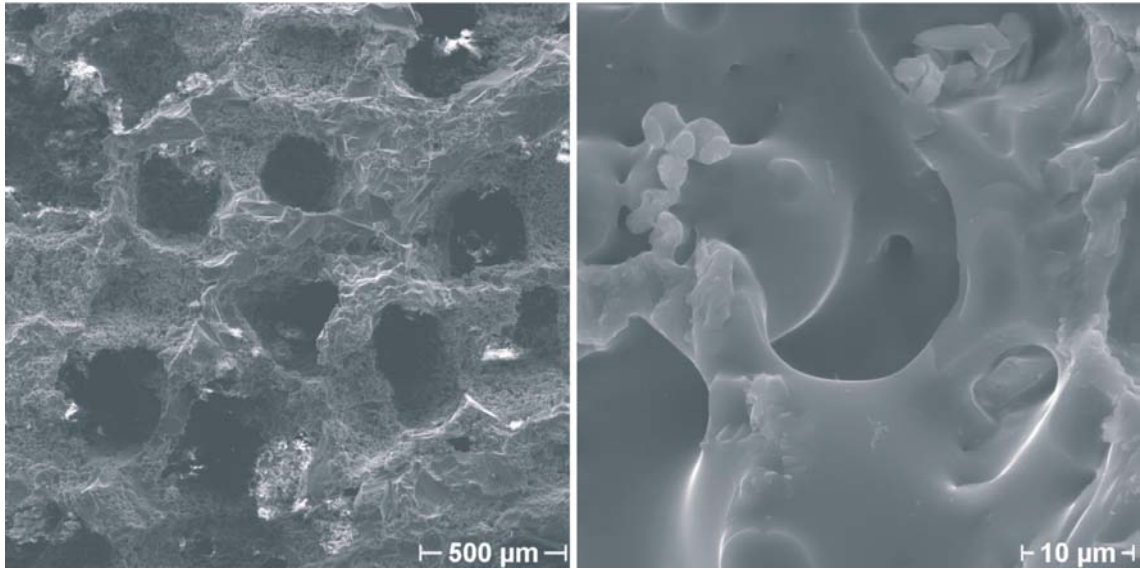


Figure 4.24: Macropores (left) and micropores (right) of sintered porous glass Mg5

The porous glass powder-reinforced polymer specimens had a porosity of about 45 %. Part of this porosity could be attributed to sodium chloride crystals. But another part of the porosity was caused by PEG 400 which acted as a pore builder as well. Figure 4.25 shows a SEM micrograph of a section of Mg5-reinforced porous polymer.

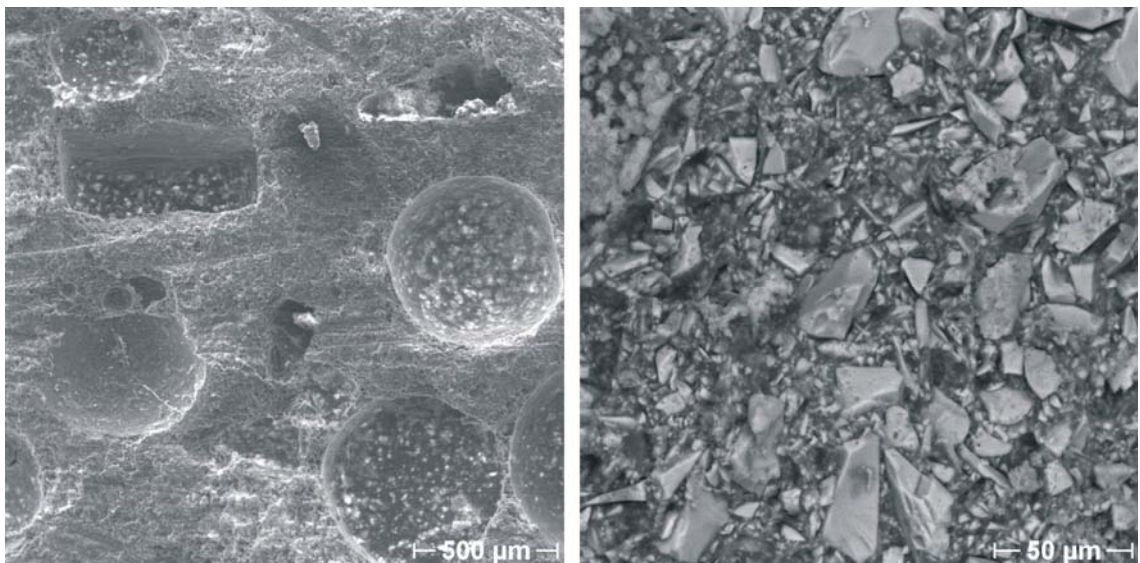


Figure 4.25: Section of Mg5-reinforced porous polymer

4.3.2 Compressive strength

The coating procedure chosen allowed coating of the inner surface of the porous specimens while leaving the open interconnective porosity unaffected. The polymer/glass ratio of the coated porous glasses was about 1:3. Polymer coating of the

porous glasses increased the compressive strength by an order of magnitude. Results are given in Table 4.5. Compressive strength of glass powder-reinforced porous polymer specimens is given in Table 4.5 and exceeded the compressive strength of the coated porous glasses considerably. In contrast to the uncoated porous glasses, the polymer/phosphate glass composites could be processed and shaped by conventional mechanical techniques such as drilling, grinding or sawing.

Table 4.5: Compressive strength of coated and uncoated sintered porous glasses and porous glass powder-reinforced polymer specimens

glass	σ_{\max} in MPa		
	uncoated	coated	polymer
Mg5	0.85 ± 0.33	4.64 ± 1.20	17.13 ± 1.65
T5	2.33 ± 0.48	7.33 ± 1.41	23.60 ± 2.72

4.3.3 Adhesive shear strength

Adhesion between polymer and polished and sintered glasses, respectively, was tested in shear strength experiments. Results are shown in Table 4.6. The schematic of the measurement procedure is shown in Figure 3.3. As the results clearly demonstrate adhesion of the polymer on the polished glasses was very low. During the experiments with polished glasses, the small glass plates came off the big ones easily and completely. None of the glass plates in the experiment were destroyed.

Table 4.6: Adhesive shear strength between polymer and polished and sintered glasses, respectively

Adhesive shear strength	
MPa	
sintered	4.13 ± 2.26
polished	0.95 ± 0.17

Measurement results for sintered non-porous glass plates were affected by the low stability of the sintered glass plates. When adhesion on sintered glasses was tested part of the glass plates fell apart during the measurement procedure while residues of the small plates were still sticking to the big ones. Hence, adhesion of the polymer on the sintered non-porous glass was considerably higher than the measurement results indicated and higher than adhesion on polished glasses. This was probably caused by the pores caused during the sintering process (Figure 4.26). Although there was no porogen added, the resulting samples show a significant amount of pores with pore sizes

up to 60 μm in diameter (cf. Chapter 4.3.1). Therefore adhesion of the polymer on sintered glasses was improved by sample topography.

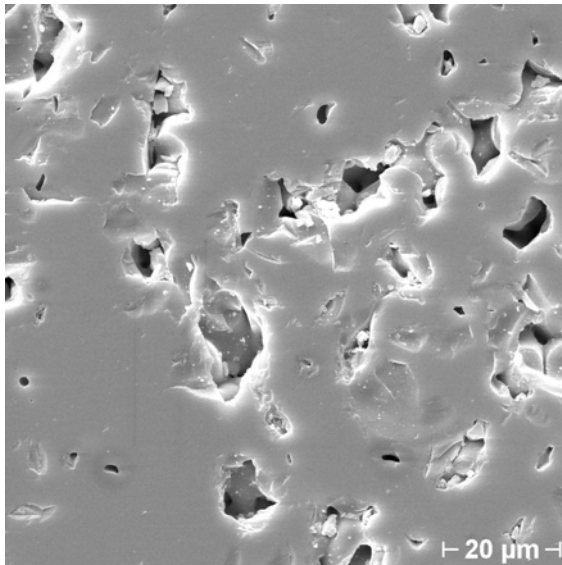


Figure 4.26: Micropores in glass Mg5 after sintering without NaCl

4.3.4 Solubility

Degradation in simulated body fluid

Degradation behavior of porous glasses and composites in SBF was tested up to 72 weeks. As Figure 4.27 shows, both glasses (Mg5 and T5) showed a linear degradation with time. Glass Mg5 (without TiO_2) degraded significantly faster than titania-containing glass T5. At 56 weeks Mg5 showed a weight loss of more than 25 wt% whereas glass T5 showed no remarkable degradation over 72 weeks. The weight loss was only about 2 wt%.

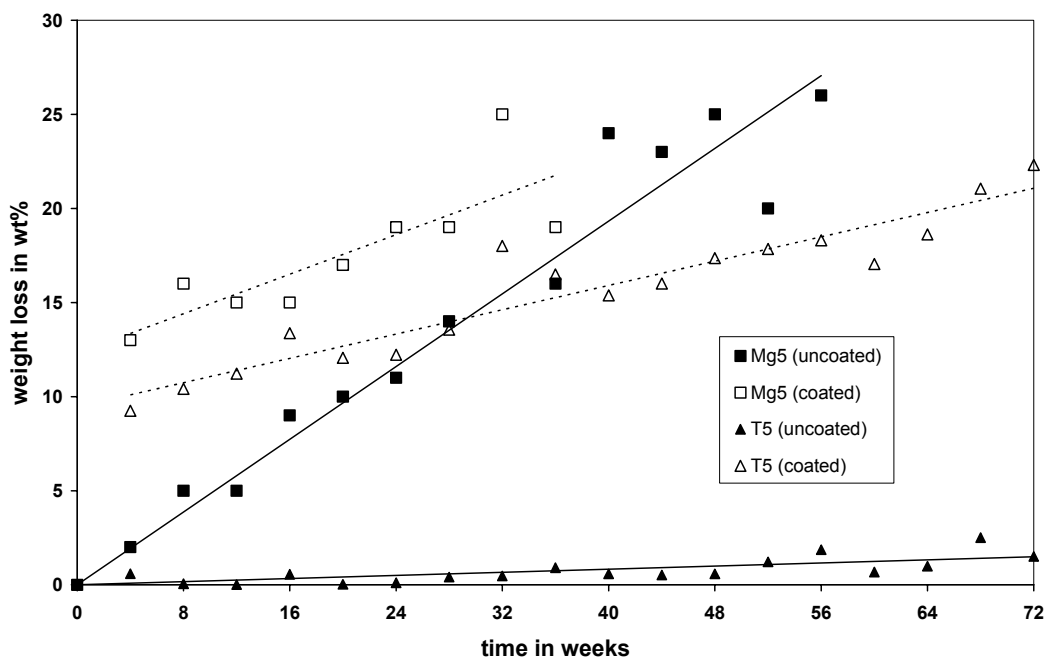


Figure 4.27: Weight loss of uncoated and polymer coated sintered porous glasses Mg5 and T5 in SBF at 37 °C (lines: regression lines)

Figure 4.27 also shows that the polymer degraded much faster than the glasses. After only four weeks, coated specimens Mg5 and T5 showed a weight loss of 13 and 9 wt%, respectively, whereas uncoated glass Mg5 only showed a weight loss of about 2 wt%. After this initial large degradation, the degradation rate decelerated and both coated specimens showed a linear degradation pattern. The two porous glasses with polymer coating are similar in their degradation behavior. This is due to the fact that the polymer dominated the degradation behavior and compensated for the different solubility of the glasses. It can be assumed that the constant degradation of coated glass T5 to a weight loss of more than 20 wt% over 72 weeks was mainly due to degradation of the polymer coating.

Degradation behavior of porous polymer specimens with glass powder reinforcement (Figure 4.28) was similar to that of coated porous glasses, i.e., the scaffolds showed a high degradation rate over the first 4 weeks which decelerated with time. Afterwards the degradation was linear. However, the degradations of reinforced polymer samples over the first 4 weeks was smaller (5 and 6 wt%) than those of polymer-coated porous glasses (9 and 13 wt%). Again, polymer with glass Mg5 showed a faster degradation than that with glass T5. After 60 weeks, the composite with glass Mg5 showed a weight

loss of more than 25 wt%, the composite with glass T5 of less than 20 wt%. Although in both cases, i.e. for coated porous glasses as well for glass-reinforced polymer specimens, the degradation of the polymer matrix dominated the degradation behaviour, apparently the structure of the glassy part modulated the solubility of the composites.

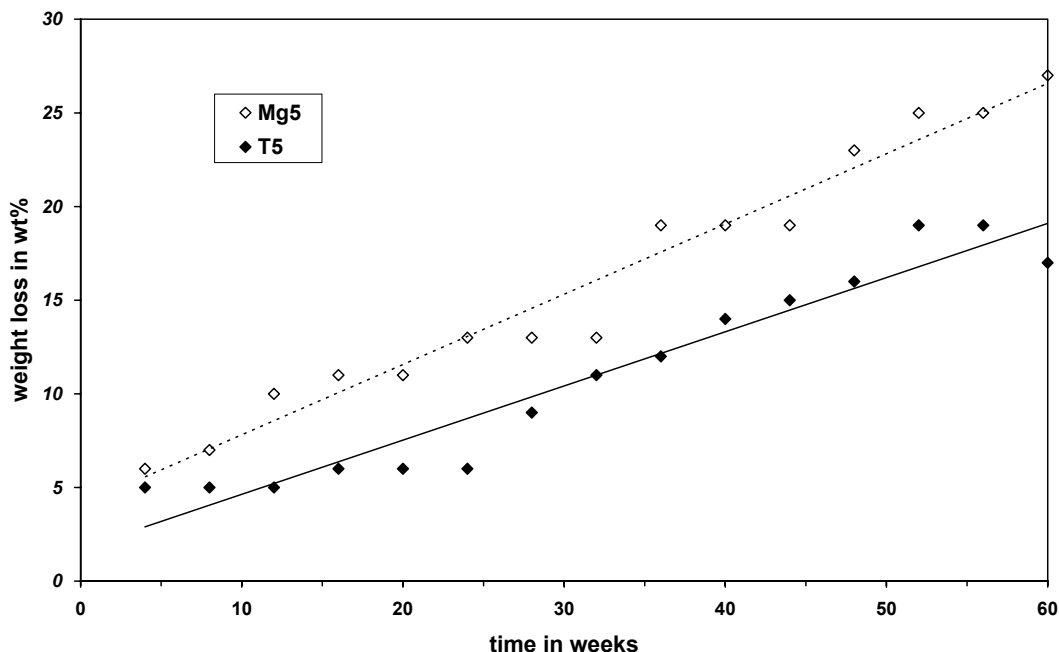


Figure 4.28: Weight loss of Mg5 and T5 glass powder-reinforced porous polymers in SBF at 37 °C (lines: regression lines)

4.3.5 Cell experiments

Proliferation

For sintered porous uncoated glasses (Figure 4.29), cell concentration at 24 h was significantly different for each glass composition and significantly lower than on TCPS control (ANOVA, $p < 0.05$). Cells proliferated on sintered porous glass T5, while the number of cells on all other glasses was similar to the seeding concentrations (50,000 cells/cm²) and also showed a relatively high variation within replicates. Cell densities at 24 h on all porous glasses were significantly lower than on polished glasses (ANOVA, $p < 0.05$; cf. Chapter 4.2.3). Figure 4.30 shows SEM micrographs of MC3T3-E1.4 cells on porous glass Mg5 after cultivation over 24 h. Few cells were attached to the surface.

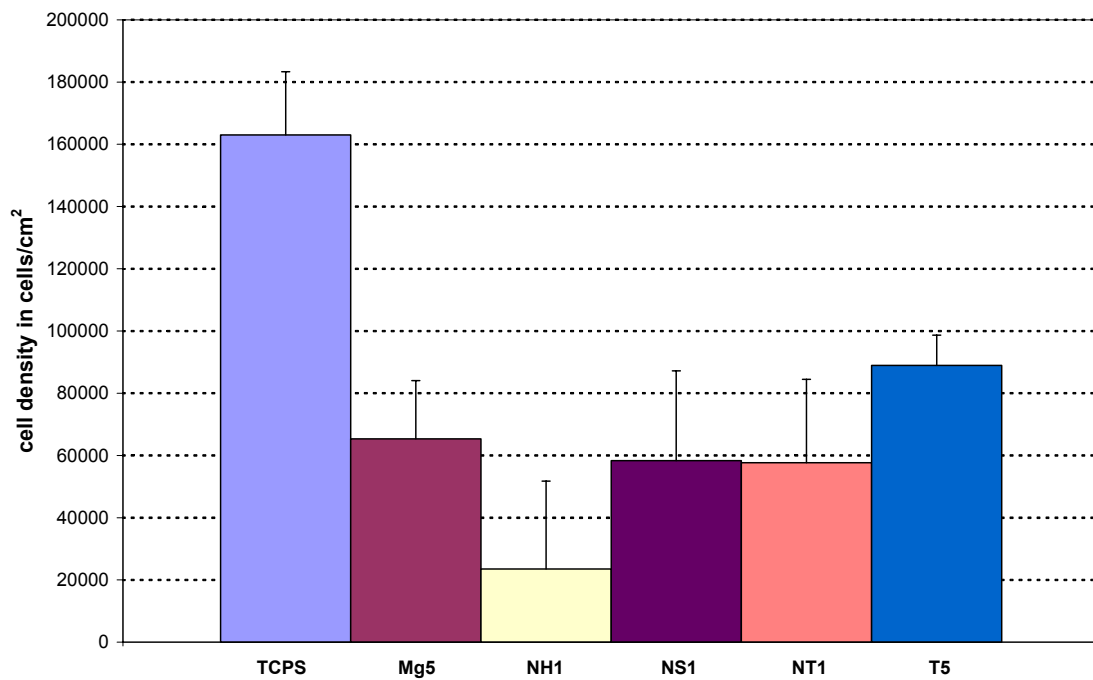


Figure 4.29: MC3T3-E1.4 concentration on porous uncoated glasses at 24 h (mean \pm standard deviation)

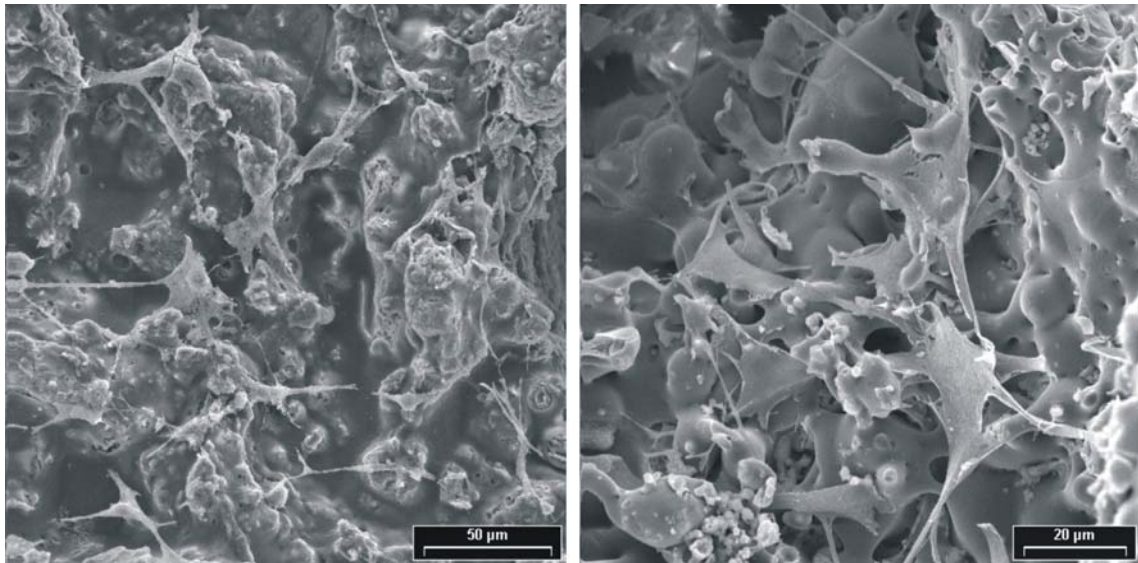


Figure 4.30: MC3T3-E1.4 cells on porous glass Mg5 after cultivation over 24 h

For three uncoated porous glasses (Mg5, NT1, T5) proliferation was tested over 72 h. As Figure 4.31 shows, for all three tested porous glasses, cell density at 72 h was significantly higher than at 24 h (ANOVA, $p < 0.05$). On all glasses cells had proliferated, i.e. cell numbers at 72 h were significantly higher than the cell concentration seeded.

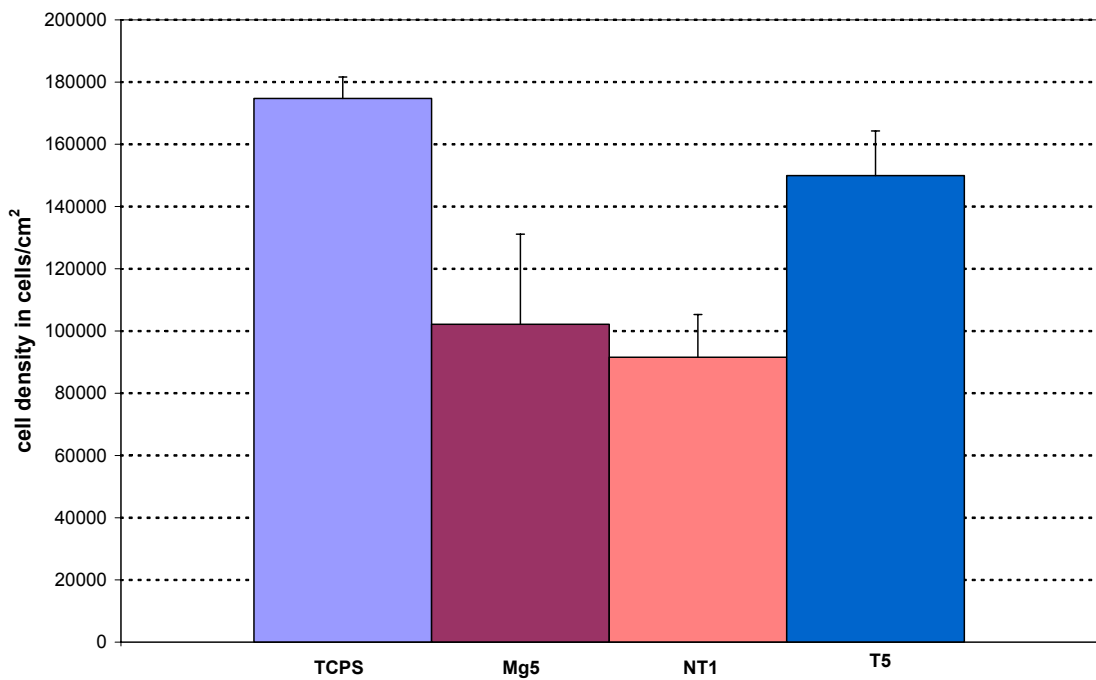


Figure 4.31: MC3T3-E1.4 concentration on porous glasses at 72 h (mean \pm standard deviation)

Due to the irregular surface of the porous specimens, identifying single cells on the surface after HE staining was difficult. However, the distribution of the stained cells in the porous structure after 2 days of cultivation on glass T5 showed that the cells had not only grown on the surface of the outer macropores but also grew into deeper lying macropores (Figure 4.32).

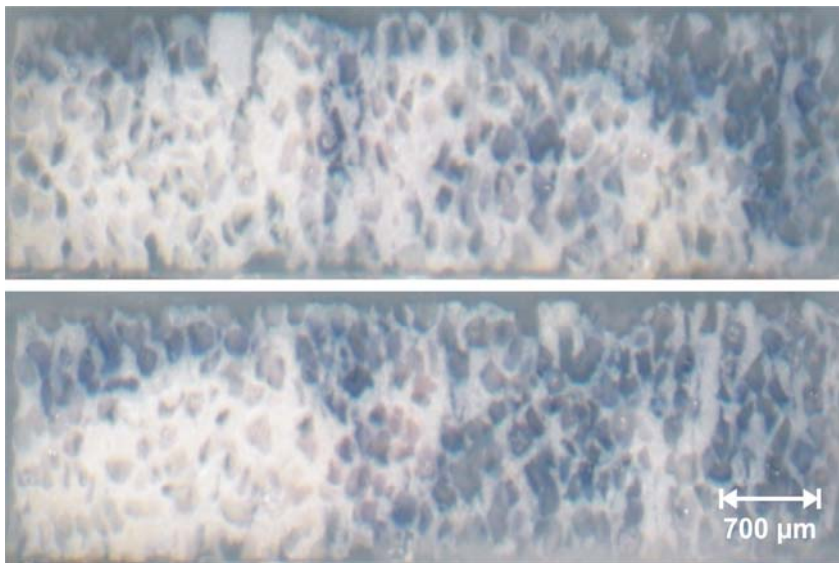


Figure 4.32: MC3T3-E1.4 cells (blue) on porous glass T5 after HE staining

Viability assay

Cell viability was assayed on porous polymer samples with Mg5 and T5 glass powder reinforcement. Porous polymer samples with CaCO_3 reinforcement were used as control. Results of the FDA/EtBr viability assay showed that after 1 and 4 days on all composites polymer/ CaCO_3 and polymer/glass (Mg5 and T5) the percentage of dead cells was less than 5%. Fluorescence micrographs (Figure 4.33) showed that the cells had not only adhered on the sample surface but had grown into a continuous cell layer on the inner surface of the macropores. Cell density after 4 days was significantly higher than after 1 day, hence, the cells proliferated.

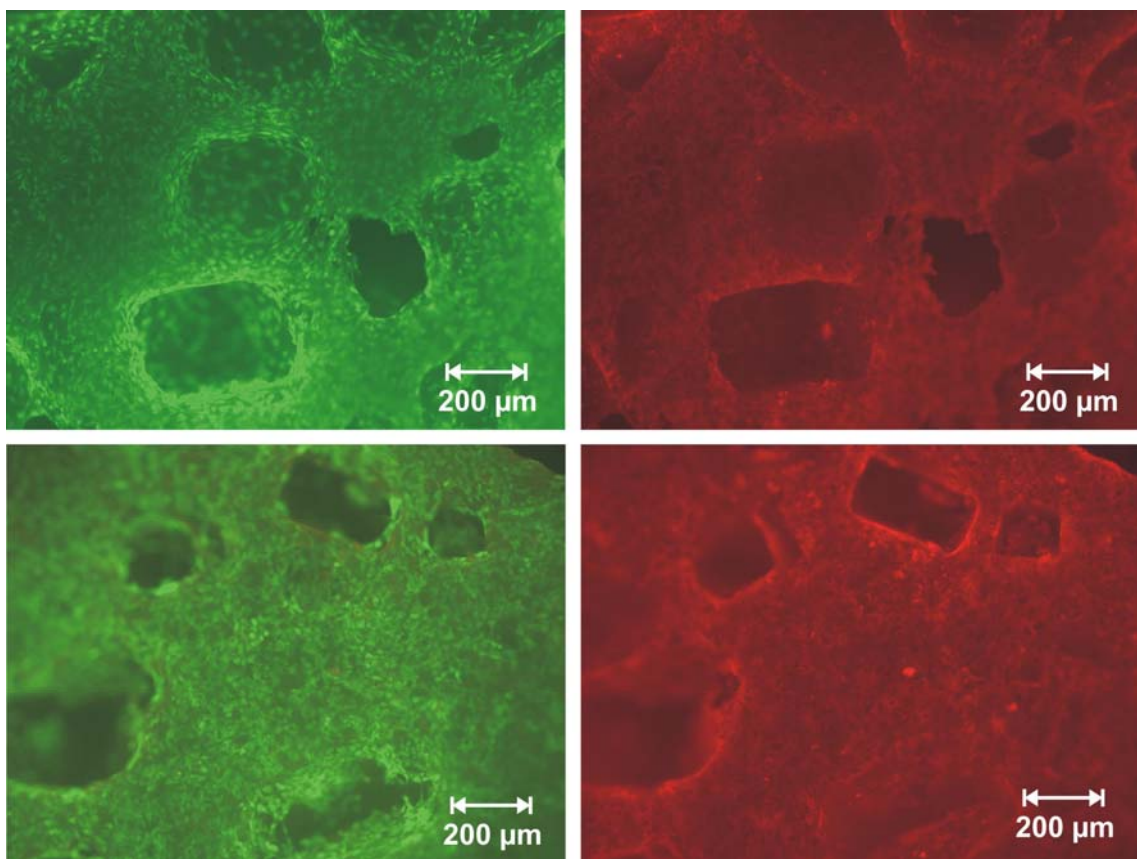


Figure 4.33: Viability of MC3T3-E1 cells on glass powder-reinforced polymer: living green fluorescent cells (left) and dead red fluorescent cells (right) on porous polymer with glass T5 (top) and Mg5 (bottom)

4.4 Glass fibers and composites

Glass fibers obtained had a diameter of 125 μm and a length of about 100 m. A micrograph of the fibers is shown in Figure 4.34. Uncoated fibers were very brittle due to corrosion of the surface. Coating of the fiber surface with organic macromer had no

noticeable effect on the stability of the fibers. Fibers were still brittle and broke into smaller pieces when winded up. Polarization microscope investigations of fibers and remaining parts of the preform showed no signs of crystallization.

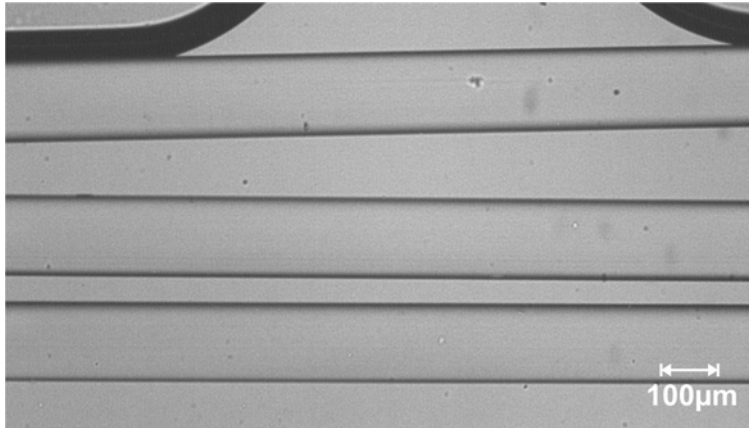


Figure 4.34: T5 glass fibers

Glass fibers were bunched, soaked with macromer and cured. The resulting fiber composites showed an elliptical profile of about 2 mm in height and 3 mm wide. Figure 4.35 shows a SEM micrograph of a section of the fiber composite. The polymer/glass ratio in the composite is about 1:3.5.

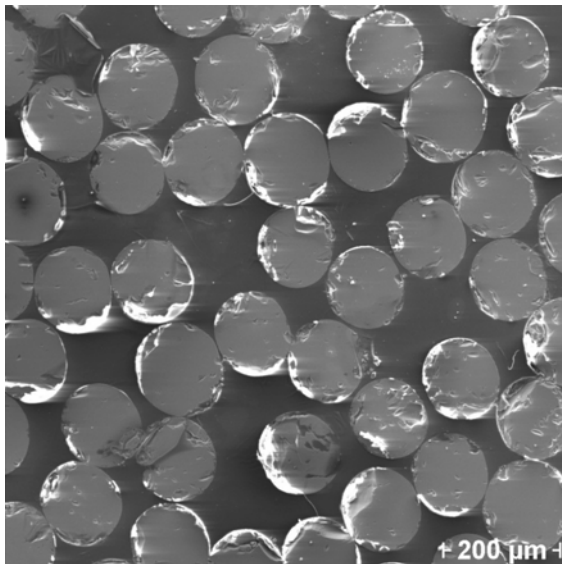


Figure 4.35: Section of polymer phosphate glass fiber composite

4-point bending strength and 3-point bending strength were investigated. The composites exhibited strengths of around 115 MPa. They did not show even fractures but broke by degrees when loaded. This is reflected in the curves of 4-point and 3-point

bending tests which show a fibrous fracture mode (Figure 4.37). If the outer fibers break, other fibers still provide stability of the composite. Figure 4.36 shows SEM micrographs of the fiber composite during 3-point bending. The micrographs show that while the outer fibers are already broken, other fibers are still unbroken. The micrographs also show delamination and branching cracks. This shows that the combination of fibers and polymer positively affected the overall stability of the material. While fibers alone show a brittle fracture mode, the combination with polymer assures that the materials does not break evenly but by degrees.

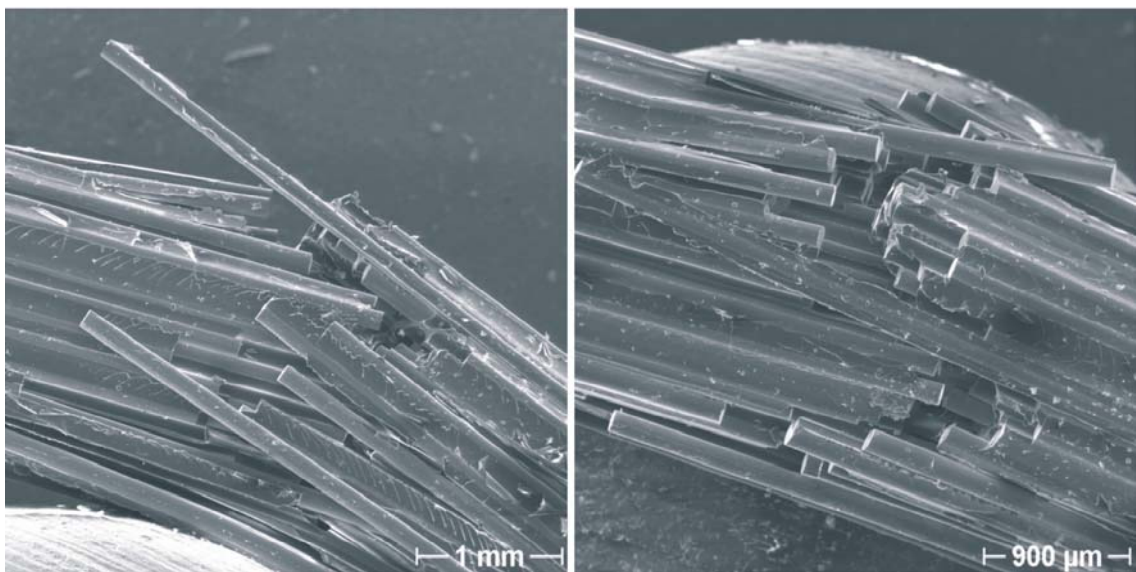


Figure 4.36: SEM micrograph of polymer phosphate glass fiber composite: fracture during 3-point bending test

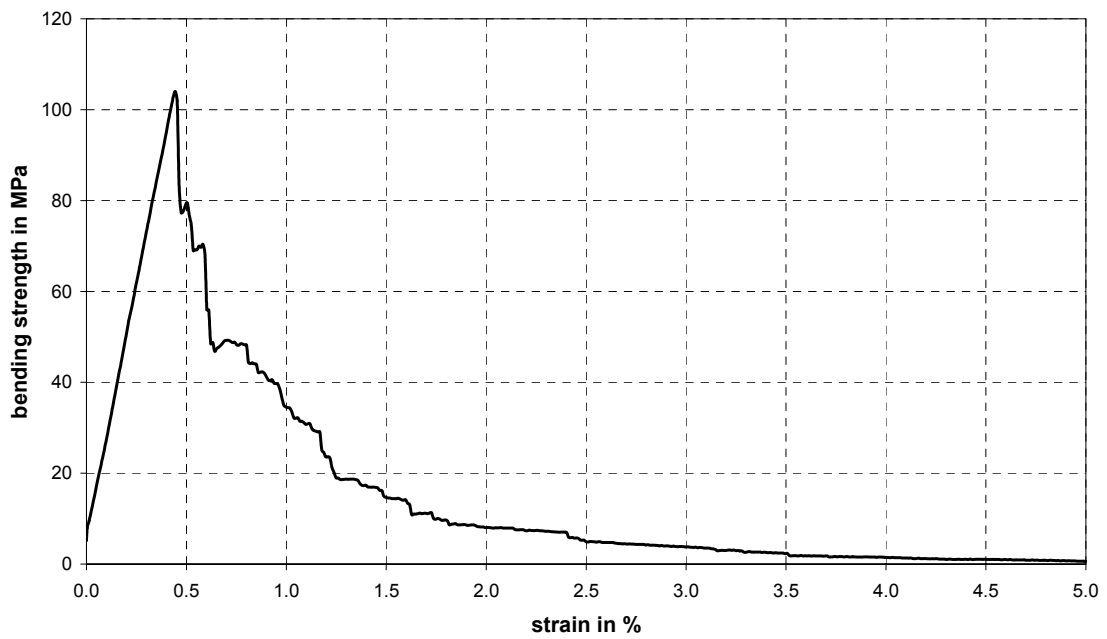
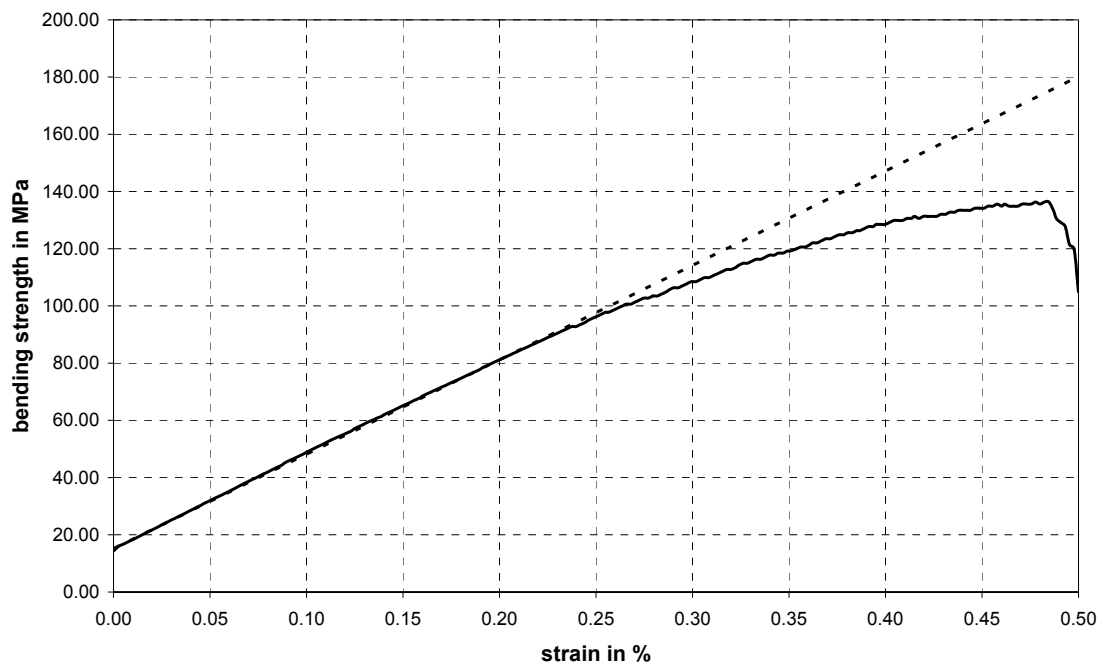


Figure 4.37: Graphs of 4-point bending test (top) and 3-point bending test (bottom)

5 Discussion

5.1 Polyphosphate glasses

The ultimate goal is to produce resorbable phosphate glasses for use as bone replacement or internal fixation material which are biocompatible, promote osteoblast proliferation and degrade at the same rate as new bone is formed.

As phosphate glasses dissolve in aqueous media they offer an immense potential for use as bioresorbable implant material. In the last few years, research mainly focused on polyphosphate glasses with phosphate concentrations in the range from 40 to 55 mol% [18,22,67]. The first set of glasses produced in this work can be counted among this group of glasses. Glasses in the system P_2O_5 -CaO-MgO- Na_2O - TiO_2 -(K_2O) with P_2O_5 concentrations between 45 and 50 mol% were produced. Glasses showed a low tendency to crystallize; they could easily be obtained in a glassy state without quenching.

This low crystallization tendency compared to invert glasses is a great advantage of polyphosphate glasses. It allows for fiber production using crucible methods as described for metaphosphate glasses containing 50 mol% P_2O_5 [68,70,75,77,78] or ultraphosphate glasses [71,76,79]. Although no fibers were actually produced of polyphosphate glasses in this work, viscosity measurements showed viscosities in the range from 10^3 to 10^5 dPa s for temperatures between 550 and 600 °C. Hence, drawing of fibers should be possible. However, with decreasing phosphate content, the tendency to crystallize increased. Glass G6, which contained 45 mol% P_2O_5 , crystallized during viscosity measurements, hence, viscosity was not determined. The same effect was reported by Ahmed *et al.* [68], who produced fibers with phosphate concentrations of 50 and 55 mol%. Of glasses containing 45 mol% P_2O_5 no fibers were obtained due to crystallization of the melt.

The increased crystallization tendency with decreasing phosphate content can be attributed to depolymerization of the phosphate network [57]. This was confirmed by

^{31}P MAS-NMR experiments. The depolymerization of phosphate chains with decreasing P_2O_5 content from 50 mol% to 45 mol% was reflected in the increase in the amount of Q^1 chain end groups and the decrease in the amount of Q^2 chain middle groups. In theory, glasses in the metaphosphate range, i.e. with 50 mol% P_2O_5 , consist of phosphate chains of infinite length or of phosphate rings, i.e., they only consist of Q^2 middle chain groups. However, glass G1, which contained 50 mol% P_2O_5 , was built up of Q^2 and Q^1 groups, experimental chain length was 17 Q^n units. Results for other glasses were similar, as the experimental chain length was shorter than the theoretical one. This can be attributed to two different facts. On the one hand, while the synthetic phosphate concentration of glass G1 was 50 mol%, the analytic content was (50.6 ± 2.2) mol%. The theoretical chain length for a P_2O_5 content of 48.4 mol%, which is $(50.6-2.2)$ mol% is only 31 Q^n units. Therefore, if the true glass composition is smaller than the synthetic one, the average chain length is less than the theoretical one. On the other hand, it was reported by Hartmann *et al.* [61] that the incorporation of Al_2O_3 leads to a higher Q^1 fraction. Since Al_2O_3 and TiO_2 can be incorporated into the glass structure in a similar way, i.e., as AlO_4 and TiO_4 or TiO_6 structural units as described by Vogel *et al.* [72], the incorporation of titania into the glasses may be the reason for shorter chain lengths.

This depolymerization of the phosphate chains also has an effect on the glass solubility. Decreasing the P_2O_5 concentration from 50 to 45 mol% resulted in a decrease in solubility by two orders of magnitude. This is due to the Q^2 units being more susceptible to hydration and subsequent hydrolysis than Q^1 groups [57,72]. However, the solubility of the glasses was not only affected by the concentration of network former but also by the concentration of network modifiers. Increasing the Na_2O concentration by up to 5 mol% in proportional exchange for CaO and MgO , increased the amount of dissolved P_2O_5 by up to an order of magnitude. This increase in solubility with decrease in CaO content and increase in Na_2O content is described in literature as well [67]. It can be attributed to the effect which the modifiers have on the glass structure. The addition of network modifiers disrupts bonds, lowering the cross-link density and increasing the number of non-bridging oxygen atoms present in the glass. However, divalent cations, such as Ca^{2+} , can serve as ionic cross-links between the non-bridging oxygen atoms of two phosphate chains [66]. The formation of such ionic cross-

links explains why the chemical durability decreased as the mole fraction of CaO in the glass decreased in exchange for monovalent Na⁺ modifier cations.

In summary, viscosity and low crystallization tendencies of the glasses are of interest for different applications, e.g. glass fiber production. However, for use as degradable biomaterials, the glasses showed too high solubilities and reacted too acidic in aqueous media. Glass solubility of polyphosphate glasses in deionized water exceeded the solubility of phosphate invert glasses (cf. Chapter 5.2) by one to three orders of magnitude. Still, the successful testing of poly- and ultraphosphate glasses in both *in vitro* and *in vivo* experiments was reported [19,23,71,111]. The variation of glass composition by increasing both the TiO₂ and CaO concentration at constant P₂O₅ content might decrease the solubility of the glasses enough for use as biomaterial as reported by Navarro *et al.* [23] and Franks *et al.* [67].

5.2 Pyrophosphate glasses

Phosphate invert glasses offer an alternative to polyphosphate glasses, since they are soluble but more stable to moisture attack [57,72]. Therefore, they exhibit a smaller degradation rate and react less acidic in aqueous media.

The pyrophosphate glass Mg5 of the composition 37 P₂O₅ - 29 CaO - 10 MgO - 24 Na₂O was developed and characterized by Vogel *et al.* [116]. Platzbecker [113] tested its biocompatibility using *in vivo* techniques by implanting porous glass cubes into the tibiae of guinea pigs. Histological investigations showed no symptoms of inflammation. The porous structure acted as a guide rail for young bony cells growing in. After three to four months the implants were completely incorporated by osteoid. The implants were degraded simultaneously. At 64 weeks post operation, a mixture of ripe bone, osteoid and small amounts of glass particles was detected.

As it is difficult to extrapolate the results obtained from *in vivo* experiments using rodents or other small animals to human beings, Hensel [112] tested porous glass cubes of glass Mg5 *in vivo* by implanting them into mini-pigs. Results were similar to the ones detected by Platzbecker [113]. The glasses showed a good biocompatibility and osteoconductivity. However, low mechanical stability and machinability caused problems during implantation.

This good biocompatibility of glass Mg5 in contrast to the large solubility of the investigated polyphosphate glasses was the reason for abandoning research on polyphosphate glasses and resuming research on invert glasses. Decreasing the P_2O_5 content makes glasses more stable to hydrolysis but also restricts the glass forming area. Hence, glasses in the pyrophosphate region show a larger tendency to crystallize than polyphosphate glasses [57]. Therefore, the aim was to vary the glass composition to control both crystallization tendency and solubility behavior. Invert glasses in the system P_2O_5 -CaO-MgO- Na_2O were found to be very sensitive to additives. Properties of the glasses can be controlled by adding small amounts of metal oxides [56].

Glass composition was varied by adding small amounts of oxides, e.g. SiO_2 , K_2O , Al_2O_3 or TiO_2 to base glass Mg5 in exchange for other components. Titanium oxide had the most distinct influence on the glass properties. Addition of 1 mol% TiO_2 (glass NT1) already resulted in a considerable decrease in solubility and crystallization tendency.

While several additives showed an influence on glass solubility, they did not affect the crystallization tendency in a noticeable way. Of all added components, only SiO_2 (glass NS1, 1 mol% SiO_2) clearly increased the solubility. This effect agreed with results published by Nagase *et al.* [131] for phosphate glasses in the poly- to metaphosphate range. Knowles *et al.* [69] found that K_2O increased the solubility of polyphosphate glasses. However, results obtained in this work were not clear. Sodium oxide was exchanged for potassium oxide, while the concentrations of all other components were fixed. Addition of 1 mol% K_2O (glass CK1) in exchange for 1 mol% Na_2O slightly decreased the solubility while exchange of 5 mol% sodium oxide for K_2O (glass CK5) resulted in a significant increase. The increase in solubility can be attributed to the larger ionic radius of potassium compared to sodium which results in a larger disrupting effect on the network structure and, hence, weakens the network [69]. Addition of ZnO showed the reverse effect than that found for K_2O . 1 mol% ZnO (glass NX1) increased the solubility while the solubility of glass NX5 (5 mol% ZnO) was similar to that of the base glass Mg5 without additives.

Other investigated components decreased the solubility. Addition of 1 mol% Fe_2O_3 decreased the solubility of the pyrophosphate glass. This effect was also found for ultra-

[71] and polyphosphate glasses [70]. According to the authors, this can be attributed to the formation of more cross-linked Fe-O-P chains. Addition of up to 5 mol% Al_2O_3 (glasses NA1 and NA5) and up to 10 mol% TiO_2 (glasses T5, NT1 to NT1 and BT1 to BT10) continuously decreased the amount of dissolved P_2O_5 in deionized water. This agrees well with results published in literature for glasses in the pyro- [72] and polyphosphate range [22] and can be attributed to the incorporation of AlO_4 , TiO_4 or TiO_6 structural units which strengthen the network. Similar to TiO_2 , addition of 1 mol% ZrO_2 (glass NZ1) also decreased the solubility.

As mentioned above, only the addition of TiO_2 showed a marked effect on the crystallization tendency. All other glasses showed a crystallization behavior which was similar to that of the base glass Mg5. In general, the tendency of pyrophosphate glasses to crystallize is large compared to polyphosphate glasses, since the reduction of the phosphate content restricts the glass formation area [57]. Glasses showed spontaneous surface crystallization and therefore had to be quenched before annealing. Incorporation of TiO_2 in the glass structure significantly decreased the crystallization tendency in the temperature range from 500 to 600 °C, which is of interest for the fabrication of sintered glass specimens or glass fibers. Since addition of TiO_2 is also known not to have any cytotoxic effect [23], glass T5, which contains 5.45 mol% TiO_2 , was chosen for further experiments.

Porous glass specimens were obtained from phosphate invert glasses by a salt sintering process. The temperature range for obtaining sintered specimens not affected by crystallization is very small. The resulting specimens had a porosity of around 65 % and pore diameters between 150 and 400 μm . The structures of the porous glasses resembled that of cancellous bone. However, compressive strength of the porous glasses is low and they are very brittle.

Degradation of porous specimens Mg5 and T5 in SBF was tested over up to 72 weeks. Both porous glasses showed a linear degradation behavior over the whole period of time. Solubility of titania-containing glass T5 was considerably lower than that of glass Mg5, which was titania-free. While glass Mg5 degraded continuously to a weight loss of more than 25 wt% in 56 weeks, glass T5 only showed a weight loss of about 2 wt% after 72 weeks. This shows that the solubility of the glasses could be changed

considerably by only minor adjustments of the glass composition. The addition of TiO₂ decreased the solubility of the glasses to a great extent. So while both glasses showed a more similar solubility in deionized water, their solubility in SBF was substantially different. The presence of a protective surface layer as observed in silica-based bioactive glasses [132] may account for this phenomenon and should be a subject of future studies. Results of degradation experiments in SBF also showed that it is difficult to extrapolate from *in vitro* degradation to *in vivo* resorption. Glass Mg5 showed a weight loss of only about 25 % over 56 weeks in SBF. However, after animal experiments over 64 weeks, only small particles of the implanted porous glass Mg5 were found by Platzbecker [113]. Since the dissolution rate of glass T5 in SBF was very low, adjustment of the glass composition might be necessary for future applications.

As described above, only addition of titanium oxide decreased the crystallization tendency of the glasses in a noticeable amount. Especially for the production of glass fibers, a low tendency to crystallize is a prerequisite. Phosphate fibers described in literature were produced using crucible methods [68,70,71,76,78]. However, due to the low viscosity of the melt and high crystallization tendency of the investigated phosphate invert glasses, this method could not be applied in this work. Therefore a preform technique was chosen for fiber production. Still, the crystallization tendency was a drawback, as on the one hand a preform must be obtained in a glassy state and on the other hand crystallization may affect the fibers during drawing. It was not possible to produce a glassy preform of glass Mg5 as the glass rods crystallized partly during annealing. However, due to the smaller crystallization tendency caused by the high TiO₂ content, preforms were obtained in a glassy state of glass T5. From this preform, glass fibers were produced. During fiber drawing at temperatures between 600 and 620 °C, no crystallization was observed. Resulting fibers and remains of the preform were investigated using polarization microscopy and showed no signs of crystallization. However, glass fibers were very brittle. Sizing of the fibers with methacrylate-modified oligolactide did not improve the stability noticeably. Therefore for future fiber production a biodegradable coating would be of interest. Resulting fibers had a diameter of about 125 μm. Decreasing of the diameter by increasing the drawing speed was difficult due to the low stability of the fibers as described above. Phosphate glass fibers

described in literature mostly showed diameters in the range from 10 to 50 μm [68,71,78]. In one case fiber diameters below 10 μm [79] were reported.

The good biocompatibility of glass Mg5 was shown in *in vivo* experiments by Platzbecker [113] and Hensel [112]. To investigate the biocompatibility of Mg5 variations, *in vitro* cell tests were carried out using MC3T3-E1.4 pre-osteoblast cells and dental pulp stem cells (DPSCs). To quantify the influence of glass composition and structure on cell growth, proliferation assays were carried out on polished non-porous glasses and sintered porous glasses. Glass compositions investigated were Mg5, T5 (5.45 mol% TiO_2), NT1 (1 mol% TiO_2), NS1 (1 mol% SiO_2), NH1 (1 mol% F^-) and CK1 (1 mol% K_2O). The presumption was, that differences in glass solubility might affect cell proliferation as described by Navarro *et al.* [23]. However, no differences in MC3T3-E1.4 proliferation on polished glasses of different compositions were found. Cells proliferated on all investigated glasses. The cell concentration after cultivation over 24 h was significantly higher than the cell concentration seeded. Proliferation over 72 h did not result in considerably higher cell concentrations. This was due to the fact that the cell layer on polished glasses at 24 h was already nearly confluent and therefore the sample surface area limited further cell growth. By contrast, proliferation of DPSCs on glasses Mg5, NT1 and T5 showed considerable differences: cells had only proliferated on glass T5, which showed the smallest solubility. Cell concentrations on glasses Mg5 and NT1 were lower than the cell concentration seeded.

MC3T3-E1.4 cell proliferation on sintered porous glasses was significantly lower than on polished glasses and also showed variation with glass composition. At 24 h, cells had only proliferated on glass T5 which had the smallest solubility. Results for the other glasses were not as clear since cell numbers showed great variation within replicates. For all porous glasses cell numbers at 24 h were much lower than on polished non-porous glasses. However, cell proliferation over 72 h resulted in considerably increased cell concentrations. So after an initial stagnation, cells proliferated on the porous glass samples. Apparently sample topography and roughness of the porous samples inhibited initial cell adhesion and subsequently cell proliferation on the glasses. It is known that the topography of a surface can profoundly affect cell attachment and spreading [133]. This resulted in considerably smaller cell concentrations on porous samples than on polished glasses after short proliferation times. However, results indicated that this

initial difference could be overcome with time, as cell concentrations on porous samples at 72 h were already significantly increased.

Differences in cell concentrations on porous glasses of different compositions may be due to a larger solubility of the porous glasses caused by increased surface area. While cell proliferation on polished glasses of different compositions was comparable, cell proliferation on porous specimens showed great variation with glass composition. It is assumed that glass solubility affected cell adhesion and subsequently cell proliferation on the glass surface. Optimized adhesion on the glasses should result in improved proliferation. Hence, to facilitate adhesion, the dissolution rate of the scaffolds needs to be adjusted. However, application of these glasses *in vivo* may require a different solubility, since a variety of factors, including pH changes and protein adhesion, will affect interaction between substrate and cells. The results of animal tests by Platzbecker [113] and Hensel [112] confirm this assumption, as glass Mg5 showed a good biocompatibility *in vivo*.

In summary, phosphate invert glasses in the system P_2O_5 -CaO-MgO- Na_2O with different additives such as TiO_2 are promising for use as both bioresorbable implant materials and degradable scaffolds in tissue engineering. Glass solubility can easily be adjusted by only minor changes in the glass composition. High crystallization tendencies were a drawback but were greatly improved by adjustment of composition. Brittleness and high elastic moduli limit the use of phosphate glasses in orthopedic surgery. However, mechanical properties can be improved by fabrication of composite materials as described in Chapter 5.4.

5.3 Modeling of solubility

The aim of modeling experiments was to find a correlation between the solubility behavior of the glasses and their chemical composition. Especially for the fabrication of degradable implant materials, a model for the estimation of glass solubility from the glass composition is of interest. Vice versa, the calculation of a glass composition from a given solubility would offer some advantages.

To reduce the number of variables, i.e. glass components, only glasses of the system P_2O_5 -CaO-MgO- Na_2O - TiO_2 were used for modeling investigations. Therefore, the

solubility data of 31 glasses was included in the calculations. 21 of the glasses were produced and characterized in this work. To increase the amount of data available for modeling, results of previous solubility investigations by Deutschbein [122] were included.

The relation between phosphate glasses and their solubility is complex. As described in Chapter 5.1, solubility depends on the glass composition as well as on the glass structure. As described by Vogel *et al.* [56], most glass properties change continuously within structural groups. However, the transition between different structural groups causes discontinuous changes of the properties. The authors described breaks in the solubility of phosphate glasses pointing at structural changes. Therefore, the use of linear models, e.g. MLR, for describing the relation between glass composition and solubility is extremely limited. The model might be useful for the modeling of solubility within one structural group. However, due to the small amount of data this was not investigated within this work. In addition, the boundaries of structural groups depend on the phosphate concentration as well as on the concentration of other components [56]. Hence, defining them is difficult without detailed structural investigations.

An artificial neural network (NN) was used for finding a correlation between the glass composition and the amount of dissolved P_2O_5 in mg/L. As neural networks represent a non-linear model, they are more useful for describing the complex relation between glass structure and solubility than linear methods. Results were presented in an observed vs. predicted plot (Figure 4.17). The observed values were the concentration of dissolved P_2O_5 measured using ICP-OES in solubility experiments. The predicted values were the values calculated by the neural network on the basis of the glass composition by fitting the values in an iterative procedure to the observed ones. Although a simple standard neural network (one hidden layer consisting of three hidden nodes) was employed, the predicted values matched the measured ones very well. The correlation coefficient in the observed vs. predicted plot was 0.9996. This showed that the model for calculating the solubility from the composition which was proposed by the NN met the actual glass solubility very well.

However, several facts limited the validity of this investigation. Although solubility experiments both in this work and by Deutschbein [122] were carried out in analogy to

DIN ISO 719 [73] and analyzed using ICP-OES, results were not necessarily comparable. No data concerning the calibration strategy used by Deutschbein were available. Hence, data provided by Deutschbein and obtained in this work were not necessarily of the same statistical population. Furthermore, statistical investigations need to be based on a minimum of data to produce a valid result. It is doubtful that the amount of data used in this experiment was enough for modeling a complex matter like the solubility of glasses of different structures. Still, artificial neural networks provided an interesting method for modeling of solubility of phosphate glasses. If based on an adequate amount of data, it might be possible to predict the solubility of a glass with sufficient accuracy. The application of neural networks for the prediction of other glass properties might be of interest as well.

5.4 Composites

Bone regeneration by use of degradable implant and fixation devices is a promising approach in orthopedic surgery. Absorbable implants obviate the need for surgical removal and they allow for the gradual transfer of load to the healing bone, thereby eliminating the problem of stress shielding. The goal is the development of a resorbable implant material which provides sufficient strength, promotes bone regeneration, and degrades in a timely accordance with bone healing or formation.

A significant amount of work on degradable polymer scaffolds for internal fixation devices or tissue engineering was published over the last few years [84-87]. The research was mostly centered on the use of poly(α -hydroxy esters). While many macromolecular compounds are bioabsorbable, only a few possess the properties necessary for bone fixation such as high mechanical strength and elastic modulus. However, low implant stiffness allows too much bone motion for satisfactory healing.

Therefore degradable polymer matrix composites are being increasingly studied. For the development of totally biodegradable implant materials, both the matrix and the reinforcement should be resorbable. However, research included both degradable and stable materials as fillers. Embedding particles of these materials into the polymer matrix is known to promote bone bonding properties and increase both the elastic modulus and the strength of the resulting composite. Additionally, the ceramic phase

can act as a hydrolysis barrier, delaying the degradation of the polymer. Currently the most studied reinforcement materials for bone implants are bioactive fillers, e.g. hydroxyapatite (HA), tricalcium phosphate (TCP) and bioactive glasses. HA is the most-used ceramic in such composite as it is similar to the inorganic phase of bone and exhibits high biocompatibility and bioactivity [95-98]. Other partially degradable composite materials include silica-based bioactive glasses (Bioglass[®]) as reinforcing phase. The glass phase is stable to hydrolysis but induces a good biocompatibility and improved mechanical properties [31,92,99].

For totally biodegradable composite materials, both the continuous phase and the reinforcement should be completely degradable. Therefore, the use of phosphate glasses as filler is of special interest. Phosphate-based glasses are an interesting range of materials, as they may dissolve completely in water depending on the composition. Furthermore, the solubility can be tailor made to suit the end application. Knowles *et al.* [100] produced completely degradable composite scaffolds of polyhydroxybutyrate and particles of a ternary calcium sodium phosphate glass. Prabhakar *et al.* [101] investigated the degradation of phosphate glass/polycaprolactone composites.

In this work, composites were prepared using a polymer based on methacrylate-modified oligolactides [27,89]. This system can be used for fabrication of polymer scaffolds as well as radically curable coating system. The resulting polymers exhibited an excellent biocompatibility in previous *in vitro* studies [88]. Based on this polymer and two phosphate invert glasses in the system P_2O_5 -CaO-MgO- Na_2O -(TiO_2), porous composite materials were produced. Phosphate content in the glasses was 34.87 and 37 mol%, respectively; the glass with the lower P_2O_5 concentration (glass T5) contained 5.45 mol% TiO_2 , glass Mg5 was titania-free.

Resorbable porous implants are of interest for regeneration of cancellous bone. Porous glass cubes were produced by a salt sintering process. Mechanical strength and machinability of the porous glass specimens were greatly improved by polymer coating of the inner surface of the macropores while maintaining the open interconnective porosity. In contrast to the uncoated porous glasses, the polymer/phosphate glass composites could be processed and shaped by conventional mechanical techniques such as drilling, grinding or sawing. Compressive strength of the composites was about five

times larger than that of uncoated porous glasses. Uncoated porous glasses showed a linear degradation in SBF. By contrast, polymer-coated porous glass specimens showed a fast degradation over the first four weeks to a weight loss of 13 wt% (glass Mg5) and 9 wt% (glass T5). With time, the degradation rate decelerated and the specimens showed a linear degradation behavior. The fast degradation in the beginning can be attributed to the degradation pattern of the polymer which dominated the overall degradation, especially in the beginning.

Glass powder-reinforced porous polymer specimens showed a compressive strength which exceeded the compressive strength of the coated porous glasses considerably. The degradation pattern was similar to that of polymer-coated porous glasses, i.e., the scaffolds showed a high degradation rate over the first 4 weeks which decelerated with time. Degradation after the first four weeks was linear. However, the degradation of reinforced polymer samples over the first four weeks was smaller (5 and 6 wt%) than that of polymer-coated porous glasses (9 and 13 wt%). Although in both cases the degradation of the polymer matrix dominated the overall degradation behavior, apparently the structure of the glassy part modulated the solubility.

Cell compatibility of porous composite materials was tested using glass powder-reinforced porous polymer samples with CaCO_3 -reinforced polymer samples as control. Results of the FDA/EtBr viability assay showed the good biocompatibility of the scaffolds. Fluorescence micrographs showed that the cells had proliferated and grown into a continuous cell layer on the inner surface of the macropores.

Degradable fiber composites are of special interest in orthopedic surgery for fabrication of internal fracture fixation devices such as pins and screws [38,94]. Conventional fixation devices of metals and alloys are stiffer than bone and therefore often require removing after healing to prevent stress shielding. By contrast, resorbable devices of degradable polymer have a low elastic modulus which allows too much bone movement for satisfactory healing. Consequently, reinforcement might provide an alternative for the development of a generally acceptable absorbable fracture fixation material. Composite materials with oriented structures were prepared using polymer and T5 glass fibers. The composites showed a fibrous fracture mode which is typical for fiber composites. Bending strength was about 115 MPa. The composites broke by degrees

when loaded. After breaking of the outer fibers, inner fibers still provided stability. The fact that the composites did not break evenly is of importance for use as implant materials. A sudden failure of an implant material might result in fatal consequences for the patient. Therefore the composite obtained by combination of fibers and polymer is clearly of advantage for use as implant material due to its good strength and its fibrous fracture mode.

In summary, the combination of resorbable phosphate glasses and degradable organic polymers is very promising for the development of bioabsorbable implant materials. While the glass system offers the possibility of solubility adjustment, the polymer matrix improves the mechanical properties and provides high compressive strength and low elastic modulus.

6 Conclusion

The aim of this work was the development and characterization of biodegradable composite materials based on phosphate glasses and a resorbable organic polymer for use as bone replacement, bone fixation devices or in tissue engineering.

Two sets of phosphate glasses were produced. First, polyphosphate glasses in the system P_2O_5 -CaO-MgO- Na_2O - TiO_2 with phosphate concentrations between 45 and 50 mol% were synthesized. The glasses showed a low tendency to crystallize; all compositions were obtained in a glassy state without quenching. ^{31}P -MAS-NMR experiments showed that the glass with 50 mol% P_2O_5 consisted of phosphate chains. With decreasing phosphate content, the amount of chain end groups increased which points at a depolymerization of phosphate chains. While phosphate glasses with 50 mol% P_2O_5 consisted of long phosphate chains or rings which are built up by chain middle (Q^2) units, glasses with lower phosphate contents consisted of smaller phosphate units, i.e. shorter phosphate chains. Viscosity measurements showed that glasses with phosphate concentrations between 46 and 50 mol% showed viscosities between 10^3 and 10^5 dPa s at 550 °C. Hence, although no fibers were actually produced of polyphosphate glasses, drawing of fibers should be possible. Viscosity measurements also showed that with depolymerization of phosphate chains the tendency to crystallize increased. Of glasses containing 45 mol% P_2O_5 no viscosity curves were obtained with the method supplied due to crystallization during measurement.

Solubility behavior of the glasses was tested in pH measurements in physiological NaCl solution. The aim was the development of a glass which gave a pH around the physiological pH of 7.36. Glass of a defined grain fraction was immersed at 37 °C over 24 h. Afterwards the pH of the solution was determined, the solution exchanged for a fresh one and the procedure repeated over at least 10 days. All investigated polyphosphate glasses gave pH values below 6.4. Glass solubility was also tested in deionized water at 98 °C. The resulting solutions were analyzed using ICP-OES. By reducing the phosphate content from 50 mol% to 45 mol% the amount of dissolved

P_2O_5 was decreased by two orders of magnitude. Still, the solubility of all glasses was very large, which was the reason for low pH values in pH experiments. For that reason another set of glasses with smaller P_2O_5 contents was produced.

In previous experiments, a phosphate invert glass of the system P_2O_5 -CaO-MgO- Na_2O was shown to be biocompatible during *in vivo* experiments. However, the high crystallization tendency of the glass was a drawback. Therefore it was decided to create a new set of glasses based on this glass Mg5 (37 P_2O_5 - 29 CaO - 10 MgO - 24 Na_2O) with the aim to produce a glass with a similar biocompatibility and solubility but with a smaller crystallization tendency. Therefore different components (Al_2O_3 , F⁻, Fe_2O_3 , K_2O , SiO_2 , TiO_2 , ZnO) were added at concentrations between 1 and 10 mol%; phosphate concentrations were between 34 and 37 mol%. However, of all the additives only TiO_2 showed a distinct influence on the crystallization behavior already at low concentrations. The crystallization tendency of glass T5 (5.45 mol% TiO_2) was reduced enough for glass fiber production. Fibers were obtained using a preform technique. Resulting fibers had a length of about 100 m in total and a diameter of about 125 μm . Polarization microscopy investigations of the fibers and the remaining parts of the preform showed no signs of crystallization.

Solubility of pyrophosphate glasses was tested in pH measurements and in distilled water at 98 °C as described for polyphosphate glasses. Most glasses gave a pH between 7 and 7.5 in physiological sodium chloride solution. The low pH values of glasses with high titania contents were attributed to the initial pH of the salt solution of around 5.8 and the low solubility of the glasses. Concentrations of dissolved P_2O_5 in deionized water were considerably smaller than for polyphosphate glasses. Solubility of invert glasses was around three orders of magnitude smaller than that of glasses containing 50 mol% P_2O_5 and around one order of magnitude smaller than the one of glasses containing 45 mol% P_2O_5 .

Porous resorbable implant materials are of interest for the regeneration of bony defects, especially as replacement for cancellous bone. Additionally, porous implants can act as a guide rail for the new bone growing in. For that reason porous glasses were produced in a salt sintering procedure. Milled glass powder with grain sizes around 10 μm was mixed with sodium chloride of grain sizes in the range from 250 to 315 μm in a volume

ratio of 1:1. Glasses were sintered at temperatures around 500 °C and afterwards the salt was dissolved in water. The resulting porous glass cubes had a porosity of around 65 %; about 15 % were caused by micropores (< 60 μm). The macropores had diameters between 150 and 400 μm.

For two porous glasses (Mg5 and T5) degradation experiments were carried out in simulated body fluid over up to 72 weeks. The solution was exchanged every two weeks and every four weeks two cubes of each composition were cleaned, dried and the weight loss was determined. Both glasses showed a linear degradation. However, while the solubility of titania-containing glass in deionized water was only about 35 % smaller than that of glass Mg5, their solubility in SBF was substantially different. After 56 weeks, glass Mg5 showed a weight loss of more than 25 wt%. Glass T5 showed only a weight loss of around 2 wt% after 72 weeks. Whether this difference in solubility in SBF was caused by surface layer formation still needs to be investigated. Results showed that to obtain a glass of small crystallization tendency and adequate solubility, the concentration of added TiO₂ needs to be optimized.

The biocompatibility of some pyrophosphate glasses was assessed in proliferation assays using two different cell lines. Proliferation of dental pulp stem cells on polished glasses was influenced by glass solubility. Cells proliferated only on glass T5 which showed the lowest glass solubility. By contrast, proliferation of MC3T3-E1.4 pre-osteoblast cells on polished glasses showed no variation with glass composition. Proliferation on porous glasses, however, was affected by both topography, i.e. sample roughness, and solubility. Cell concentrations on all porous samples were significantly smaller than on polished samples and also showed variation with glass composition. Again, cells proliferated only on glass T5 during 24 h experiments. Cell densities after 72 h experiments were greatly increased; cells had proliferated on all investigated glass compositions. This showed that while the sample roughness apparently affected initial cell adhesion, it did not prevent cell proliferation.

Besides the development of a phosphate glass suitable for use as degradable bone replacement, another aim of this work was the fabrication of composite materials based on phosphate glasses and degradable polymers. Composite materials consisting of phosphate glasses and methacrylate-modified oligolactides were produced in

cooperation with Innovent Technologieentwicklung Jena e.V. where the polymer was developed and synthesized. Composite materials with an open porosity as well as composite materials with oriented structures were prepared and characterized with respect to their mechanical properties, degradation in simulated body fluid and their cytocompatibility.

The polymer was used for fabrication of porous polymer specimens and for thinly coating the inner surface of sintered porous glass cubes. The polymer coating of the porous glasses greatly improved their compressive strength and machinability. Compressive strength of coated porous glasses was between 4 and 8 MPa in contrast to 0.8 to 2.3 MPa for uncoated specimens. Porous glass powder-reinforced polymer scaffolds showed a compressive strength which was even larger than that of coated porous glasses (17 to 24 MPa). Based on glass fibers and polymer, composite materials with oriented structures were obtained. These composite materials showed the typical fibrous fracture mode and gave bending strengths of around 115 MPa. Degradation of composite materials was carried out as described for sintered porous glasses. Composite materials showed a large weight loss to up to 13 wt% over the first four weeks. Afterwards the degradation pattern was linear to a weight loss of about 25 wt% at 60 weeks. This showed that the polymer was degraded significantly faster than the glass.

Cytocompatibility of the composite materials was tested using a viability assay. MC3T3-E1 osteoblast-like cells were seeded onto porous glass powder-reinforced polymer samples. After one and four days the percentage of dead cells was less than 5 %. Cells had grown into a confluent layer and also covered pores. Cell concentration at four days was significantly larger than at one day. Hence, cells proliferated. Therefore, results showed a good biocompatibility of the composite scaffolds.

In summary, polyphosphate were too acidic and too soluble for use as implant materials. However, due to their low crystallization tendency and their potential use for fiber production, it might be of interest to lower their solubility by increasing amounts of suitable additives, e.g. TiO_2 . Phosphate invert glasses showed promising results for use as bone replacement materials. Their high crystallization tendency was greatly improved by addition of TiO_2 . However, this also affected glass solubility to a great extent. Hence, the concentration of additives needs to be adjusted.

Mechanical properties were greatly improved by fabrication of composite materials using a degradable polymer based on methacrylate-modified oligolactide and phosphate glasses. Compressive strength of porous composites was greatly improved compared to porous glasses. These porous composite materials are of interest for use as bioresorbable bone replacement, e.g. for regeneration of cancellous bone, or as degradable scaffolds in tissue engineering. Combination of glass fibers and polymer produced composite materials with oriented structures which might be of interest for use as bone fixation devices such as screws or pins. Both invert glasses and composite materials showed good biocompatibility in initial cytocompatibility tests.

Bibliography

- [1] Wintermantel E, Ha SW.
Biokompatible Werkstoffe und Bauweisen: Implantate für Medizin und Umwelt.
Berlin, Heidelberg, New York: Springer; 1998.
- [2] Ravaglioli A, Krajewski A.
Bioceramics: materials, properties, applications.
London, New York, Tokyo, Melbourne: Chapman & Hall; 1992.
- [3] Vogel W, Höland W.
The development of bioglass ceramics for medical applications.
Angewandte Chemie-International Edition in English 1987;26(6):527-44.
- [4] Vogel W.
Glass chemistry. 2nd ed.
Berlin, Heidelberg, New York, London: Springer; 1994.
- [5] Kokubo T.
Bioactive glass ceramics - properties and applications.
Biomaterials 1991;12(2):155-63.
- [6] Ohgushi H, Ishimura M, Habata T, Tamai S.
Porous ceramics for intra-articular depression fracture.
In: Wise DL, editor.
Biomaterials and bioengineering handbook.
New York, Basel: Marcel Dekker; 2000. p. 397-405.
- [7] Ohtsuki C, Kushitani H, Kokubo T, Kotani S, Yamamuro T.
Apatite formation on the surface of ceravital-type glass-ceramic in the body.
J Biomed Mater Res 1991;25(11):1363-70.
- [8] Moisescu C, Jana C, Habelitz S, Carl G, Rüssel C.
Oriented fluoroapatite glass-ceramics.
J Non-Cryst Solids 1999;248(2-3):176-82.
- [9] Habelitz S, Kullar A, Marshall SJ, DenBesten PK, Balooch M, Marshall GW, et al.
Amelogenin-guided crystal growth on fluoroapatite glass-ceramics.
J Dent Res 2004;83(9):698-702.

- [10] Gheysen G, Ducheyne P, Hench LL, Demeester P.
Bioglass composites - A potential material for dental application.
Biomaterials 1983;4(2):81-4.
- [11] Roether JA, Gough JE, Boccaccini AR, Hench LL, Maquet V, Jerome R.
Novel bioresorbable and bioactive composites based on bioactive glass and polylactide foams for bone tissue engineering.
J Mater Sci: Mater Med 2002;13(12):1207-14.
- [12] Verrier S, Blaker JJ, Maquet V, Hench LL, Boccaccini AR.
PDLLA/Bioglass (R) composites for soft-tissue and hard-tissue engineering: an *in vitro* cell biology assessment.
Biomaterials 2004;25(15):3013-21.
- [13] Foppiano S, Marshall SJ, Marshall GW, Saiz E, Tomsia AP.
The influence of novel bioactive glasses on *in vitro* osteoblast behavior.
J Biomed Mater Res A 2004;71A(2):242-9.
- [14] De Diego MA, Coleman NJ, Hench LL.
Tensile properties of bioactive fibers for tissue engineering applications.
J Biomed Mater Res 2000;53(3):199-203.
- [15] Hench LL.
Bioactive materials: The potential for tissue regeneration.
J Biomed Mater Res 1998;41(4):511-8.
- [16] Gough JE, Christian P, Scotchford CA, Rudd CD, Jones IA.
Synthesis, degradation, and *in vitro* cell responses of sodium phosphate glasses for craniofacial bone repair.
J Biomed Mater Res 2002;59(3):481-9.
- [17] Gough JE, Christian P, Scotchford CA, Jones IA.
Long-term craniofacial osteoblast culture on a sodium phosphate and a calcium/sodium phosphate glass.
J Biomed Mater Res A 2003;66A(2):233-40.
- [18] Knowles JC.
Phosphate based glasses for biomedical applications.
J Mater Chem 2003;13(10):2395-401.
- [19] Bitar M, Salih V, Mudera V, Knowles JC, Lewis MP.
Soluble phosphate glasses: *in vitro* studies using human cells of hard and soft tissue origin.
Biomaterials 2004;25(12):2283-92.

- [20] Ahmed I, Lewis M, Olsen I, Knowles JC.
Phosphate glasses for tissue engineering: Part 1. Processing and characterisation of a ternary-based P_2O_5 -CaO- Na_2O glass system.
Biomaterials 2004;25(3):491-9.
- [21] Franks K, Salih V, Knowles JC, Olsen I.
The effect of MgO on the solubility behavior and cell proliferation in a quaternary soluble phosphate based glass system.
J Mater Sci-Mater Med 2002;13(6):549-56.
- [22] Navarro M, Ginebra MP, Clement J, Martinez S, Avila G, Planell JA.
Physicochemical degradation of titania-stabilized soluble phosphate glasses for medical applications.
J Am Ceram Soc 2003;86(8):1345-52.
- [23] Navarro M, Ginebra MP, Planell JA.
Cellular response to calcium phosphate glasses with controlled solubility.
J Biomed Mater Res A 2003;67A(3):1009-15.
- [24] Vogel J, Wange P, Hartmann P.
Phosphate glasses and glass-ceramics for medical applications.
Glastech Ber Glass Sci Technol 1997;70(7):220-3.
- [25] Vogel J.
Porous glasses by a salt sintering process.
In: Stoch L, editor.
Porous and special glasses. Polish Ceramic Soc., Krakow; 1998. p. 105-11.
- [26] Vogel J, Schulze KJ, Reif D, Hartmann P, Platzbecker U, Leuner B.
Resorbable porous phosphate invert glasses - first *in vitro* and *in vivo* results.
In: Sedel L, Rey C, editors.
Bioceramics, Volume 10.
Oxford: Pergamon; 1997. p. 57-60.
- [27] Schnabelrauch M, Vogt S, Larcher Y, Wilke I.
Biodegradable polymer networks based on oligolactide macromers: synthesis, properties and biomedical applications.
Biomolecular Engineering 2002;19(2-6):295-8.
- [28] Cui YJ, Zhao M, Tang XZ, Luo YP.
Novel micro-crosslinked poly(organophosphazenes) with improved mechanical properties and controllable degradation rate as potential biodegradable matrix.
Biomaterials 2004;25(3):451-7.

- [29] Qian ZY, Li S, He Y, Zhang HL, Liu XB.
Hydrolytic degradation study of biodegradable polyesteramide copolymers based on epsilon-caprolactone and 11-aminoundecanoic acid.
Biomaterials 2004;25(11):1975-81.
- [30] Blaker JJ, Gough JE, Maquet V, Notingher I, Boccaccini AR.
In vitro evaluation of novel bioactive composites based on Bioglass (R)-filled polylactide foams for bone tissue engineering scaffolds.
Journal of Biomedical Materials Research Part A 2003;67A(4):1401-11.
- [31] Lu HH, El-Amin SF, Scott KD, Laurencin CT.
Three-dimensional, bioactive, biodegradable, polymer-bioactive glass composite scaffolds with improved mechanical properties support collagen synthesis and mineralization of human osteoblast-like cells in vitro.
J Biomed Mater Res A 2003;64A(3):465-74.
- [32] Vogt S, Carl G, Vogel J, Schnabelrauch M.
Resorbable polymer coatings for highly porous phosphate glasses.
Phosphorus Research Bulletin 2002;13:249-53.
- [33] Maquet V, Boccaccini AR, Pravata L, Notingher I, Jerome R.
Porous poly(alpha-hydroxyacid)/Bioglass (R) composite scaffolds for bone tissue engineering. I: preparation and in vitro characterisation.
Biomaterials 2004;25(18):4185-94.
- [34] Jaakkola T, Rich J, Tirri T, Narhi T, Jokinen M, Seppala J, et al.
In vitro Ca-P precipitation on biodegradable thermoplastic composite of poly(epsilon-caprolactone-co-DL-lactide) and bioactive glass (S53P4).
Biomaterials 2004;25(4):575-81.
- [35] Zhang K, Wang YB, Hillmyer MA, Francis LF.
Processing and properties of porous poly(L-lactide)/bioactive glass composites.
Biomaterials 2004;25(13):2489-500.
- [36] Ontañón M, Aparicio C, Ginebra MP, Planell JA.
Structure and mechanical properties of bone.
In: Elices M., editor.
Structural biological materials: Design and structure-property relationships.
Amsterdam, Lausanne, New York, Oxford, Singapore, Tokyo: Pergamon; 2000.
p. 31-71.
- [37] Park SH, Llinás A, Goel VK, Keller JC.
Hard tissue replacements.
In: Park JB, Bronzino JD, editors.
Biomaterials - principles and applications.
Boca Raton, London, New York, Washington DC: CRC Press; 2003. p. 173-94.

- [38] Choueka J, Charvet JL, Alexander H, Oh YH, Joseph G, Blumenthal NC, et al. Effect of annealing temperature on the degradation of reinforcing fibers for absorbable implants. *J Biomed Mater Res* 1995;29(11):1309-15.
- [39] Lakes RS. Composite biomaterials. In: Park JB, Bronzino JD, editors. *Biomaterials - principles and applications*. Boca Raton, London, New York, Washington DC: CRC Press; 2003. p. 79-93.
- [40] Fleck C. Struktur und mechanische Eigenschaften kortikalen Knochens unter quasistatischer und zyklischer Beanspruchung. Kaiserslautern: Lehrstuhl für Werkstoffkunde, Universität Kaiserslautern; 2005.
- [41] Brunski JB. Metals. In: Ratner DB, Hoffman AS, Schoen FJ, Lemons JE, editors. *Biomaterials science: An introduction to materials in medicine*. San Diego, London, Boston, New York, Sydney, Tokyo, Toronto: Academic Press; 1996. p. 37-50.
- [42] Silver FH, Christiansen DL. *Biomaterials science and biocompatibility*. New York, Berlin, Heidelberg, Barcelona, Hong Kong, London: Springer; 1999.
- [43] Hench LL. Ceramics, glasses and glass-ceramics. In: Ratner DB, Hoffman AS, Schoen FJ, Lemons JE, editors. *Biomaterials science: An introduction to materials in medicine*. San Diego, London, Boston, New York, Sydney, Tokyo, Toronto: Academic Press; 1996. p. 73-84.
- [44] Hench LL. Biomaterials: a forecast for the future. *Biomaterials* 1998;19(16):1419-23.
- [45] Rokkanen PU. Bioabsorbable polymers for medical applications with an emphasis on orthopedic surgery. In: Dumitriu S, editor. *Polymeric biomaterials*. 2 ed. New York, Basel: Marcel Dekker; 2005. p. 545-62.

- [46] Matzen PF.
Praktische Orthopädie. 2nd ed.
Leipzig: Barth; 1990.
- [47] Tsiridis E, Schizas C.
Bone fracture fixation.
In: Wnek GE, Bowlin GL, editors.
Encyclopedia of biomaterials and biomedical engineering.
New York, Basel: Marcel Dekker; 2004. p. 180-5.
- [48] Pistner H.
Osteosynthese mit bioresorbierbaren Materialien.
Reinbek: Einhorn-Press Verlag; 1999.
- [49] Neves NM, Mano JF, Reis RL.
Biodegradable composites for biomedical applications.
In: Reis RL, San Roman J, editors.
Biodegradable systems in tissue engineering and regenerative medicine.
Boca Raton, London, New York, Washington DC: CRC Press; 2005. p. 91-113.
- [50] Suuronen R, Lindqvist C.
Bone plates and screws, bioabsorbable.
In: Wnek GE, Bowlin GL, editors.
Encyclopedia of biomaterials and biomedical engineering.
New York, Basel: Marcel Dekker; 2004. p. 199-205.
- [51] Kohn J, Langer R.
Bioresorbable and bioerodible materials.
In: Ratner DB, Hoffman AS, Schoen FJ, Lemons JE, editors.
Biomaterials science: An introduction to materials in medicine.
San Diego, London, Boston, New York, Sydney, Tokyo, Toronto: Academic
Press; 1996. p. 64-73.
- [52] Hasirci V.
Biodegradable biomedical polymers.
In: Wise DL, editor.
Biomaterials and bioengineering handbook.
New York, Basel: Marcel Dekker; 2000. p. 141-55.
- [53] Claes L, Ignatius A.
Development of new, biodegradable implants.
Chirurg 2002;73(10):990-6.
- [54] Clément J, Manero JM, Planell JA, Avila G, Martinez S.
Analysis of the structural changes of a phosphate glass during its dissolution in
simulated body fluid.
J Mater Sci: Mater Med 1999;10(12):729-32.

- [55] Jäger C, Hartmann P, Witter R, Braun M.
New 2D NMR experiments for determining the structure of phosphate glasses: a review.
J Non-Cryst Solids 2000;263(1-4):61-72.
- [56] Vogel J, Wange P, Hartmann P.
Effect of composition changes on the structure and properties of phosphate glasses in the pyrophosphate region.
Glastech Ber Glass Sci Technol 1997;70(1):23-7.
- [57] Walter G, Vogel J, Hoppe U, Hartmann P.
The structure of CaO-Na₂O-MgO-P₂O₅ invert glass.
J Non-Cryst Solids 2001;296(3):212-23.
- [58] Witter R, Hartmann P, Vogel J, Jäger C.
Measurements of chain length distributions in calcium phosphate glasses using 2D P-31 double quantum NMR.
Solid State Nucl Magn Reson 1998;13(3):189-200.
- [59] van Wazer JR.
Phosphorus and its compounds.
New York: Interscience; 1958.
- [60] Brow RK.
Review: the structure of simple phosphate glasses.
J Non-Cryst Solids 2000;263(1-4):1-28.
- [61] Hartmann P, Vogel J, Schnabel B.
NMR-Study of phosphate-glasses and glass-ceramic structures.
J Non-Cryst Solids 1994;176(2-3):157-63.
- [62] Hoppe U, Walter G, Kranold R, Stachel D.
Structural specifics of phosphate glasses probed by diffraction methods: a review.
J Non-Cryst Solids 2000;263(1-4):29-47.
- [63] Walter G, Hoppe U, Kranold R, Stachel D.
Structural characterization of magnesium phosphate-glasses by X-ray diffraction.
Phys Chem Glasses 1994;35(6):245-52.
- [64] Brow RK, Kirkpatrick RJ, Turner GL.
The short-range structure of sodium-phosphate glasses 1. MAS NMR-studies.
J Non-Cryst Solids 1990;116(1):39-45.

- [65] Hoppe U.
A structural model for phosphate glasses.
J Non-Cryst Solids 1996;195(1-2):138-47.
- [66] Bunker BC, Arnold GW, Wilder JA.
Phosphate glass dissolution in aqueous solutions.
J Non-Cryst Solids 1984;64(3):291-316.
- [67] Franks K, Abrahams I, Knowles JC.
Development of soluble glasses for biomedical use Part I: *In vitro* solubility measurement.
J Mater Sci: Mater Med 2000;11(10):609-14.
- [68] Ahmed I, Lewis M, Olsen I, Knowles JC.
Phosphate glasses for tissue engineering: Part 2. Processing and characterisation of a ternary-based P_2O_5 -CaO- Na_2O glass fibre system.
Biomaterials 2004;25(3):501-7.
- [69] Knowles JC, Franks K, Abrahams I.
Investigation of the solubility and ion release in the glass system K_2O - Na_2O -CaO- P_2O_5 .
Biomaterials 2001;22(23):3091-6.
- [70] Ahmed I, Collins CA, Lewis MP, Olsen I, Knowles JC.
Processing, characterisation and biocompatibility of iron-phosphate glass fibres for tissue engineering.
Biomaterials 2004;25(16):3223-32.
- [71] Lin ST, Krebs SL, Kadiyala S, Leong KW, Lacourse WC, Kumar B.
Development of bioabsorbable glass fibers.
Biomaterials 1994;15(13):1057-61.
- [72] Vogel J, Wange P, Knoche S, Rüssel C.
Chemical solubility of phosphate glasses in the system Na_2O -CaO-MgO- P_2O_5 - Al_2O_3 - TiO_2 in aqueous solutions of different pH values.
Glass Sci Technol 2004;77(2):82-7.
- [73] DIN ISO 719: Wasserbeständigkeit von Glasgrieß bei 98°C. Deutsches Institut für Normung, Berlin; 1989.
- [74] Clupper DC, Gough JE, Embanga PM, Notingher I, Hench LL, Hall MM.
Bioactive evaluation of 45S5 bioactive glass fibres and preliminary study of human osteoblast attachment.
J Mater Sci: Mater Med 2004;15(7):803-8.

- [75] Stockhorst H, Brückner R.
Structure sensitive measurements on phosphate-glass fibers.
J Non-Cryst Solids 1986;85(1-2):105-26.
- [76] Pähler G, Brückner R.
Mechanical properties and structural aspects of binary phosphate glass fibers.
J Non-Cryst Solids 1982;49(1-3):487-96.
- [77] Milberg ME, Daly MC.
Structure of oriented sodium metaphosphate glass fibers.
J Chem Phys 1963;39(11):2966-&.
- [78] Abou Neel EA, Ahmed I, Pratten J, Nazhat SN, Knowles JC.
Characterisation of antibacterial copper releasing degradable phosphate glass fibres.
Biomaterials 2005;26(15):2247-54.
- [79] Shah R, Sinanan ACM, Knowles JC, Hunt NP, Lewis MP.
Craniofacial muscle engineering using a 3-dimensional phosphate glass fibre construct.
Biomaterials 2005;26(13):1497-505.
- [80] Andriano KP, Daniels AU, Heller J.
In vitro and in vivo degradation studies of absorbable poly(orthoester) proposed for internal tissue fixation studies.
In: Wise DL, editor.
Biomaterials and bioengineering.
New York, Basel: Marcel Dekker; 2000. p. 577-601.
- [81] Stankus JJ, Guan JJ, Wagner WR.
Elastomers, biodegradable.
In: Wnek GE, Bowlin GL, editors.
Encyclopedia of biomaterials and biomedical engineering.
New York, Basel: Marcel Dekker; 2004. p. 484-93.
- [82] Rokkanen PU.
Bioabsorbable polymers for medical applications with an emphasis on orthopedic surgery.
In: Dumitriu S, editor.
Polymeric biomaterials. 2nd ed.
New York, Basel: Marcel Dekker; 2002. p. 545-62.
- [83] Wright DD.
Degradable polymer composites.
In: Wnek GE, Bowlin GL, editors.
Encyclopedia of biomaterials and biomedical engineering.
New York, Basel: Marcel Dekker; 2004. p. 423-30.

- [84] Kellomäki M, Niiranen H, Puumanen K, Ashammakhi N, Waris T, Törmälä P. Bioabsorbable scaffolds for guided bone regeneration and generation. *Biomaterials* 2000;21(24):2495-505.
- [85] Ishaug SL, Crane GM, Miller MJ, Yasko AW, Yaszemski MJ, Mikos AG. Bone formation by three-dimensional stromal osteoblast culture in biodegradable polymer scaffolds. *J Biomed Mater Res* 1997;36(1):17-28.
- [86] Deschamps AA, van Apeldoorn AA, Hayen H, de Bruijn JD, Karst U, Grijpma DW, et al. *In vivo* and *in vitro* degradation of poly(ether ester) block copolymers based on poly(ethylene glycol) and poly(butylene terephthalate). *Biomaterials* 2004;25(2):247-58.
- [87] Guan JJ, Sacks MS, Beckman EJ, Wagner WR. Biodegradable poly(ether ester urethane)urea elastomers based on poly(ether ester) triblock copolymers and putrescine: synthesis, characterization and cytocompatibility. *Biomaterials* 2004;25(1):85-96.
- [88] Vogt S, Berger S, Wilke I, Larcher Y, Weisser J, Schnabelrauch M. Design of oligolactone-based scaffolds for bone tissue engineering. *Bio-Medical Materials and Engineering* 2005;15(1-2):73-85.
- [89] Vogt S, Larcher Y, Beer B, Wilke I, Schnabelrauch M. Fabrication of highly porous scaffold materials based on functionalized oligolactides and preliminary results on their use in bone tissue engineering. *European Cells and Materials* 2002;4:30-8.
- [90] Leonor IB, Sousa RA, Reis RL. Development of bioactive composites based on biodegradable systems for bone replacement applications. In: Reis RL, San Roman J, editors. *Biodegradable systems in tissue engineering and regenerative medicine*. Boca Raton, London, New York, Washington DC: CRC Press; 2005. p. 115-26.
- [91] Wang CW, Sastry AM. Composites. In: Wnek GE, Bowlin GL, editors. *Encyclopedia of biomaterials and biomedical engineering*. New York, Basel: Marcel Dekker; 2004. p. 355-62.
- [92] Stamboulis A, Hench LL, Boccaccini AR. Mechanical properties of biodegradable polymer sutures coated with bioactive glass. *J Mater Sci: Mater Med* 2002;13(9):843-8.

- [93] Jaakkola T, Rich J, Tirri T, Narhi T, Jokinen M, Seppala J, et al.
In vitro Ca-P precipitation on biodegradable thermoplastic composite of poly(ϵ -caprolactone-co-DL-lactide) and bioactive glass (S53P4).
Biomaterials 2004;25(4):575-81.
- [94] Slivka MA, Chu CC, Adisaputro IA.
Fiber-matrix interface studies on bioabsorbable composite materials for internal fixation of bone fractures. 1. Raw material evaluation and measurement of fiber-matrix interfacial adhesion.
J Biomed Mater Res 1997;36(4):469-77.
- [95] Knowles JC, Hastings GW, Ohta H, Niwa S, Boeree N.
Development of a degradable composite for orthopedic use - *In vivo* biomechanical and histological evaluation of 2 bioactive degradable composites based on the polyhydroxybutyrate polymer.
Biomaterials 1992;13(8):491-6.
- [96] Ural E, Kesenci K, Fambri L, Migliaresi C, Piskin E.
Poly(D,L-lactide/ ϵ -caprolactone)/hydroxyapatite composites.
Biomaterials 2000;21(21):2147-54.
- [97] Marra KG, Szem JW, Kumta PN, DiMilla PA, Weiss LE.
In vitro analysis of biodegradable polymer blend/hydroxyapatite composites for bone tissue engineering.
J Biomed Mater Res 1999;47(3):324-35.
- [98] Helwig E, Sandner B, Gopp U, Vogt F, Wartewig S, Henning S.
Ring-opening polymerization of lactones in the presence of hydroxyapatite.
Biomaterials 2001;22(19):2695-702.
- [99] Maquet V, Boccaccini AR, Pravata L, Notingher I, Jerome R.
Porous poly(α -hydroxyacid)/Bioglass[®] composite scaffolds for bone tissue engineering. I: preparation and *in vitro* characterisation.
Biomaterials 2004;25(18):4185-94.
- [100] Knowles JC, Hastings GW.
In vitro and *in vivo* Investigation of a range of phosphate glass-reinforced polyhydroxybutyrate-based degradable composites.
J Mater Sci: Mater Med 1993;4(2):102-6.
- [101] Prabhakar RL, Brocchini S, Knowles JC.
Effect of glass composition on the degradation properties and ion release characteristics of phosphate glass - polycaprolactone composites.
Biomaterials 2005;26(15):2209-18.

- [102] Vallittu PK.
Some aspects of the tensile strength of unidirectional glass fibre-polymethyl methacrylate composite used in dentures.
Journal of Oral Rehabilitation 1998;25(2):100-5.
- [103] Lee YK, Song J, Lee SB, Kim KM, Choi SH, Kim CK, et al.
Proliferation, differentiation, and calcification of preosteoblast-like MC3T3-E1 cells cultured onto noncrystalline calcium phosphate glass.
J Biomed Mater Res A 2004;69A(1):188-95.
- [104] Sudo H, Kodama HA, Amagai Y, Yamamoto S, Kasai S.
In vitro differentiation and calcification in a new clonal osteogenic cell-line derived from newborn mouse calvaria.
J Cell Biol 1983;96(1):191-8.
- [105] Huang WB, Carlsen B, Rudkin G, Berry M, Ishida K, Yamaguchi DT, et al.
Osteopontin is a negative regulator of proliferation and differentiation in MC3T3-E1 pre-osteoblastic cells.
Bone 2004;34(5):799-808.
- [106] Wang D, Christensen K, Chawla K, Xiao GZ, Krebsbach PH, Franceschi RT.
Isolation and characterization of MC3T3-E1 preosteoblast subclones with distinct *in vitro* and *in vivo* differentiation mineralization potential.
J Bone Miner Res 1999;14(6):893-903.
- [107] Gronthos S, Mankani M, Brahimi J, Robey PG, Shi S.
Postnatal human dental pulp stem cells (DPSCs) *in vitro* and *in vivo*.
Proc Natl Acad Sci U S A 2000;97(25):13625-30.
- [108] Gronthos S, Brahimi J, Li W, Fisher LW, Cherman N, Boyde A, et al.
Stem cell properties of human dental pulp stem cells.
J Dent Res 2002;81(8):531-5.
- [109] Freshney RI.
Culture of animal cells: A manual of basic technique. 4th ed.
New York: Wiley-Liss; 1994.
- [110] Mosmann T.
Rapid Colorimetric Assay for Cellular Growth and Survival - Application to Proliferation and Cyto-Toxicity Assays.
J Immunol Methods 1983;65(1-2):55-63.
- [111] Salih V, Franks K, James M, Hastings GW, Knowles JC, Olsen I.
Development of soluble glasses for biomedical use Part II: The biological response of human osteoblast cell lines to phosphate-based soluble glasses.
J Mater Sci: Mater Med 2000;11(10):615-20.

- [112] Hensel MJ.
Tierexperimentelle Testung neuentwickelter Phosphatgläser, einer Phosphatglaskeramik und einer mit einer Glaskeramik beschichteten Cobalt/Chrom-Legierung am Minischwein [Dissertation].
Dresden: Medizinische Fakultät Carl Gustav Carus der Technischen Universität Dresden; 2000.
- [113] Platzbecker U.
Tierexperimentelle Untersuchungen zur Resorbierbarkeit von drei neuentwickelten porösen Biogläsern/Bioglaskeramiken [Dissertation].
Dresden: Medizinische Fakultät Carl Gustav Carus der Technischen Universität Dresden; 1996.
- [114] Wagstaff FE, Brown SD, Cutler IB.
The influence of H₂O and O₂ atmospheres on the crystallisation of vitreous silica.
Phys Chem Glasses 1964;5(3):76-81.
- [115] Wagstaff FE, Richards KJ.
Preparation and crystallization behavior of oxygen-deficient vitreous silica.
J Am Ceram Soc 1965;48(7):382-&.
- [116] Vogel J.
Abschlussbericht zum BMFT Teilprojekt "Resorbierbare, poröse Biogläser/Bioglaskeramiken" Friedrich-Schiller-Universität Jena; 1993.
- [117] Vogt S, Vogel J, Schnabelrauch M.
Resorbable polymer coatings for highly porous bioglasses.
European Journal of Trauma 2002;2:119-21.
- [118] Tas AC.
Synthesis of biomimetic Ca-hydroxyapatite powders at 37 degrees C in synthetic body fluids.
Biomaterials 2000;21(14):1429-38.
- [119] Otto M.
Chemometrics: Statistics and computer application in analytical chemistry.
Weinheim, New York, Chichester, Brisbane, Singapore, Toronto: Wiley-VCH; 1999.
- [120] Danzer K, Hobert H, Fischbacher C, Jagemann KU.
Chemometrik: Grundlagen und Anwendungen.
Berlin, Heidelberg, New York: Springer; 2001.

- [121] Kellner R, Mermet JM, Otto M, Widmer HM.
Analytical chemistry.
Weinheim, New York, Chichester, Brisbane, Singapore, Toronto: Wiley-VCH;
1998.
- [122] Deutschbein S.
Grundlagenuntersuchungen zur Steuerung des Löslichkeitsverhaltens spezieller
Phosphatgläser [Diplomarbeit] Friedrich-Schiller-Universität Jena; 1995.
- [123] Yue Y, Rüssel C, Carl G, Braun M, Jäger C.
Structural order of extruded calcium metaphosphate glasses.
Phys Chem Glasses 2000;41(1):12-6.
- [124] Yue YZ, Carl G, Rüssel C.
Rheological properties of calcium metaphosphate melts during extrusion.
Glastech Ber Glass Sci Technol 1999;72(3):67-75.
- [125] Braun M, Yue Y, Rüssel C, Jäger C.
Two-dimensional nuclear magnetic resonance evidence for structural order in
extruded phosphate glasses.
J Non-Cryst Solids 1998;241(2-3):204-7.
- [126] Arbuzov VI, Yue Y, Carl G, Rüssel C.
Study of extrusion induced structure modification in calcium metaphosphate
glasses by the method of post-radiation chronospectroscopy.
Glastech Ber Glass Sci Technol 1998;71C:256-9.
- [127] Schnabelrauch M, Vogel J, Vogt S.
Abschlussbericht zum Projekt "Entwicklung von bioresorbierbaren,
polymerverstärkten Gläsern hoher Porosität".
Jena: INNOVENT Technologieentwicklung Jena e.V.; 2002.
- [128] Vogel, J.
Unpublished Work. (2005)
- [129] Scholze H.
Glas: Natur, Struktur und Eigenschaften. 3rd ed.
Berlin, Heidelberg, New York, London, Paris, Tokyo: Springer; 1988.
- [130] Ehrt D, Vogel W.
Radiation effects in glasses.
Nuclear Instruments & Methods in Physics Research Section B-Beam
Interactions with Materials and Atoms 1992;65(1-4):1-8.
- [131] Nagase M, Abe Y, Chigira M, Udagawa E.
Toxicity of silica-containing calcium-phosphate glasses demonstrated in mice.
Biomaterials 1992;13(3):172-5.

-
- [132] Skipper LJ, Sowrey FE, Pickup DM, Fitzgerald V, Rashid R, Drake KO, et al. Structural studies of bioactivity in sol-gel-derived glasses by X-ray spectroscopy. *J Biomed Mater Res A* 2004;70A(2):354-60.
- [133] Gough JE, Notingher I, Hench LL. Osteoblast attachment and mineralized nodule formation on rough and smooth 45S5 bioactive glass monoliths. *J Biomed Mater Res A* 2004;68A(4):640-50.

Appendix

A Synthetic glass composition

Table A.1: Synthetic glass composition (mol%) of polyphosphate glasses

glass	P ₂ O ₅	CaO	MgO	Na ₂ O	K ₂ O	TiO ₂
G1	50.00	20.00	2.00	25.00	-	3.00
G2	48.00	24.00	4.00	21.50	-	2.50
G5	46.00	20.00	4.00	28.50	-	1.50
G6	45.00	20.00	4.00	29.50	-	1.50
G7	46.00	16.00	8.00	28.00	-	2.00
G8	45.00	16.00	8.00	29.00	-	2.00
G1N30	50.00	15.45	1.55	30.00	-	3.00
G2N25	48.00	21.00	3.50	25.00	-	2.50
G2N30	48.00	16.70	2.80	30.00	-	2.50
G5N32	46.00	17.00	3.50	32.00	-	1.50
G6N32	45.00	18.00	3.50	32.00	-	1.50
G7N31	46.00	14.00	7.00	31.00	-	2.00
G8N32	45.00	14.00	7.00	32.00	-	2.00
G1K5	50.00	15.45	1.55	25.00	5.00	3.00
G2K3.5	48.00	21.00	3.50	21.50	3.50	2.50
G2K8.5	48.00	16.70	2.80	21.50	8.50	2.50
G2N25K5	48.00	16.70	2.80	25.00	5.00	2.50
G5K3.5	46.00	17.00	3.50	28.50	3.50	1.50
G6K2.5	45.00	18.00	3.50	29.50	2.50	1.50
G7K3	46.00	14.00	7.00	28.00	3.00	2.00
G8K3	45.00	14.00	7.00	29.00	3.00	2.00
D4	52.50	23.70	4.30	19.50	-	-
D3T3	48.30	24.00	4.40	19.60	-	3.70
D3T2	48.00	24.70	4.70	20.10	-	2.50

Table A.2: Synthetic glass composition (mol%) of pyrophosphate glasses

glass	P₂O₅	CaO	MgO	Na₂O	additive	
Mg5	37.00	29.00	10.00	24.00	-	
T5	34.87	27.45	9.65	22.57	5.45	TiO ₂
NT1	37.00	28.54	9.84	23.62	1.00	TiO ₂
NT5	37.00	26.70	9.21	22.10	5.00	TiO ₂
NT10	37.00	24.40	8.41	20.19	10.00	TiO ₂
BT1	37.00	28.26	9.74	24.00	1.00	TiO ₂
BT5	37.00	25.28	8.72	24.00	5.00	TiO ₂
BT10	37.00	21.56	7.44	24.00	10.00	TiO ₂
CK1	37.00	29.00	10.00	23.00	1.00	K ₂ O
CK5	37.00	29.00	10.00	19.00	5.00	K ₂ O
NA1	37.00	28.54	9.84	23.62	1.00	Al ₂ O ₃
NA5	37.00	26.70	9.21	22.10	5.00	Al ₂ O ₃
NF1	37.00	28.54	9.84	23.62	1.00	Fe ₂ O ₃
NH1	37.00	28.54	9.84	23.62	1.00	F ⁻
NS1	37.00	28.54	9.84	23.62	1.00	SiO ₂
NX1	37.00	28.54	9.84	23.62	1.00	ZnO
NX5	37.00	26.70	9.21	22.10	5.00	ZnO
NZ1	37.00	28.54	9.84	23.62	1.00	ZrO ₂

B Analytic glass composition

Table B.1: Analytic glass composition (mol%) of polyphosphate glasses

glass	P ₂ O ₅	CaO	MgO	Na ₂ O	K ₂ O	TiO ₂
G1	50.6 ± 2.2	21.1 ± 0.3	2.2 ± 0.6	23.0 ± 0.5	-	3.0 ± 0.1
G2	48.1 ± 2.1	25.8 ± 0.3	4.1 ± 0.6	19.4 ± 0.5	-	2.6 ± 0.1
G5	46.3 ± 2.0	22.3 ± 0.3	4.2 ± 0.6	25.6 ± 0.5	-	1.6 ± 0.1
G6	45.1 ± 1.9	23.2 ± 0.2	4.1 ± 0.5	26.0 ± 0.4	-	1.6 ± 0.1
G7	45.5 ± 2.0	18.5 ± 0.3	9.8 ± 0.5	24.1 ± 0.4	-	2.2 ± 0.1
G8	46.1 ± 2.0	19.4 ± 0.2	8.1 ± 0.5	24.2 ± 0.4	-	2.1 ± 0.1
G1N30	51.3 ± 2.2	20.3 ± 0.3	1.7 ± 0.5	23.9 ± 0.4	-	2.8 ± 0.1
G2N25	48.1 ± 2.0	23.0 ± 0.3	3.7 ± 0.6	22.5 ± 0.5	-	2.7 ± 0.1
G5N32	46.0 ± 2.0	19.0 ± 0.3	3.9 ± 0.6	29.5 ± 0.5	-	1.6 ± 0.1
G6N32	44.9 ± 1.9	20.5 ± 0.3	4.3 ± 0.6	28.8 ± 0.4	-	1.5 ± 0.1
G7N31	44.5 ± 1.9	16.3 ± 0.3	8.9 ± 0.6	28.2 ± 0.5	-	2.0 ± 0.1
G8N32	45.2 ± 2.0	16.7 ± 0.2	8.0 ± 0.5	28.1 ± 0.4	-	2.0 ± 0.1
G1K5	50.6 ± 2.2	16.4 ± 0.3	1.7 ± 0.6	23.4 ± 0.5	5.2 ± 0.1	2.7 ± 0.1
G2K3.5	46.7 ± 2.0	22.6 ± 0.3	3.8 ± 0.6	20.9 ± 0.5	3.5 ± 0.1	2.5 ± 0.1
G5K3.5	45.7 ± 2.0	18.8 ± 0.3	4.1 ± 0.5	26.5 ± 0.4	3.6 ± 0.1	1.4 ± 0.1
G6K2.5	44.9 ± 1.9	20.1 ± 0.3	4.3 ± 0.5	26.7 ± 0.4	2.5 ± 0.1	1.4 ± 0.1
G7K3	45.1 ± 2.0	15.2 ± 0.2	8.3 ± 0.4	26.5 ± 0.4	3.0 ± 0.1	1.9 ± 0.1
G8K3	42.9 ± 1.8	14.5 ± 0.3	10.7 ± 0.5	27.3 ± 0.4	2.9 ± 0.1	1.7 ± 0.1

Table B.2: Analytic glass composition (mol%) of pyrophosphate glasses

glass	P ₂ O ₅	CaO	MgO	Na ₂ O	additive	
Mg5	36.93 ± 0.74	29.39 ± 0.21	10.05 ± 0.13	23.63 ± 0.30	-	
T5	34.04 ± 0.76	28.84 ± 0.22	10.48 ± 0.14	20.86 ± 0.31	5.78 ± 0.13	TiO ₂
NT1	36.88 ± 0.75	29.37 ± 0.22	9.91 ± 0.13	22.73 ± 0.31	1.11 ± 0.13	TiO ₂
CK1	36.98 ± 0.74	29.41 ± 0.21	10.05 ± 0.13	22.60 ± 0.31	0.97 ± 0.18	K ₂ O
NA1	36.84 ± 0.75	29.05 ± 0.22	9.91 ± 0.13	23.02 ± 0.31	1.18 ± 0.04	Al ₂ O ₃
NH1	36.82 ± 0.74	29.00 ± 0.21	9.85 ± 0.13	23.32 ± 0.30	n/a	F ⁻
NS1	36.80 ± 0.73	29.08 ± 0.21	9.88 ± 0.13	23.05 ± 0.30	1.19 ± 0.11	SiO ₂

C Solubility results

Table C.1: Polyphosphate glasses: dissolved oxides in mg/L (time-constant solubility)

glass	P ₂ O ₅	CaO	MgO	Na ₂ O	K ₂ O	TiO ₂
G1	10314.7 ± 1409.2	1771.2 ± 16.4	132.2 ± 3.9	2196.0 ± 37.5	-	149.3 ± 4.9
G2	628.5 ± 32.9	110.5 ± 5.0	14.8 ± 4.0	141.7 ± 10.5	-	7.7 ± 5.0
G5	300.7 ± 34.2	43.9 ± 5.1	6.3 ± 4.1	96.9 ± 10.6	-	n/a
G6	253.3 ± 10.9	38.0 ± 0.5	7.0 ± 0.4	76.5 ± 1.0	-	4.2 ± 0.5
G7	239.4 ± 10.2	21.8 ± 0.5	15.4 ± 0.4	71.3 ± 1.0	-	3.8 ± 0.5
G8	304.8 ± 13.5	30.4 ± 0.5	16.0 ± 0.4	88.0 ± 0.9	-	5.81 ± 0.5
G1N30	19679.7 ± 2670.5	2459.11 ± 34.5	174.2 ± 3.9	5125.8 ± 73.1	-	223.3 ± 4.8
G2N25	1895.0 78.3	293.1 ± 4.8	41.1 ± 4.0	448.9 ± 10.0	-	34.0 ± 5.0
G5N32	981.8 ± 40.4	141.0 ± 5.0	22.2 ± 4.0	306.6 ± 10.2	-	16.2 ± 5.0
G6N32	599.9 ± 28.5	89.4 ± 0.4	16.3 ± 0.4	156.1 ± 45.6	-	11.5 ± 0.5
G7N31	371.46 ± 16.8	40.7 ± 0.5	20.5 ± 0.4	109.8 ± 0.9	-	9.1 ± 0.5
G8N32	499.6 ± 23.4	57.2 ± 0.5	24.3 ± 0.4	144.3 ± 0.9	-	12.8 ± 0.5
G7K3	464.6 ± 214.4	70.0 ± 0.5	25.48 ± 0.4	167.6 ± 45.6	58.0 ± 34.3	7.2 ± 0.5
G8K3	391.0 ± 17.8	37.3 ± 0.5	23.0 ± 0.4	109.5 ± 0.9	23.5 ± 0.5	8.0 ± 0.5

Table C.2: Pyrophosphate glasses: dissolved oxides in mg/L (time-constant solubility)

glass	P ₂ O ₅	CaO	MgO	Na ₂ O	additive	
Mg5	26.35 ± 1.37	3.05 ± 0.31	1.25 ± 0.05	8.74 ± 2.82	-	
T5	17.34 ± 3.11	2.15 ± 0.37	0.65 ± 0.23	6.34 ± 1.09	0.33 ± 0.24	TiO ₂
NT1	22.98 ± 1.37	3.08 ± 0.31	1.20 ± 0.05	7.76 ± 2.82	0.14 ± 0.16	TiO ₂
NT5	19.23 ± 1.37	2.08 ± 0.31	0.73 ± 0.05	5.94 ± 2.82	0.75 ± 0.16	TiO ₂
NT10	15.49 ± 1.37	1.05 ± 0.31	0.39 ± 0.05	4.98 ± 2.82	0.56 ± 0.16	TiO ₂
BT1	25.38 ± 1.37	2.65 ± 0.31	1.22 ± 0.05	8.68 ± 2.82	0.24 ± 0.16	TiO ₂
BT5	22.64 ± 1.37	2.45 ± 0.31	0.94 ± 0.05	7.82 ± 2.82	1.02 ± 0.16	TiO ₂
BT10	16.53 ± 1.37	0.85 ± 0.31	0.37 ± 0.05	6.08 ± 2.82	0.77 ± 0.16	TiO ₂
CK1	24.98 ± 1.37	3.04 ± 0.31	1.46 ± 0.05	8.33 ± 2.82	0.49 ± 0.64	K ₂ O
CK5	28.20 ± 1.37	3.75 ± 0.31	1.62 ± 0.05	7.56 ± 2.82	2.60 ± 0.64	K ₂ O
NA1	23.02 ± 1.37	4.00 ± 0.31	1.69 ± 0.05	9.80 ± 2.82	0.71 ± 0.26	Al ₂ O ₃
NA5	19.38 ± 1.37	2.85 ± 0.31	0.74 ± 0.05	5.67 ± 2.82	2.00 ± 0.26	Al ₂ O ₃
NF1	21.40 ± 1.37	2.52 ± 0.31	1.03 ± 0.05	6.91 ± 2.82	0.19 ± 0.22	Fe ₂ O ₃
NH1	27.16 ± 1.37	3.26 ± 0.31	1.52 ± 0.05	8.96 ± 2.82	n/a	F ⁻
NS1	35.24 ± 1.37	4.78 ± 0.31	1.97 ± 0.05	11.60 ± 2.82	3.95 ± 0.91	SiO ₂
NX1	34.73 ± 1.37	4.87 ± 0.31	1.95 ± 0.05	11.19 ± 2.82	0.32 ± 0.19	ZnO
NX5	25.93 ± 1.37	3.22 ± 0.31	1.24 ± 0.05	7.88 ± 2.82	1.22 ± 0.19	ZnO
NZ1	21.38 ± 1.37	2.03 ± 0.31	0.99 ± 0.05	6.99 ± 2.82	0.19 ± 0.36	ZrO ₂

Table C.3: Glass composition and dissolved P₂O₅ of glasses after Deutschbein [122]

glass	glass composition					dissolved
	P ₂ O ₅	CaO	MgO	Na ₂ O	TiO ₂	mg/L
1	38.9	30.5	5.6	25.0		77.9
2	43.0	28.5	5.3	23.1		112.2
3	47.6	26.2	4.8	47.6		526.9
4	52.5	23.7	4.3	19.5		10079.4
1T2	37.9	29.8	5.4	24.3	2.6	11.5
2T2	43.5	26.9	5.1	22.1	2.4	64.1
2T4	43.9	25.7	4.7	20.9	4.8	0.0
3T2	48.0	24.7	4.7	20.1	2.5	274.9
3T3	48.3	24.0	4.4	19.6	3.7	274.9
4T2	53.0	22.1	4.1	18.2	2.6	1786.8
4T3	54.1	20.9	3.9	17.1	3.9	916.3

Table C.4: Time-dependent solubility: dissolved oxides in mg/L

glass	time min	Na₂O	CaO	MgO	TiO₂
G1	60	992,16	815,34	61,04	128,08
	120	1426,81	1178,18	92,94	79,46
	300	1942,32	1388,11	114,25	85,63
	480	2024,69	1263,65	110,09	7,02
G2	60	39,90	57,01	6,22	n/a
	120	104,54	128,90	19,04	2,93
	300	375,74	431,28	70,45	10,56
	480	592,68	666,84	113,94	8,19
G5	60	44,07	47,03	5,45	n/a
	120	64,50	63,53	8,71	n/a
	300	133,89	96,07	17,79	3,69
	480	183,68	78,46	19,83	3,28
G6	60	39,16	41,42	6,72	4,27
	120	50,63	49,45	8,47	5,50
	300	78,39	62,42	12,57	7,37
	480	96,13	62,98	9,86	n/a
G7	60	26,22	19,10	11,09	3,33
	120	35,29	20,21	13,88	3,96
	300	61,39	35,85	23,36	7,52
	480	80,98	39,26	29,48	9,21
G8	60	36,42	31,88	13,43	5,60
	120	41,75	35,11	15,05	6,48
	300	69,03	47,12	23,54	10,07
	480	95,11	55,25	30,89	12,45

D Glass data

Table D.1: Polyphosphate glasses: glass data

glass	pH*	density g/cm ³	T _g °C	lg η (550°C) (η in dPa s)	lg η (600°C) (η in dPa s)
G1	5.19	2.6	379	3.94	(3.06)**
G2	5.81	2.64	394	4.40	(3.39)***
G5	6.10	2.63	372	3.38	2.64
G6	6.34	2.64	373	n/a	n/a
G7	6.25	2.64	391	n/a	n/a
G8	6.23	2.64	384	n/a	n/a
G1N30	4.19	2.58	394	n/a	n/a
G2N25	5.37	2.61	383	n/a	n/a
G2N30	n/a	n/a	363	n/a	n/a
G5N32	6.19	2.61	n/a	n/a	n/a
G6N32	6.37	2.63	n/a	n/a	n/a
G7N31	6.39	2.62	378	n/a	n/a
G8N32	6.29	2.61	371	n/a	n/a
G1K5	3.78	n/a	n/a	n/a	n/a
G2K3.5	5.77	2.61	369	n/a	n/a
G2K8.5	5.40	2.58	336	n/a	n/a
G2N25K5	5.43	2.6	n/a	n/a	n/a
G5K3.5	6.25	2.61	n/a	n/a	n/a
G6K2.5	6.38	2.63	n/a	n/a	n/a
G7K3	n/a	2.62	n/a	n/a	n/a
G8K3	n/a	2.63	n/a	n/a	n/a
D4	n/a	2.56	360	3.57	2.86
D3T3	4.79	2.61	411	4.24	(3.21/3.42)**
D3T2	4.93	2.61	407	n/a	n/a

* refers to the pH in physiological salt solution after immersion over 24 h

** affected by non-Newtonian flow

*** affected by crystallization

Table D.2: Pyrophosphate glasses: glass data

glass	pH*	density g/cm ³	T_g °C
Mg5	7.54	2.73	419
T5	7.14	2.77	470
NT1	7.31	2.74	433
NT5	6.89	2.74	456
NT10	6.57	2.78	487
BT1	7.32	2.72	432
BT5	6.92	2.73	451
BT10	6.59	2.75	466
CK1	7.28	2.69	416
CK5	7.18	2.7	411
NA1	6.89	2.73	437
NA5	n/a	2.74	472
NF1	6.89	2.73	430
NH1	7.16	2.68	423
NS1	6.95	2.67	419
NX1	n/a	2.72	n/a
NX5	n/a	2.78	n/a
NZ1	6.89	n/a	432

* refers to the pH in physiological salt solution after immersion over 24 h

Table D.3: Crystal phases of glasses Mg5, T5, NT1, NS1, NH1, CK1 and NA1

Glass	Temperature °C	Crystal phase
Mg5	520; 560	Ca ₂ P ₂ O ₇
		Mg ₂ P ₂ O ₇
		Na ₄ P ₂ O ₇
T5	540	Ca ₂ P ₂ O ₇
		CaMgP ₂ O ₇
		Mg ₂ P ₂ O ₇
	600	Na ₄ P ₂ O ₇
		Ca ₂ P ₂ O ₇
		CaMgP ₂ O ₇
NT1	520; 580	Mg ₂ P ₂ O ₇
		Na ₄ P ₂ O ₇
		NaPO ₃
NS1	500; 560	Ca ₂ P ₂ O ₇
		Mg ₂ P ₂ O ₇
NH1	500	Ca ₂ P ₂ O ₇
	540	Ca ₂ P ₂ O ₇
CK1	500; 560	Mg ₂ P ₂ O ₇
		Ca ₂ P ₂ O ₇
NA1	600	Mg ₂ P ₂ O ₇
		Ca ₂ P ₂ O ₇
		NaMgPO ₄

Figures

Figure 2.1:	Internal fracture fixation using wires (left), screws (center and right) and plates (right) (after Matzen [46])	15
Figure 2.2:	Basic phosphate and silicate tetrahedra in glass structures	17
Figure 2.3:	Schematic of the invert glass structure (after Vogel [4])	18
Figure 3.1:	Schematic of the fiber rig (IPHT).....	38
Figure 3.2:	Reaction schematic of the macromer synthesis.....	40
Figure 3.3:	Schematic of the adhesive shear strength measurement procedure....	42
Figure 3.4:	Schematic of the neural network used for modeling investigations...	48
Figure 4.1:	³¹ P MAS-NMR spectra (bottom) and central resonances (top) of glasses G1, G2, G5 and G6	50
Figure 4.2:	³¹ P chemical shifts: Gauss fit of Q ¹ (red curves) and Q ² (green curves) peaks of glasses G1, G2, G5 and G6	51
Figure 4.3:	Viscosity (rotating viscometer) of glasses D4, D3T3, G1, G2 and G5	53
Figure 4.4:	pH of polyphosphate glasses in physiological NaCl solution (mean ± standard deviation)	55
Figure 4.5:	pH of glass D4 in physiological NaCl solution over 16 days (line: regression line).....	56
Figure 4.6:	Ratio P ₂ O ₅ /other components in solution vs. ratio P ₂ O ₅ /other components in the glass (line: ratio 1:1).....	57
Figure 4.7:	Dissolved P ₂ O ₅ vs. P ₂ O ₅ content in the glass for low (left) and high (right) alkali oxide contents.....	58
Figure 4.8:	Time-dependent solubility of glass G1.....	59
Figure 4.9:	Time-dependent solubility of glasses G2, G5, G6, G7 and G8.....	60
Figure 4.10:	Crystalline surface layers after tempering for 30 min at 540 °C: Glasses Mg5 (left) and T5 (right).....	62
Figure 4.11:	X-ray spectra of powder and crystalline surface of glass T5 (tempered for 30 min at 600 °C)	63
Figure 4.12:	Crystallization of pyrophosphate glasses (tempered for 30 min).....	64
Figure 4.13:	Viscosity curve (beam bending viscometer) of glass T5.....	64
Figure 4.14:	pH of glasses in physiological NaCl solution (mean ± confidence interval) (top); weight loss after 10 days in physiological NaCl solution (bottom)	65
Figure 4.15:	Total oxides dissolved (mean ± 95% confidence interval)	66
Figure 4.16:	MLR: observed by predicted plot and 95 % confidence band (correlation coefficient: 0.93; red: pyrophosphate glasses, green: polyphosphate glasses, blue: meta-/ultraphosphate glasses).....	67
Figure 4.17:	NN: observed by predicted plot (correlation coefficient: 0.9996; red: pyrophosphate glasses, green: polyphosphate glasses, blue: meta-/ultraphosphate glasses).....	68

Figure 4.18:	MC3T3-E1.4 concentration on polished glasses at 24 h (mean \pm standard deviation)	69
Figure 4.19:	MC3T3-E1.4 concentration on polished glasses at 72 h (mean \pm standard deviation)	70
Figure 4.20:	MC3T3-E1.4 cell layer on polished glass Mg5 at 24 h (left: confluent cell layer; right: cell layer and exposed glass surface).....	70
Figure 4.21:	DPSC concentration on polished glasses at 24 h (mean \pm standard deviation).....	71
Figure 4.22:	Absorbance of γ -irradiated glasses corrected by absorbance of non-irradiated glasses	72
Figure 4.23:	MC3T3-E1.4 concentration on heat-sterilized polished glasses at 24 h (mean \pm standard deviation)	73
Figure 4.24:	Macropores (left) and micropores (right) of sintered porous glass Mg5.....	74
Figure 4.25:	Section of Mg5-reinforced porous polymer	74
Figure 4.26:	Micropores in glass Mg5 after sintering without NaCl.....	76
Figure 4.27:	Weight loss of uncoated and polymer coated sintered porous glasses Mg5 and T5 in SBF at 37 °C (lines: regression lines)	77
Figure 4.28:	Weight loss of Mg5 and T5 glass powder-reinforced porous polymers in SBF at 37 °C (lines: regression lines)	78
Figure 4.29:	MC3T3-E1.4 concentration on porous uncoated glasses at 24 h (mean \pm standard deviation)	79
Figure 4.30:	MC3T3-E1.4 cells on porous glass Mg5 after cultivation over 24 h	79
Figure 4.31:	MC3T3-E1.4 concentration on porous glasses at 72 h (mean \pm standard deviation)	80
Figure 4.32:	MC3T3-E1.4 cells (blue) on porous glass T5 after HE staining	80
Figure 4.33:	Viability of MC3T3-E1 cells on glass powder-reinforced polymer: living green fluorescent cells (left) and dead red fluorescent cells (right) on porous polymer with glass T5 (top) and Mg5 (bottom).....	81
Figure 4.34:	T5 glass fibers.....	82
Figure 4.35:	Section of polymer phosphate glass fiber composite	82
Figure 4.36:	SEM micrograph of polymer phosphate glass fiber composite: fracture during 3-point bending test	83
Figure 4.37:	Graphs of 4-point bending test (top) and 3-point bending test (bottom)	84

Tables

Table 3.1:	Synthetic glass composition (mol%) of polyphosphate glasses.....	35
Table 3.2:	Synthetic glass composition (mol%) of pyrophosphate glasses.....	36
Table 4.1:	Glass compositions in mol% and metal oxide fraction (x) of glasses G1, G2, G5 and G6	49
Table 4.2:	^{31}P MAS-NMR chemical shifts in ppm for Q^1 and Q^2 groups.....	50
Table 4.3:	Relative concentrations of the Q^n units determined by ^{31}P MAS-NMR and experimental and theoretical average chain lengths L	52
Table 4.4:	Viscosity (η) at 550 °C and 600 °C.....	54
Table 4.5:	Compressive strength of coated and uncoated sintered porous glasses and porous glass powder-reinforced polymer specimens	75
Table 4.6:	Adhesive shear strength between polymer and polished and sintered glasses, respectively.....	75
Table A.1:	Synthetic glass composition (mol%) of polyphosphate glasses	118
Table A.2:	Synthetic glass composition (mol%) of pyrophosphate glasses.....	119
Table B.1:	Analytic glass composition (mol%) of polyphosphate glasses	120
Table B.2:	Analytic glass composition (mol%) of pyrophosphate glasses	120
Table C.1:	Polyphosphate glasses: dissolved oxides in mg/L (time-constant solubility).....	121
Table C.2:	Pyrophosphate glasses: dissolved oxides in mg/L (time-constant solubility).....	122
Table C.3:	Glass composition and dissolved P_2O_5 of glasses after Deutschbein [122]	122
Table D.1:	Polyphosphate glasses: glass data	124
Table D.2:	Pyrophosphate glasses: glass data	125
Table D.3:	Crystal phases of glasses Mg5, T5, NT1, NS1, NH1, CK1 and NA1	126

Danksagung

Herrn Prof. Dr. Christian Rüssel danke ich für die Möglichkeit, meine Doktorarbeit am Otto-Schott-Institut durchzuführen, für die interessante Themenstellung sowie für die Betreuung der Arbeit.

Frau Prof. Dr. Dörte Stachel danke ich für die Übernahme des Zweitgutachtens sowie für Ihre stete Diskussionsbereitschaft und freundliche Unterstützung.

Dr. Stefan Habelitz, Dr. Wu Li, Prof. Dr. Sally J. Marshall, Dr. Grayson W. Marshall, Dr. Silvia Foppiano, Grace Nonomura und Larry Watanabe danke ich für die Möglichkeit, Untersuchungen an der UCSF durchzuführen, sowie für Hilfe und Anregungen während meiner Zeit dort und danach.

Dr. Matthias Schnabelrauch und Dr. Sebastian Vogt danke ich für die Herstellung der Polymerproben und Komposite, für die Abbauuntersuchungen in simulierter Körperflüssigkeit sowie für ihre zahlreichen Anregungen und die stete hilfsbereite Diskussionsbereitschaft. Dr. Jürgen Weisser danke ich für die Durchführung der FDA/EtBr-Zelltests.

Angelika Hacker danke ich für unzählige Arbeiten und Hilfen im Laboralltag und das freundschaftliche Arbeitsklima im Labor.

Dr. Peter Wange und Dr. Jürgen Vogel danke ich für ihren Rat und viele Anregungen.

Dr. Jörg Kraft, Prof. Dr. Klaus Danzer, Brunhilde Dressler, Dr. Dirk Merten, Ines Kamp und Susan Rudzinski danke ich für ihre Unterstützung bei der Durchführung und Auswertung der analytischen Messungen.

Dr. Günter Völksch und Renate Lemanczyk danke ich für die Untersuchungen am Rasterelektronenmikroskop.

Gabriele Möller, Bernd Keinert, Bettina Hartmann, Gerlinde Loesche, Steffi Ebbinghaus, Elke Wagner, Lutz Preißer und Rainer Weiß danke ich für die durchgeführten Probenvorbereitungen, Untersuchungen, Messungen und Arbeiten.

Dr. Peter Hartmann danke ich für die Durchführung der ^{31}P MAS-NMR Messungen.

Dr. Jens Kobelke danke ich für die Möglichkeit, Glasfasern am IPHT herzustellen.

Erik Heurich danke ich für die Hilfe bei den Kristallisationsuntersuchungen.

Sämtlichen Doktoranden, Diplomanden und Mitarbeitern des Otto-Schott-Instituts danke ich für die angenehme Arbeitsatmosphäre und die gute Zusammenarbeit.

Dr. Sandra Hornschuh danke ich für ihr Interesse an meiner Arbeit, ihre freundschaftliche Hilfe und das Korrekturlesen. Meinem Freund, Dr. Rainer Brüning, danke ich für seine Geduld und große Hilfe, sein Vertrauen sowie die schöne gemeinsame Zeit.

Selbständigkeitserklärung

Ich erkläre, dass ich die vorliegende Arbeit selbständig und unter Verwendung der angegebenen Hilfsmittel, persönlichen Mitteilungen und Quellen angefertigt habe.

Jena, den 06. Mai 2005

Delia Brauer

Lebenslauf

Persönliche Daten

Name: Delia Silke Brauer
Geburtsdatum: 28.07.1976
Geburtsort: Berlin-Neukölln
Familienstand: ledig

Ausbildungsdaten

Aug. 1989 - Mai 1996 Campe-Gymnasium Holzminden
Mai 1996 Abitur
Okt. 1996 - Sept. 2001 Studium der Chemie (Umweltchemie) an der Friedrich-Schiller-Universität Jena
Sept. 1998 Vordiplom
Sept. 1999 - Feb. 2000 Auslandssemester an der University of Northumbria at Newcastle, Newcastle upon Tyne, UK
Nov. 2000 - Sept. 2001 Diplomarbeit; Betreuer: Prof. Dr. J.W. Einax, Institut für Anorganische und Analytische Chemie der Friedrich-Schiller-Universität Jena
Thema: „Herabsetzung der Nachweisgrenze in der Elektroanalytik durch Anwendung der Wavelet-Transformation“
Sept. 2001 Diplom in Chemie (Umweltchemie)
Okt. 2001 - Juni 2002 wissenschaftliche Mitarbeiterin am Institut für Anorganische und Analytische Chemie der Friedrich-Schiller-Universität Jena
seit Juli 2002 wissenschaftliche Mitarbeiterin am Otto-Schott-Institut für Glaschemie der Friedrich-Schiller-Universität Jena
Promotionsarbeit; Betreuer: Prof. Dr. C. Rüssel, Otto-Schott-Institut für Glaschemie der Friedrich-Schiller-Universität Jena
Thema: „Degradable phosphate glasses and composite materials for biomedical applications“
Juni 2004 - Nov. 2004 Forschungsaufenthalt an der University of California, San Francisco, USA

Jena, den 06. Mai 2005

Delia Brauer